Activation of Ionic Species by Visible Light Photoredox Catalysis

Dissertation

Zur Erlangung des Doktorgrades der Naturwissenschaften

(Dr. rer. nat.)

an der Fakultät für Chemie und Pharmazie

der Universität Regensburg

vorgelegt von

Thea Hering

aus München

2016

The experimental work was carried out between December 2012 and January 2016 at the University of Regensburg, Institute of Organic Chemistry under the supervision of Prof. Dr. Burkhard König.

Date of submission: 18.03.2016

Date of colloquium: 04.05.2016

Board of examiners:

Prof Dr. Olga Garcia Mancheño	(Chair)
Prof. Dr. Burkhard König	(1st Referee)
Prof. Dr. Robert Wolf	(2nd Referee)
Prof. Dr. Frank-Michael Matysik	(Examiner)

To my family

&

Christian

"Ich bin immer noch verwirrt, aber auf einem höheren Niveau"

Enrico Fermi

Table of Contents

1. THE PHOTOREDOX CATALYZED MEERWEIN ADDITION REACTION: INTERMOLECULAR AMINO-ARYLATION OF ALKENES 1
  - 1.1. Introduction 3
  - 1.2. Results and Discussion 4
  - 1.3. Conclusion 10
  - 1.4. Experimental Part 11
    - 1.4.1. General Methods and Material 11
    - 1.4.2. General Procedures 11
    - 1.4.3. Reaction Optimization 21
    - 1.4.4. Radical Capturing Experiments 23
    - 1.4.5. Carbenium Ion Trapping Experiments 24
    - 1.4.6. ^{1}H and ^{13}C NMR Spectra of Selected Compounds 25
  - 1.5. References 31

2. VISIBLE LIGHT PHOTOOXIDATION OF NITRATE: THE DAWN OF A NOCTURNAL RADICAL 35
  - 2.1. Introduction 37
  - 2.2. Results and Discussion 38
  - 2.3. Conclusion 45
  - 2.4. Experimental Section 45
    - 2.4.1. General Information 45
    - 2.4.2. CV- Measurement 46
    - 2.4.3. Spectroscopic Investigations 47
    - 2.4.4. Synthetic Procedures 51
    - 2.4.5. Proposed Mechanism for the Photooxidation of Compound 9 54
  - 2.5. References 55

3. HALOGENASE INSPIRED OXIDATIVE CHLORINATION USING FLAVIN PHOTOCATALYSIS 59
  - 3.1. Introduction 60
  - 3.2. Conclusion 66

3.3. Experimental Section 66
3.3.1. General Information 66
3.3.2. General Procedure for the Photocatalytic Chlorination 67
3.3.3. GC-FID Measurements 67
3.3.4. Control Reactions 68
3.3.5. Reactions with Peracetic Acid 69
3.3.6. Optimization of the Reaction Conditions 70
3.3.7. UV/VIS Spectroscopy 72

3.4. References 74

4. PHOTOCATALYTIC ACTIVATION OF *N*−CHLORO COMPOUNDS FOR THE CHLORINATION OF ARENES 77

4.1. Introduction 79

4.2. Activation of *N*−Chloramines 80

4.3. Activation of NCS 85

4.4. Conclusion 89

4.5. Experimental Section 89
4.5.1. General Information 89
4.5.2. Synthesis of *N*−Chloramines 90
4.5.3. General Procedure for the Photocatalytic Activation of *N*−Chloro Compounds 90
4.5.4. CV- Measurements 91

4.6. References 92

5. SUMMARY 95

6. ZUSAMMENFASSUNG 97

7. ABBREVIATIONS 99

8. CURRICULUM VITAE 101

9. DANKSAGUNG 103

CHAPTER 1

1. The Photoredox Catalyzed Meerwein Addition Reaction: Intermolecular Amino-Arylation of Alkenes

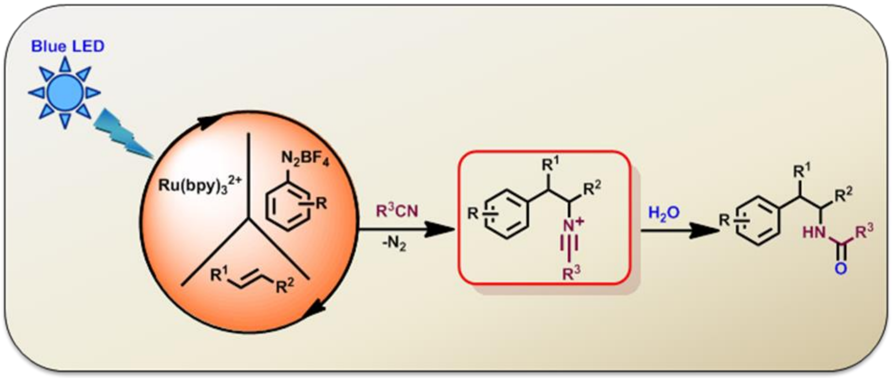
Blue LED
$Ru(bpy)_3^{2+}$
N_2BF_4
R
R^1
R^2
R^3CN
$-N_2$
R
R^1
R^2
N^+
R^3
H_2O
R
R^1
R^2
HN
R^3
O

This chapter was published in: D. P. Hari, T. Hering, B. König, *Angew. Chem., Int. Ed.* **2014**, *53*, 725-728. - reproduced with permission from John Wiley & Sons
DP carried out the reactions in Tables 1, 2 and 3. TH carried out the reactions in Table 4 and Scheme 1-2. DP wrote the manuscript. BK supervised the project and is corresponding author.

1.1. Introduction

The Meerwein arylation is a valuable synthetic transformation based on aryl radical chemistry (Scheme 1-1).[1-13] The classic Meerwein arylation has two alternative reaction pathways: (a) a Meerwein arylation-elimination, in which aryl-alkene cross coupling products are formed exclusively, and (b) a Meerwein arylation-addition, in which the aryl radical and a halogen atom add to an olefinic substrate.[2] The addition of other atoms instead of halogen has also been reported.[2] However, photo Meerwein arylations were so far only applied for the formation of aryl-alkene coupling products and not extended to the valuable alkene addition products[14-17] obtainable under classical Meerwein arylation conditions.[18-26] The challenge in obtaining the addition product is the competing reaction of the trapping reagent or nucleophile with the diazonium salt leading to undesired products.[2]

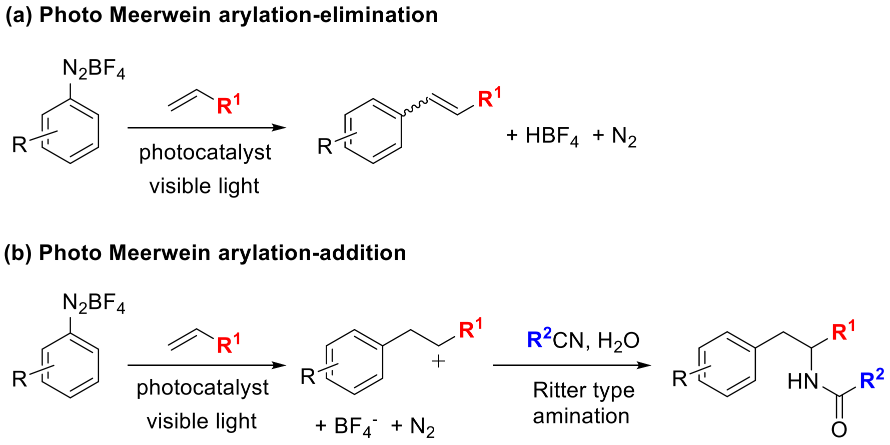

Scheme 1-1. Types of photo Meerwein arylation reactions: (a) photo Meerwein arylation-elimination, (b) photo Meerwein arylation-addition.

The Ritter-type amination reaction is a most useful transformation for the formation of C−N bonds and has been used in industrial processes for the synthesis of the anti-HIV drug Crixivan, the alkaloid aristotelone, and Amantadine.[17, 27-35] We utilize the Ritter reaction conditions to trap the carbenium ion, which is generated during the photoredox Meerwein arylation reaction leading to a photoredox catalyzed Meerwein arylation-addition process allowing the intermolecular amino-arylation of alkenes mediated by visible light.

1.2. Results and Discussion

Our initial studies began with an attempted reaction of diazonium salt **1a** (0.25 mmol) with 5 eq. of styrene **2a** using 2 mol% of $[Ru(bpy)_3]Cl_2$ in 1.0 mL of CH_3CN containing 10 eq. of water under visible light irradiation for 4 h at 20 °C; the desired product **3a** was obtained in 42% yield (Table 1-1) along with 1,2-diphenylethanol as a byproduct.

Table 1-1. Optimizing reaction conditions.

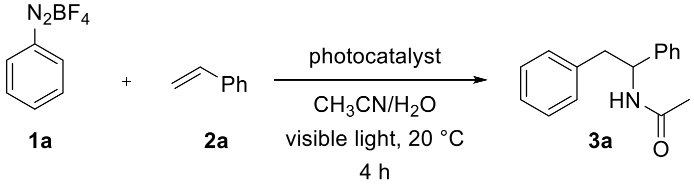

Entry	Conditions	Yield (%)[a]
1	$[Ru(bpy)_3]Cl_2$ (2 mol%), **2a** (5 eq.)	42[b]
2	$[Ru(bpy)_3]Cl_2$ (2 mol%), **2a** (5 eq.)	75
3	$[Ru(bpy)_3]Cl_2$ (2 mol%), **2a** (5 eq.)	65[c]
4	$[Ru(bpy)_3]Cl_2$ (2 mol%), **2a** (5 eq.)	74[d]
5	$[Ru(bpy)_3]Cl_2$ (0.5 mol%), **2a** (5 eq.)	75
6	$[Ru(bpy)_3]Cl_2$ (0.5 mol%), **2a** (2 eq.)	88
7	$[Ru(bpy)_3]Cl_2$ (0.5 mol%), **2a** (1.1 eq.)	72
9	Eosin Y (0.5 mol%), **2a** (2 eq.)	38
10	$Ir(ppy)_3$ (0.5 mol%), **2a** (2 eq.)	76
11	Rhodamine B (0.5 mol%), **2a** (2 eq.)	5
12	Rose Bengal (0.5 mol%), **2a** (2 eq.)	37
13	$C_{50}H_{40}CuF_6N_2OP_3$ (0.5 mol%), **2a** (2 eq.)	21
14	no photocatalyst, **2a** (2 eq.)	5
15	$[Ru(bpy)_3]Cl_2$ (0.5 mol%), **2a** (2 eq.), no light	0

[a] GC yield determined by using a calibrated internal standard. [b] The reaction was carried out with 10 eq. of H_2O. [c] The reaction was carried out in 0.5 mL of CH_3CN. [d] The reaction was carried out in 2.0 mL of CH_3CN. Unless otherwise mentioned in all other cases the reactions were carried out in 1.0 mL of CH_3CN using 1 eq. of H_2O.

We examined the amount of water, catalyst loading and different eq. of styrene on this multi-component photoreaction. To our delight the desired product **3a** was obtained in 88% yield when diazonium salt **1a** (0.25 mmol), 0.5 mol% of $[Ru(bpy)_3]Cl_2$, 2 eq. of styrene **2a** and 1 eq. of water were used in 1.0 mL of CH_3CN (Table 1-1, entry 6). The reaction yields of **3a** are significantly affected by the amount of water: a larger amount of water results in the formation of the 1,2-diphenylethanol (Table 1-1, entry 1 *vs.* 2).

After having optimized the reaction conditions we screened different photocatalysts (Table 1-1, entries 6, 9-13). $[Ru(bpy)_3]Cl_2$ was found to be the best one for this transformation. To prove the significance of the photoreaction, we carried out control experiments without light and without the photocatalyst $[Ru(bpy)_3]Cl_2$. As expected, we observed 0 and 5% of product yield, respectively (Table 1-1, entries 15 and 14). When we employed dichloromethane as a solvent and 10 eq. of acetonitrile in this photoreaction, product **3a** was obtained in 70% yield.[36] This shows that the use of the organic nitrile as a solvent is not required. In addition, we also replaced the photocatalyst and visible light by copper catalysts, which are commonly employed in Meerwein arylations. However, under these conditions the reaction does not proceed showing that the photoredox system is essential.[36]

Furthermore, we investigated the scope of the diazonium salts for this photoreaction and the results were summarized in Table 1-2. Aryl diazonium salts bearing electron withdrawing, neutral and donating substituents react smoothly affording the corresponding products in good to excellent yields. Several functional groups including ester, nitro, halide, ether, alkyl groups are tolerated in the photoreaction. In addition to aryl diazonium salts, heteroaryl diazonium salt **1j** was used in this reaction to giving the corresponding product **3j** in 75% yield (Table 1-2, entry 10). Carbon-halogen bonds remain intact during the photoreaction providing access to halogen substituted amides in a single step (Table 1-2, entries 5 and 9). The halide functional groups can be used for further transformations by transition metal catalyzed or organometallic reactions.

Table 1-2. Scope of the aryl diazonium salts.[a]

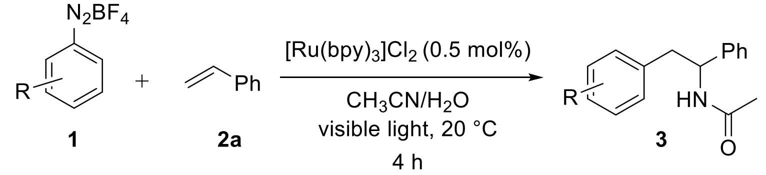
N_2BF_4
R
+
Ph
1
2a
$[Ru(bpy)_3]Cl_2$ (0.5 mol%)
CH_3CN/H_2O
visible light, 20 °C
4 h
R
Ph
HN
O
3

Entry	Substrate	Product	Yield (%)[b]
1	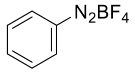 **1a**	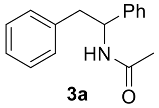 **3a**	82
2	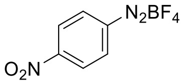 **1b**	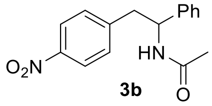 **3b**	92
3	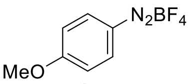 **1c**	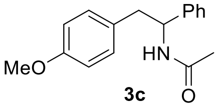 **3c**	70
4	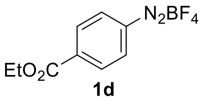 **1d**	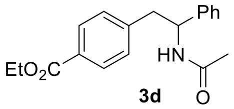 **3d**	82
5	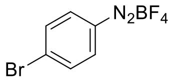 **1e**	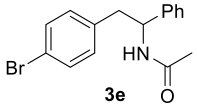 **3e**	76
6	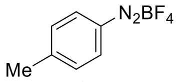 **1f**	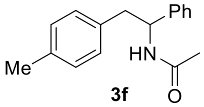 **3f**	70
7	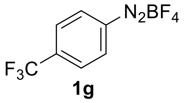 **1g**	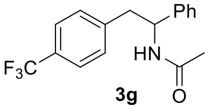 **3g**	73
8	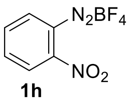 **1h**	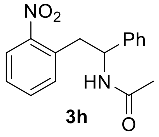 **3h**	87
9	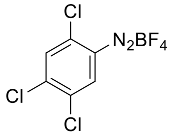 **1i**	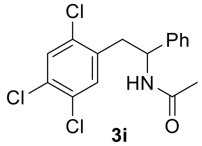 **3i**	50
10	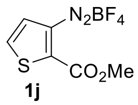 **1j**	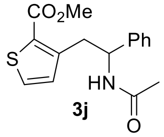 **3j**	75
11	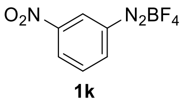 **1k**	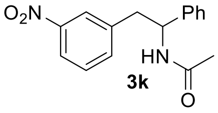 **3k**	70

[a] The reaction was performed with **1** (0.25 mmol), styrene **2a** (2 eq.), $[Ru(bpy)_3]Cl_2$ (0.005 eq.) and 1 eq. of H_2O in 1.0 mL of CH_3CN. [b] Isolated yields after purification by flash column chromatography.

We then expanded the scope of the reaction by varying the nitrile, which proved to be of general applicability in the photoreaction. The products obtained from the reactions of diazonium salt **1b** and styrenes **2a** with different nitriles are shown in Table 1-3. The results demonstrate that primary, secondary, and tertiary alkyl nitriles undergo cleanly the transformation providing the corresponding products in good to excellent yields. We were also pleased to find that cyclopropane carbonitrile was tolerated well affording the corresponding product **3m** in 65% yield after 4 h blue light irradiation at room temperature (Table 1-3, entry 3).

Table 1-3. Scope of nitriles.[a]

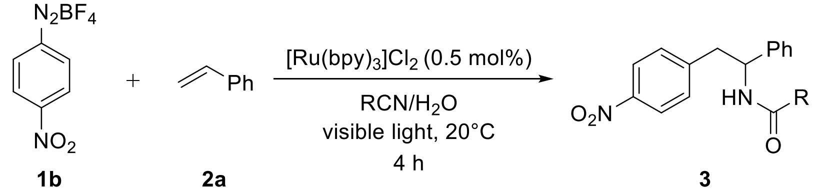

1b **2a** **3**

Entry	Nitrile	Product	Yield (%)[b]
1	CH_3CN	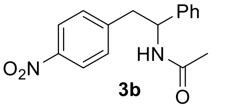 **3b**	92
2	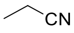	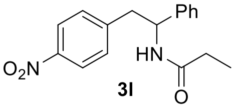 **3l**	84
3	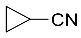	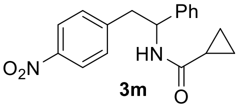 **3m**	65
4	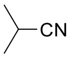	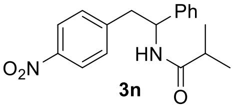 **3n**	71
5	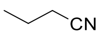	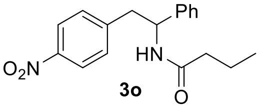 **3o**	80
6	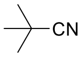	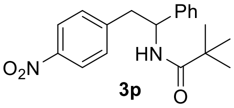 **3p**	72
7	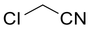	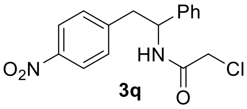 **3q**	60

[a] The reaction was performed with **1b** (0.25 mmol), styrene **2a** (2 eq.), $[Ru(bpy)_3]Cl_2$ (0.005 eq.) and 1 eq. of H_2O in 1.0 mL of nitrile. [b] Isolated yields after purification by flash column chromatography using silica gel.

Table 1-4. Scope of alkenes.[a]

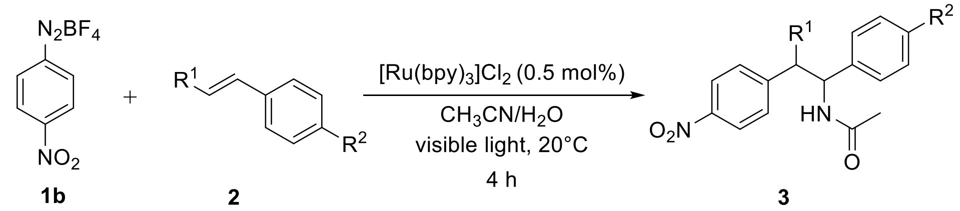

N_2BF_4
NO_2
1b
+
R^1
R^2
2
$[Ru(bpy)_3]Cl_2$ (0.5 mol%)
CH_3CN/H_2O
visible light, 20°C
4 h
R^1
R^2
O_2N
HN
O
3

Entry	R^1	R^2	Product	Yield (%)[b]
1	H	H	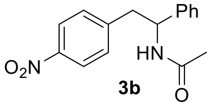 3b	92
2	Ph	H	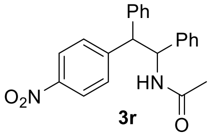 3r	53
3	H	Cl	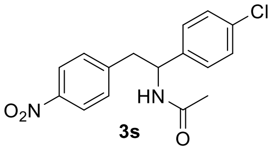 3s	87
4	COOMe	H	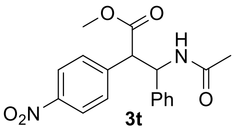 3t	20
5	Me	H	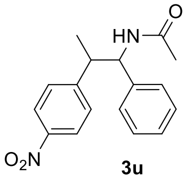 3u	75[c]
6	H	COOH	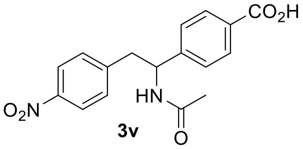 3v	97
7	H	Me	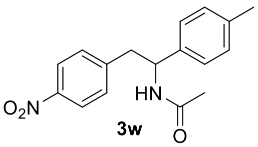 3w	55
8	COMe	H	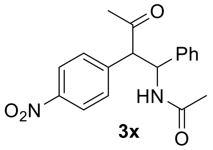 3x	43

[a] The reaction was performed with **1b** (0.25 mmol), alkene **2** (2 eq.), $[Ru(bpy)_3]Cl_2$ (0.005 eq.) and 1 eq. of water in 1.0 mL of CH_3CN. [b] Isolated yields after purification by flash column chromatography using silica gel. [c] dr (65:35).

Having established the scope towards both diazonium salts and nitriles in this photoreaction, we investigated various alkenes. The results are summarized in the Table 1-4. Styrenes with electron withdrawing, neutral and donating substitution at *para* position smoothly give the corresponding products in moderate to excellent yields upon irradiation for 4 h (Table 1-4, entries 1, 3, 6, and 7). In addition, this photoreaction could also be applied to internal alkenes. The reaction of diazonium salt **1b** with trans-*β*-methyl-styrene regioselectively provided the corresponding product **3u** in 75% yield (dr 65:35).[17] Notably, trans-stilbene, cinnamic acid ester, and benzalacetone can be used in this multi-component photoreaction and afford the corresponding products as single regioisomers in moderate yields (Table 1-4, entries 2, 4, and 8).

To further demonstrate the importance of the photoreaction products, we applied to the synthesis of 3-aryl-3,4-dihydroisoquinolines by adopting the previously reported method by Larsen and his co-workers (Scheme 1-2).[37-38] The reaction of diazonium salt **1a** with styrene **2a** under standard photoreaction conditions provided the corresponding product **3a**, which was then further converted into 3-aryl-3,4-dihydroisoquinoline **4** using oxalyl chloride and $FeCl_3$.[37]

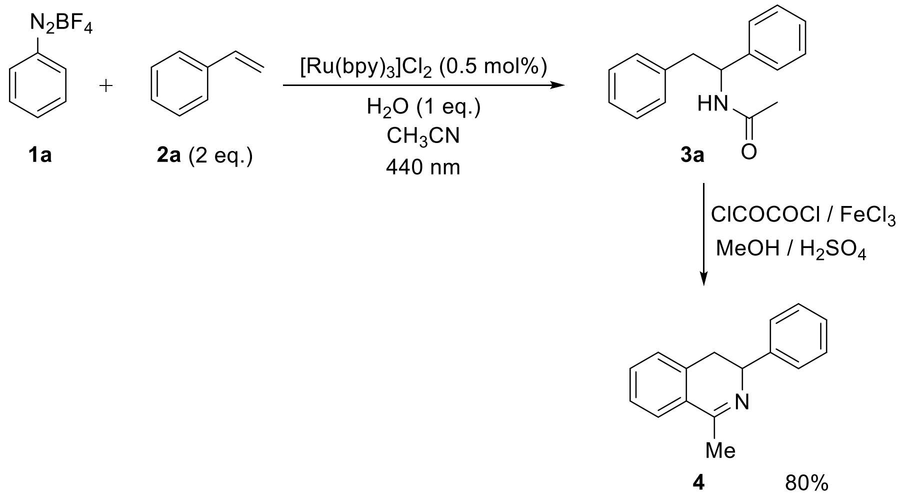

Scheme 1-2. Application of the photoreaction in the synthesis of 3-aryl-3,4-dihydroisoquinoline.

The suggested mechanism of the photoreaction based on trapping of intermediates and related literature reports is depicted in Scheme 1-3.[17-18, 39-48] Aryl radical **5** is formed initially by a single electron transfer from the excited state of the photocatalyst $Ru(bpy)_3^{2+*}$ to diazonium salt **1a**. Addition of aryl radical **5** to alkene **2** yields the corresponding radical intermediate **6**, which is then further oxidized to give carbenium intermediate **7**.[22] Finally, the intermediate **7** is attacked by a nitrile (R^3CN), followed by hydrolysis to give the amino-arylated product **3a**.[17]

Radical intermediate **6** is either oxidized by the strong oxidant Ru(bpy)$_3^{3+}$ to complete the photocatalytic cycle or by the diazonium salt **1a** in a chain transfer mechanism. Radical intermediates **5** and **6** were trapped with TEMPO, which supports radical intermediates during the photoreaction.[20-22] In addition, the carbenium ion intermediate was also trapped with water and methanol, these results indicate the formation of intermediate **7** in the reaction (see Experimental Section).

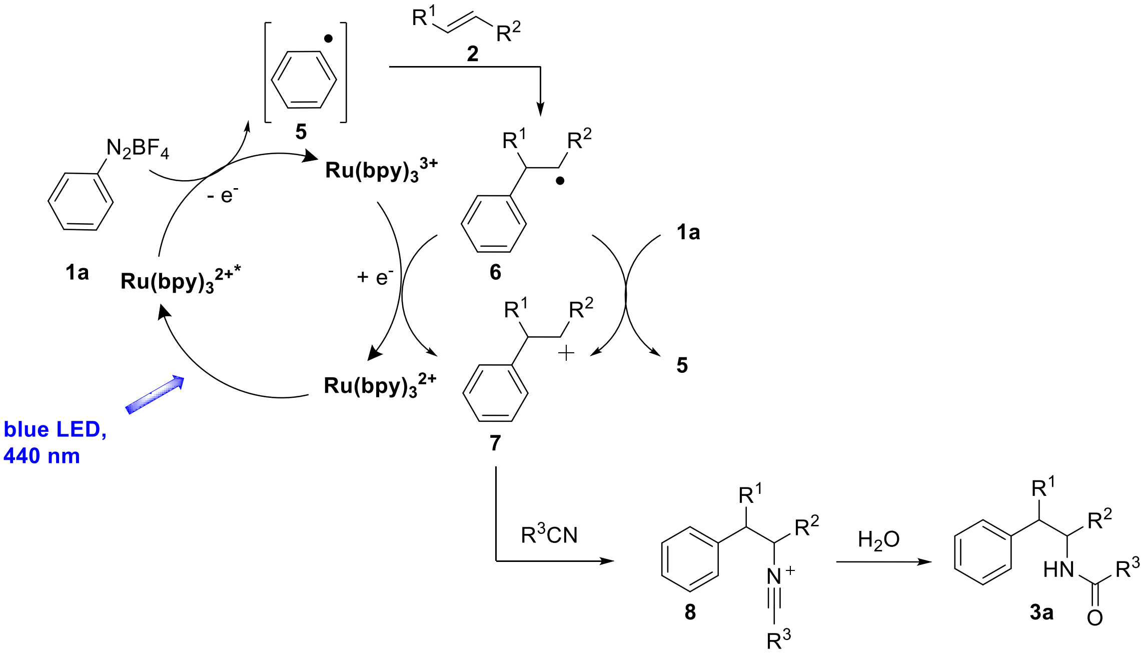

Scheme 1-3. Proposed mechanism for the Photo-Meerwein addition reaction.

1.3. Conclusion

In conclusion, the reported protocol allows the formation of C$_{alkyl}$–N bonds by an intermolecular amino-arylation of alkenes mediated by visible light. It is, to the best of our knowledge, the first example of a photocatalytic Meerwein addition reaction. The multi-component reaction gives efficient access to different types of amides under mild reaction conditions tolerating a broad range of functional groups. The substrate scopes of diazonium salts, nitriles, and alkenes are large. Many products of the photoreaction are not easily accessible by other methods and have due to the presence of halide functional groups the potential for further synthetic elaboration. Exemplarily, one photoreaction product was used for the synthesis of a 3-aryl-3,4-dihydroisoquinoline. Experiments to elucidate the mechanism of the reaction in detail, and applications of the reaction to the synthesis of other potential biologically active molecules are ongoing in our laboratory.

1.4. Experimental Part

1.4.1. General Methods and Material

Proton NMR spectra were recorded on a Bruker Avance 300 MHz spectrometer in $CDCl_3$ and dimethyl sulfoxide-d_6 solutions with internal solvent signal peak at 7.26 ppm and 2.50 ppm respectively. Carbon NMR were recorded at 75 MHz spectrometer in $CDCl_3$ and dimethyl sulfoxide-d_6 solutions and referenced to the internal solvent signal at 77.16 ppm and 39.52 ppm respectively. Proton NMR data are reported as follows: chemical shift (ppm), multiplicity (s = singlet, d = doublet, t = triplet, q = quartet, quint = quintet, dd = doublet of doublets, ddd = doublet of doublet of doublets, td = triplet of doublets, qd = quartet of doublets, m = multiplet, br. s. = broad singlet), and coupling constants (Hz). All reactions were monitored by thin-layer chromatography (TLC) using Merck silica gel plates 60 F254; visualization was accomplished with short wave UV light (254 nm). Standard flash chromatography was performed using silica gel of particle size 40−63 µm. All other commercially available reagents and solvents were used without any further purification.

Irradiation Sources: High Power LEDs of different wavelengths were used for irradiation of the reaction mixtures: Philips LUXEON® Rebel (purple, λ_{max} = 400 ± 10 nm, 1000 mA, 1.2 W), Philips LUXEON® Rebel LXML-TRo1-0225 (blue, λ_{max} = 440 ± 10 nm, 700 mA, 3.0 W) and Philips LUXEON® Rebel (green, λ_{max} = 520 ± 15 nm, 145 lm @700mA, 1.0 W)

1.4.2. General Procedures

Procedure for the preparation of aryl diazonium tetrafluoroborates[49]

The appropriate aniline (10 mmol) was dissolved in a mixture of 3.4 mL of hydrofluoroboric acid (50%) and 4 mL of distilled water. The reaction mixture was cooled to 0 °C using an ice bath, and then sodium nitrite ($NaNO_2$) solution (0.69 g in 1.5 mL water) was added drop wise. The resulting reaction mixture was stirred for 40 min at 0-5 °C and the obtained precipitate was collected by filtration, dried and re-dissolved in a minimum amount of acetone. Diethyl ether was added until precipitation of diazonium tetrafluoroborate, which was filtered, washed several times with small portions of diethyl ether and dried under vacuum.

General procedure for the reaction of arenediazonium tetrafluoroborates with alkenes

In a 5 mL snap vial equipped with magnetic stirring bar the catalyst [Ru(bpy)$_3$]Cl$_2$ (0.005 eq.), arenediazonium tetrafluoroborate **1** (1 eq., 0.25 mmol), alkene **2** (2 eq.), and water (1 eq.) were dissolved in 1 mL of CH$_3$CN, and the resulting reaction mixture was degassed by three "pump-freeze-thaw" cycles *via* a syringe needle. The vial was irradiated through the vial's plane bottom side using 440 nm blue LEDs with cooling device maintaining a temperature around 20 °C. After 4 h of irradiation, the reaction mixture was transferred to a separating funnel, diluted with dichloromethane and washed with 15 mL of water. The aqueous layer was washed three times (3 x 15 mL) with dichloromethane. The combined organic phases were dried over Na$_2$SO$_4$, filtered and concentrated in vacuum. Purification of the crude product was achieved by flash column chromatography using petrol ether/ethyl acetate (1:3 to 1:1) as eluent.

N-(1,2-Diphenylethyl)acetamide (3a)[37]

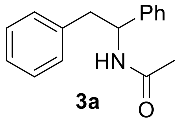

3a

^{1}H NMR (300 MHz, CDCl$_3$): δ ppm 7.48 – 7.12 (m, 8H), 7.13 – 6.92 (m, 2H), 5.81 (s, 1H), 5.28 (q, *J* = 7.3 Hz, 1H), 3.11 (d, *J* = 7.1 Hz, 2H), 1.93 (s, 3H).

^{13}C NMR (75 MHz, CDCl$_3$): δ ppm 169.4, 141.6, 137.4, 129.4, 128.7, 128.5, 127.5, 126.8, 126.7, 54.5, 42.6, 23.5.

HR-MS (ESI): [M+H]$^+$ calculated for C$_{16}$H$_{18}$NO: 241.1416 found: 241.1416

Mp: 150-152 °C

N-(2-(4-Nitrophenyl)-1-phenylethyl)acetamide (3b)

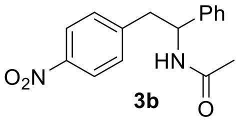

3b

^{1}H NMR (300 MHz, CDCl$_3$): δ ppm 8.06 (d, *J* = 8.7 Hz, 2H), 7.37 – 7.24 (m, 3H), 7.24 – 7.14 (m, 4H), 5.83 (d, *J* = 7.5 Hz, 1H), 5.25 (dd, *J* = 14.5, 7.8 Hz, 1H), 3.34 (dd, *J* = 13.5, 6.5 Hz, 1H), 3.16 (dd, *J* = 13.5, 8.1 Hz, 1H), 1.97 (s, 3H).

^{13}C NMR (75 MHz, CDCl$_3$):δ ppm 169.4, 146.7, 145.4, 140.2, 130.2, 129.0, 128.1, 126.8, 123.5, 54.7, 42.2, 23.4.

HR-MS (ESI): [M+H]$^+$ calculated for C$_{16}$H$_{17}$N$_2$O$_3$: 285.1234, found: 285.1234

Mp: 158-160 °C

N-(2-(4-Methoxyphenyl)-1-phenylethyl)acetamide (3c)

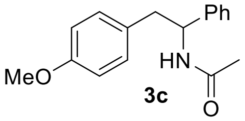

3c

^{1}H NMR (300 MHz, $CDCl_3$): δ ppm 7.35 – 7.23 (m, 3H), 7.22 – 7.16 (m, 2H), 6.94 (d, *J* = 8.7 Hz, 2H), 6.76 (d, *J* = 8.7 Hz, 2H), 5.83 (s, 1H), 5.22 (q, *J* = 7.2 Hz, 1H), 3.76 (s, 3H), 3.04 (d, *J* = 7.0 Hz, 2H), 1.93 (s, 3H).

^{13}C NMR (75 MHz, $CDCl_3$):δ ppm 169.4, 158.3, 141.7, 130.4, 129.3, 128.6, 127.5, 126.8, 113.8, 55.3, 54.6, 41.7, 23.5.

HR-MS (ESI): [M+H]$^+$ calculated for $C_{17}H_{20}NO_2$ 270.1489, found: 270.1490

Mp: 143-146 °C

Ethyl 4-(2-acetamido-2-phenylethyl)benzoate (3d)

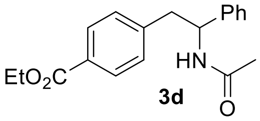

3d

^{1}H NMR (300 MHz, $CDCl_3$): δ ppm 7.89 (d, *J* = 8.3 Hz, 2H), 7.35 – 7.24 (m, 3H), 7.21 – 7.15 (m, 2H), 7.11 (d, *J* = 8.3 Hz, 2H), 5.81 (d, *J* = 7.1 Hz, 1H), 5.27 (q, *J* = 7.5 Hz, 1H), 4.34 (q, *J* = 7.1 Hz, 2H), 3.17 (qd, *J* = 13.6, 7.2 Hz, 2H), 1.94 (s, 3H), 1.37 (t, *J* = 7.1 Hz, 3H).

^{13}C NMR (75 MHz, $CDCl_3$): δ ppm 169.4, 166.7, 142.8, 140.9, 129.7, 129.4, 128.9, 128.8, 127.8, 126.8, 61.0, 54.6, 42.5, 23.5, 14.7.

HR-MS (ESI): [M+H]$^+$ calculated for $C_{19}H_{22}NO_3$: 312.1594, found: 312.1597

Mp: 144-146 °C

N-(2-(4-Bromophenyl)-1-phenylethyl)acetamide (3e)

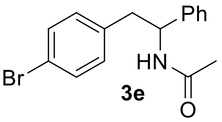

3e

^{1}H NMR (300 MHz, $CDCl_3$): δ ppm 7.36 – 7.24 (m, 5H), 7.22 – 7.13 (m, 2H), 6.90 (d, *J* = 8.3 Hz, 2H), 5.78 (d, *J* = 7.7 Hz, 1H), 5.22 (dd, *J* = 14.8, 7.5 Hz, 1H), 3.20 – 2.85 (m, 2H), 1.95 (s, 3H).

^{13}C NMR (75 MHz, $CDCl_3$):δ ppm 169.4, 140.9, 136.5, 131.5, 131.2, 128.8, 127.8, 126.8, 120.6, 54.6, 41.9, 23.6.

HR-MS (ESI): [M+H]$^+$ calculated for $C_{16}H_{17}BrNO$: 318.0488, found: 318.0488

Mp: 187-189 °C

N-(1-Phenyl-2-(p-tolyl)ethyl)acetamide (3f)

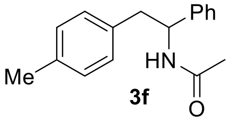

3f

^{1}H NMR (300 MHz, $CDCl_3$): δ ppm 7.34 – 7.19 (m, 5H), 7.03 (d, *J* = 7.8 Hz, 2H), 6.93 (d, *J* = 8.0 Hz, 2H), 5.89 (d, *J* = 7.7 Hz, 1H), 5.25 (q, *J* = 7.3 Hz, 1H), 3.06 (d, *J* = 7.1 Hz, 2H), 2.29 (s, 3H), 1.92 (s, 3H).

^{13}C NMR (75 MHz, $CDCl_3$):δ ppm 169.4, 141.8, 136.2, 134.2, 129.3, 129.1, 128.6, 127.4, 126.7, 54.5, 42.2, 23.5, 21.1.

HR-MS (ESI): $[M+H]^+$ calculated for $C_{17}H_{19}NO$: 254.1539, found: 254.1542

Mp: 134-136 °C

N-(1-Phenyl-2-(4-(trifluoromethyl)phenyl)ethyl)acetamide (3g)

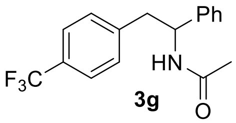

3g

^{1}H NMR (300 MHz, $CDCl_3$): δ ppm 7.46 (d, *J* = 8.1 Hz, 2H), 7.37 – 7.24 (m, 3H), 7.24 – 7.11 (m, 4H), 5.83 (d, *J* = 7.8 Hz, 1H), 5.27 (q, *J* = 7.5 Hz, 1H), 3.24 (dd, *J* = 13.6, 6.8 Hz, 1H), 3.13 (dd, *J* = 13.6, 7.7 Hz, 1H), 1.95 (s, 3H).

^{13}C NMR (75 MHz, $CDCl_3$): δ ppm 169.4, 141.7, 140.8, 129.7, 128.9, 127.9, 126.8, 125.3 (q, *J* = 3.6 Hz), 54.6, 42.3, 23.5.

HR-MS (ESI): $[M+H]^+$ calculated for $C_{17}H_{17}F_3NO$: 308.1257, found: 308.1259

Mp: 177-179 °C

N-(2-(2-Nitrophenyl)-1-phenylethyl)acetamide (3h)

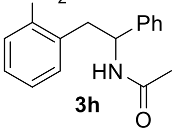

3h

^{1}H NMR (300 MHz, $CDCl_3$): δ ppm 7.86 (dd, *J* = 8.1, 1.1 Hz, 1H), 7.54 (td, *J* = 7.6, 1.2 Hz, 1H), 7.47 – 7.26 (m, 7H), 6.38 (d, *J* = 8.2 Hz, 1H), 5.35 (ddd, *J* = 10.0, 8.5, 5.5 Hz, 1H), 3.43 (dd, *J* = 13.9, 10.2 Hz, 1H), 3.30 (dd, *J* = 13.9, 5.4 Hz, 1H), 1.84 (s, 3H).

^{13}C NMR (75 MHz, CDCl$_3$):δ ppm 169.5, 150.1, 141.6, 133.3, 133.0, 132.5, 128.9, 128.0, 127.9, 126.5, 124.8, 54.6, 38.6, 23.4.

HR-MS (ESI): [M+H]$^+$ calculated for C$_{16}$H$_{17}$N$_2$O$_3$: 285.1234, found: 285.1236

Mp: 170-172 °C

N-(1-Phenyl-2-(2,4,5-trichlorophenyl)ethyl)acetamide (3i)

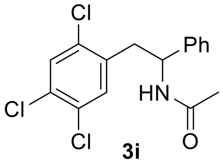

3i

^{1}H NMR (300 MHz, CDCl$_3$): δ ppm 7.44 (s, 1H), 7.39 – 7.23 (m, 6H), 5.89 (d, *J* = 8.0 Hz, 1H), 5.30 (dd, *J* = 15.0, 8.2 Hz, 1H), 3.26 – 3.09 (m, 2H), 1.94 (s, 3H).

^{13}C NMR (75 MHz, CDCl$_3$):δ ppm 169.4, 140.9, 135.9, 133.1, 132.5, 131.6, 131.1, 130.8, 129.0, 128.1, 126.6, 53.7, 39.2, 23.5.

HR-MS (ESI): [M+H]$^+$ calculated for C$_{16}$H$_{15}$Cl$_3$NO: 342.0214, found: 342.0218

Mp: 170-172 °C

Methyl 3-(2-acetamido-2-phenylethyl)thiophene-2-carboxylate (3j)

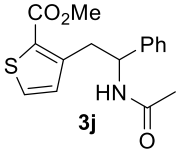

3j

^{1}H NMR (300 MHz, CDCl$_3$): δ ppm 7.44 (d, *J* = 5.1 Hz, 1H), 7.41 – 7.29 (m, 5H), 6.98 (m, 2H), 5.34 – 5.02 (m, 1H), 3.91 (s, 3H), 3.64 (dd, *J* = 13.7, 11.0 Hz, 1H), 3.19 (dd, *J* = 13.7, 4.3 Hz, 1H), 1.85 (s, 3H).

^{13}C NMR (75 MHz, CDCl$_3$): δ ppm 169.5, 164.5, 147.1, 142.7, 131.3, 131.2, 128.7, 127.5, 126.4, 55.3, 52.4, 35.9, 23.4.

HR-MS (ESI): [M+H]$^+$ calculated for C$_{16}$H$_{15}$NO$_3$S: 304.1002, found: 304.1003

Mp: 199-201 °C

N-(2-(3-Nitrophenyl)-1-phenylethyl)acetamide (3k)

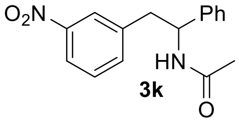

^{1}H NMR (300 MHz, CDCl$_3$): δ ppm 8.03 (dt, J = 7.4, 2.1 Hz, 1H), 7.89 (d, J = 1.8 Hz, 1H), 7.45 – 7.37 (m, 2H), 7.37 – 7.24 (m, 3H), 7.23 – 7.14 (m, 2H), 5.95 (d, J = 7.6 Hz, 1H), 5.25 (q, J = 7.6 Hz, 1H), 3.30 (dd, J = 13.6, 7.0 Hz, 1H), 3.16 (dd, J = 13.6, 7.6 Hz, 1H), 1.95 (s, 3H).

^{13}C NMR (75 MHz, CDCl$_3$): δ ppm 169.5, 148.2, 140.4, 139.8, 135.6, 129.3, 129.0, 128.2, 126.8, 124.4, 121.8, 54.8, 42.1, 23.5.

HR-MS (ESI): $[M+H]^+$ calculated for $C_{16}H_{17}N_2O_3$: 285.1234, found: 285.1236

Mp: 172-174 °C

N-(2-(4-Nitrophenyl)-1-phenylethyl)propionamide (3l)

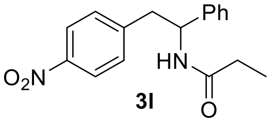

^{1}H NMR (300 MHz, CDCl$_3$): δ ppm 8.05 (d, J = 8.7 Hz, 2H), 7.38 – 7.23 (m, 3H), 7.24 – 7.12 (m, 4H), 5.88 (d, J = 7.6 Hz, 1H), 5.25 (dd, J = 14.6, 7.7 Hz, 1H), 3.33 (dd, J = 13.5, 6.6 Hz, 1H), 3.16 (dd, J = 13.5, 8.0 Hz, 1H), 2.18 (q, J = 7.6 Hz, 2H), 1.10 (t, J = 7.6 Hz, 3H).

^{13}C NMR (75 MHz, CDCl$_3$): δ ppm 173.2, 146.9, 145.6, 140.4, 130.3, 129.0, 128.1, 126.8, 123.6, 54.6, 42.4, 29.8, 9.8.

HR-MS (ESI): $[M+H]^+$ calculated for $C_{17}H_{19}N_2O_3$: 299.1390, found: 299.1391

Mp: 163-165 °C

N-(2-(4-Nitrophenyl)-1-phenylethyl)cyclopropanecarboxamide (3m)

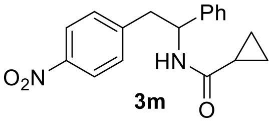

^{1}H NMR (300 MHz, CDCl$_3$): δ ppm 8.05 (d, J = 8.7 Hz, 2H), 7.36 – 7.27 (m, 3H), 7.24 – 7.14 (m, 4H), 5.98 (s, 1H), 5.23 (dd, J = 14.2, 7.9 Hz, 1H), 3.37 (dd, J = 13.4, 6.2 Hz, 1H), 3.16 (dd, J = 13.4, 8.3 Hz, 1H), 1.41 – 1.27 (m, 1H), 0.98 – 0.85 (m, 2H), 0.84 – 0.57 (m, 2H).

^{13}C NMR (75 MHz, CDCl$_3$): δ ppm 173.1, 146.8, 145.6, 140.3, 130.3, 129.0, 128.2, 126.9, 123.6, 55.1, 42.5, 14.9, 7.6, 7.5.

HR-MS (ESI): [M+H]$^+$ calculated for $C_{18}H_{19}N_2O_3$: 310.1317, found: 310.1315

Mp: 180-182 °C

N-(2-(4-Nitrophenyl)-1-phenylethyl)isobutyramide (3n)

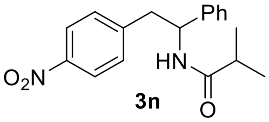

3n

^{1}H NMR (300 MHz, CDCl$_3$): δ ppm 8.06 (d, *J* = 8.8 Hz, 2H), 7.37 – 7.27 (m, 3H), 7.24 – 7.15 (m, 4H), 5.78 (d, *J* = 7.1 Hz, 1H), 5.25 (dd, *J* = 14.6, 7.6 Hz, 1H), 3.32 (dd, *J* = 13.5, 6.7 Hz, 1H), 3.18 (dd, *J* = 13.5, 7.8 Hz, 1H), 2.42 – 2.13 (m, 1H), 1.10 (t, *J* = 2.0 Hz, 3H), 1.08 (t, *J* = 3.5 Hz, 3H).

^{13}C NMR (75 MHz, CDCl$_3$): δ ppm 176.4, 146.8, 145.6, 140.4, 130.3, 129.0, 128.1, 126.8, 123.6, 54.4, 42.4, 35.8, 19.8, 19.5.

HR-MS (ESI): [M+H]$^+$ calculated for $C_{18}H_{21}N_2O_3$: 313.1547, found: 313.1550

Mp: 178-180 °C

N-(2-(4-nitrophenyl)-1-phenylethyl)butyramide (3o)

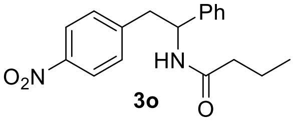

3o

^{1}H NMR (300 MHz, CDCl$_3$): δ ppm 8.05 (d, *J* = 11.0 Hz, 2H), 7.36 – 7.26 (m, 3H), 7.24 – 7.13 (m, 4H), 5.81 (d, *J* = 7.5 Hz, 1H), 5.27 (dd, *J* = 14.7, 7.7 Hz, 1H), 3.33 (dd, *J* = 13.5, 6.7 Hz, 1H), 3.16 (dd, *J* = 13.5, 7.9 Hz, 1H), 2.13 (t, *J* = 7.4 Hz, 2H), 1.61 (td, *J* = 14.4, 7.0 Hz, 2H), 0.87 (t, *J* = 7.4 Hz, 3H).

^{13}C NMR (75 MHz, CDCl$_3$): δ ppm 172.4, 146.8, 145.6, 140.4, 130.3, 128.9, 128.1, 126.7, 123.6, 54.6, 42.4, 38.8, 19.2, 13.8.

HR-MS (ESI): [M+H]$^+$ calculated for $C_{18}H_{21}N_2O_3$: 312.1474, found: 312.1475

Mp: 162-164 °C

N-(2-(4-nitrophenyl)-1-phenylethyl)pivalamide (3p)

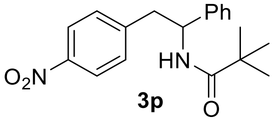

3p

^{1}H NMR (300 MHz, CDCl$_3$): δ ppm δ 8.07 (d, *J* = 8.7 Hz, 2H), 7.37 – 7.26 (m, 3H), 7.25 – 7.12 (m, 4H), 5.91 (d, *J* = 7.4 Hz, 1H), 5.24 (q, *J* = 7.4 Hz, 1H), 3.30 (dd, *J* = 13.5, 6.7 Hz, 1H), 3.18 (dd, *J* = 13.5, 7.7 Hz, 1H), 1.14 (s, 9H)

^{13}C NMR (75 MHz, CDCl$_3$): δ ppm 177.9, 146.9, 145.6, 140.5, 130.3, 129.1, 128.1, 126.7, 123.6, 54.4, 42.4, 38.9, 27.6.

HR-MS (ESI): [M+H]$^+$ calculated for $C_{19}H_{23}N_2O_3$: 327.1703, found: 327.1709

Mp: 163-165 °C

2-Chloro-*N*-(2-(4-nitrophenyl)-1-phenylethyl)acetamide (3q)

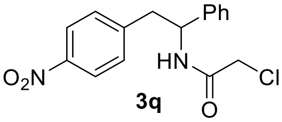

3q

^{1}H NMR (300 MHz, CDCl$_3$): δ ppm 8.08 (d, *J* = 8.7 Hz, 2H), 7.40 – 7.27 (m, 3H), 7.25 – 7.13 (m, 4H), 6.92 (d, *J* = 7.9 Hz, 1H), 5.26 (dd, *J* = 15.1, 7.5 Hz, 1H), 4.02 (s, 2H), 3.33 (dd, *J* = 13.5, 6.9 Hz, 1H), 3.22 (dd, *J* = 13.5, 7.6 Hz, 1H).

^{13}C NMR (75 MHz, CDCl$_3$): δ ppm 165.3, 147.0, 144.8, 139.5, 130.3, 129.2, 128.4, 126.7, 123.7, 54.9, 42.7, 42.4.

HR-MS (ESI): [M+H]$^+$ calculated for $C_{16}H_{16}ClN_2O_3$: 319.0844, found: 319.0848

Mp: 158-160 °C

N-(2-(4-Nitrophenyl)-1,2-diphenylethyl)acetamide (3r)

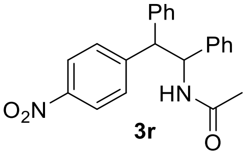

3r

^{1}H NMR (300 MHz, CDCl$_3$): δ ppm 8.16 (d, *J* = 8.8 Hz, 2H), 7.53 (d, *J* = 8.7 Hz, 2H), 7.25 – 6.99 (m, 10H), 6.04 – 5.84 (m, 1H), 5.77 (d, *J* = 9.4 Hz, 1H), 4.44 (d, *J* = 10.9 Hz, 1H), 1.80 (s, 3H).

^{13}C NMR (75 MHz, CDCl$_3$): δ ppm 169.1, 149.3, 146.9, 140.3, 139.9, 129.4, 128.8, 128.7, 128.4, 127.7, 127.3, 127.2, 123.9, 57.6, 55.6, 23.4.

HR-MS (ESI): [M+H]$^+$ calculated for $C_{22}H_{21}N_2O_3$: 361.1547, found: 361.1551

Mp: 210-212 °C

*N-(*1-(4-Chlorophenyl)-2-(4-nitrophenyl)ethyl)acetamide (3s)

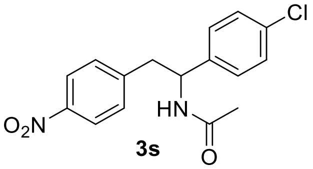
3s

^{1}H NMR (300 MHz, CDCl$_3$): δ ppm 8.07 (d, *J* = 8.8 Hz, 2H), 7.27 (d, *J* = 8.4 Hz, 2H), 7.20 (d, *J* = 8.7 Hz, 2H), 7.12 (d, *J* = 8.4 Hz, 2H), 5.96 (d, *J* = 7.8 Hz, 1H), 5.23 (q, *J* = 7.6 Hz, 1H), 3.28 (dd, *J* = 13.6, 6.9 Hz, 1H), 3.12 (dd, *J* = 13.6, 7.9 Hz, 1H), 1.95 (s, 3H).

^{13}C NMR (75 MHz, CDCl$_3$): δ ppm 169.5, 146.9, 145.1, 139.0, 133.9, 130.2, 129.1, 128.2, 123.7, 54.1, 42.1, 23.4.

HR-MS (ESI): [M+H]$^+$ calculated for $C_{16}H_{16}ClN_2O_3$: 319.0844, found: 319.0848

Mp: 190-192 °C

Methyl 3-acetamido-2-(4-nitrophenyl)-3-phenylpropanoate (3t)

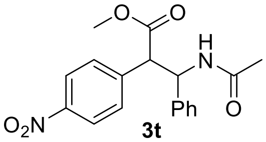
3t

^{1}H NMR (300 MHz, CDCl$_3$): δ ppm 8.18 (d, *J* = 8.8 Hz, 2H), 7.56 (d, *J* = 8.8 Hz, 2H), 7.41 – 7.27 (m, 5H), 5.88 (d, *J* = 9.4 Hz, 1H), 5.77 (t, *J* = 9.7 Hz, 1H), 4.25 (d, *J* = 9.9 Hz, 1H), 3.52 (s, 3H), 1.76 (s, 3H).

^{13}C NMR (75 MHz, CDCl$_3$): δ ppm 170.8, 169.1, 147.8, 142.6, 139.1, 130.1, 129.0, 128.5, 127.4, 123.8, 57.2, 55.0, 52.6, 23.3.

HR-MS (ESI): [M+H]$^+$ calculated for $C_{18}H_{19}N_2O_5$: 343.1288, found: 343.1291

Mp: 191-193 °C

N-(2-(4-nitrophenyl)-1-phenylpropyl)acetamide (3u)

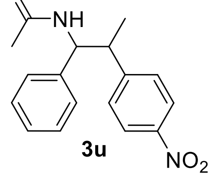
3u

Major Isomer: ^{1}H NMR (300 MHz, CDCl$_3$): δ ppm 8.15 (d, *J* = 8.8 Hz, 2H), 7.42 – 7.28 (m, 5H), 7.25 – 7.17 (m, 2H), 5.66 (d, *J* = 9.1 Hz, 1H), 5.24 (t, *J* = 9.0 Hz, 1H), 3.29 (dq, *J* = 14.0, 7.0 Hz, 1H), 1.78 (s, 3H), 1.18 (d, *J* = 7.0 Hz, 3H).

^{13}C NMR (75 MHz, CDCl$_3$): δ ppm 169.0, 151.1, 147.0, 140.3, 128.9, 128.8, 128.0, 127.2, 123.8, 58.1, 45.7, 23.4, 19.2.

HR-MS (ESI): [M+H]$^+$ calculated for $C_{17}H_{19}N_2O_3$: 298.1301, found: 298.1302

Mp: 195-196 °C

Minor Isomer: ^{1}H NMR (300 MHz, CDCl$_3$): δ ppm 8.03 (d, *J* = 8.8 Hz, 2H), 7.24 – 7.12 (m, 5H), 7.05 – 6.91 (m, 2H), 5.85 (d, *J* = 8.7 Hz, 1H), 5.23 (t, *J* = 8.8 Hz, 1H), 3.47 – 3.10 (dq, *J* = 14.1, 7.0 Hz, 1H), 2.02 (s, 3H), 1.39 (d, *J* = 7.0 Hz, 3H).

^{13}C NMR (75 MHz, CDCl$_3$): δ ppm 169.6, 150.8, 146.7, 139.6, 129.1, 128.7, 127.9, 127.3, 123.5, 58.6, 45.5, 23.6, 18.4.

4-(1-Acetamido-2-(4-nitrophenyl)ethyl)benzoic acid (3v)

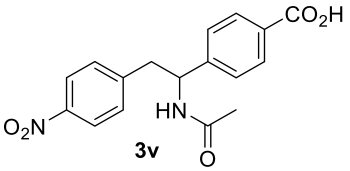

3v

^{1}H NMR (300 MHz, DMSO-*d*$_6$): δ ppm 12.91 (s, 1H), 8.51 (d, *J* = 8.7 Hz, 1H), 8.14 (d, *J* = 8.7 Hz, 2H), 7.90 (d, *J* = 8.3 Hz, 2H), 7.51 (dd, *J* = 13.5, 8.5 Hz, 4H), 5.17 (td, *J* = 9.1, 6.0 Hz, 1H), 3.11 (qd, *J* = 13.6, 7.8 Hz, 2H), 1.76 (s, 3H).

^{13}C NMR (75 MHz, DMSO-*d*$_6$): δ ppm 168.6, 167.1, 147.8 146.8, 146.2, 130.5, 129.5, 129.4, 126.8, 123.2, 53.4, 41.9, 22.5.

HR-MS (ESI): [M+H]$^+$ calculated for $C_{17}H_{17}N_2O_5$: 329.1132, found: 329.1136

Mp: 248-250 °C

N-(2-(4-nitrophenyl)-1-(*p*-tolyl)ethyl)acetamide (3w)

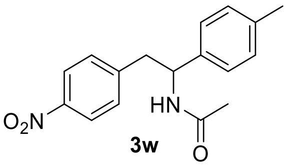

3w

^{1}H NMR (300 MHz, CDCl$_3$): δ ppm 8.01 (d, *J* = 8.8 Hz, 2H), 7.16 (d, *J* = 8.7 Hz, 2H), 7.12 – 6.98 (m, 4H), 5.75 (d, *J* = 7.7 Hz, 1 H), 5.15 (dd, *J* = 14.3, 8.0 Hz, 1H), 3.29 (dd, *J* = 13.5, 6.3 Hz, 1H), 3.09 (dd, *J* = 13.5, 8.2 Hz, 1H), 2.28 (s, 3H), 1.91 (s, 3H).

^{13}C NMR (75 MHz, $CDCl_3$): δ ppm 169.4, 146.8, 145.7, 138.0, 137.2, 130.3, 129.7, 126.8, 123.6, 54.6, 42.4, 23.5, 21.2.

ESI-MS: [$M+H^+$]: Calculated: 299.1390, found: 299.1391

Mp: 197-199 °C

N-(2-(4-Nitrophenyl)-3-oxo-1-phenylbutyl)acetamide (3x)

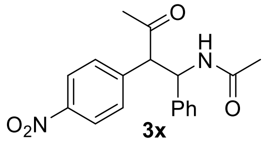

3x

^{1}H NMR (300 MHz, $CDCl_3$): δ ppm 8.16 (d, *J* = 8.8 Hz, 2H), 7.42 (d, *J* = 8.7 Hz, 2H), 7.34 – 7.16 (m, 5H), 7.03 (d, *J* = 9.2 Hz, 1H), 5.51 (dd, *J* = 9.2, 6.0 Hz, 1H), 4.55 (d, *J* = 6.0 Hz, 1H), 2.05 (s, 3H), 1.95 (s, 3H).

^{13}C NMR (75 MHz, $CDCl_3$): δ ppm 208.0, 169.6, 147.6, 142.5, 139.6, 129.7, 128.9, 127.9, 126.8, 124.2, 62.3, 55.8, 31.1, 23.5.

Mp: 84-86 °C

1.4.3. Reaction Optimization

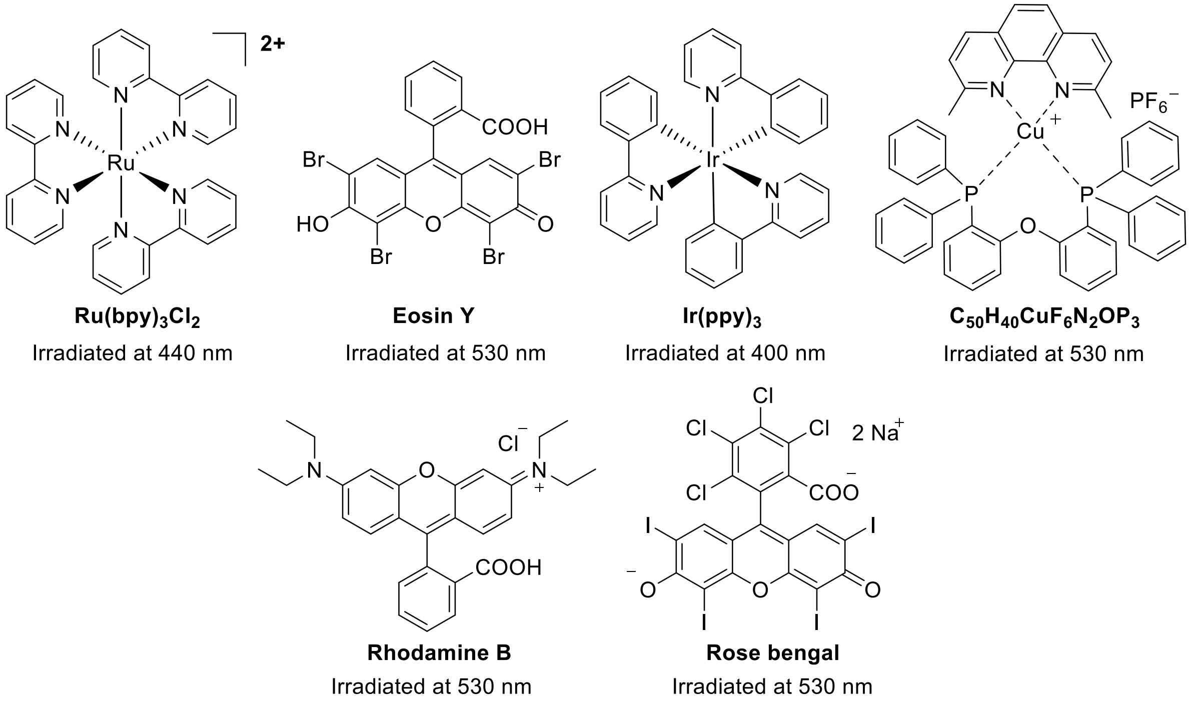

Ru(bpy)$_3$Cl$_2$
Irradiated at 440 nm

Eosin Y
Irradiated at 530 nm

Ir(ppy)$_3$
Irradiated at 400 nm

$C_{50}H_{40}CuF_6N_2OP_3$
Irradiated at 530 nm

Rhodamine B
Irradiated at 530 nm

Rose bengal
Irradiated at 530 nm

Figure 1-1. Structures of the employed photocatalyst described in Table 1-1.

Table 1-5. Screening with Copper catalyst and solvent screening.[a]

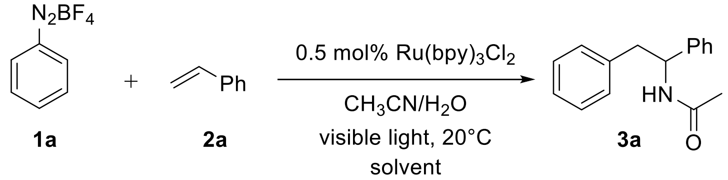
N2BF4
1a
+
Ph
2a
0.5 mol% Ru(bpy)3Cl2
CH3CN/H2O
visible light, 20°C
solvent
Ph
HN
O
3a

Entry	Conditions	Yield (%)[b]
1	20 mol% Cu powder, no photocatalyst, no light, 1.0 mL CH_3CN	0
2	20 mol% CuCl, no photocatalyst, no light, 1.0 mL CH_3CN	0
3	20 mol% $CuCl_2$, no photocatalyst, no light, 1.0 mL CH_3CN	0
4	$[Ru(bpy)_3]Cl_2$ (0.5 mol%), 10 eq. of CH_3CN, DMSO (0.850 mL), 440 nm	0[c]
5	$[Ru(bpy)_3]Cl_2$ (0.5 mol%), 20 eq. of CH_3CN, DMSO (0.700 mL), 440 nm	0[c]
6	$[Ru(bpy)_3]Cl_2$ (0.5 mol%), 30 eq. of CH_3CN, DMSO (0.550 mL), 440 nm	0[c]
7	$[Ru(bpy)_3]Cl_2$ (0.5 mol%), 10 eq. of CH_3CN, DCM (0.850 mL), 440 nm	68
8	$[Ru(bpy)_3]Cl_2$ (0.5 mol%), 20 eq. of CH_3CN, DCM (0.700 mL), 440 nm	77
9	$[Ru(bpy)_3]Cl_2$ (0.5 mol%). 30 eq. of CH_3CN, DCM (0.550 mL), 440 nm	82

[a] The reaction was performed with **1a** (0.25 mmol), styrene **2a** (2 eq.), and 1 eq. of water. [b] GC yield determined by using a calibrated internal standard. [c] Obtained more than 80% of stilbene.

Synthesis of 3-aryl-3,4-dihydroisoquinoline[37]

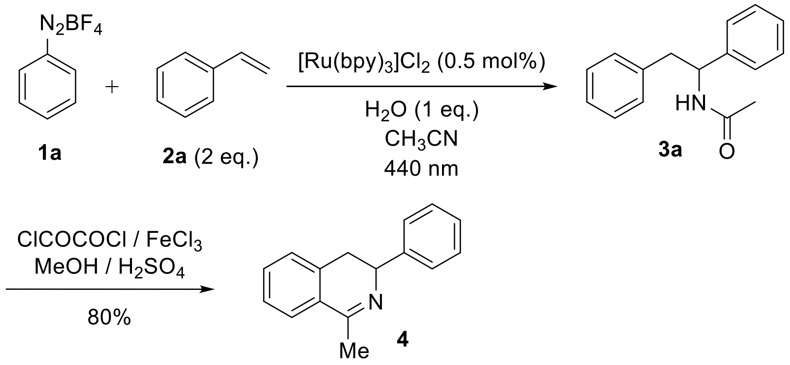
N2BF4
1a
+
2a (2 eq.)
[Ru(bpy)3]Cl2 (0.5 mol%)
H2O (1 eq.)
CH3CN
440 nm
HN
O
3a
ClCOCOCl / FeCl3
MeOH / H2SO4
80%
N
Me
4

Scheme 1-4. Synthesis of 3-aryl-3,4-dihydroisoquinoline (**4**).

1-Methyl-3-phenyl-3,4-dihydroisoquinoline (4)[37]

^{1}H NMR (400 MHz, $CDCl_3$): δ ppm 7.57 (dd, *J* = 7.5, 1.2 Hz, 1H), 7.51 – 7.43 (m, 2H), 7.43 – 7.31 (m, 4H), 7.32 – 7.24 (m, 1H), 7.20 (d, *J* = 7.2 Hz, 1H), 4.57 (ddd, *J* = 13.8, 5.3, 2.2 Hz, 1H), 3.02 – 2.78 (m, 2H), 2.51 (d, *J* = 2.2 Hz, 3H).

1.4.4. Radical Capturing Experiments

Experimental procedure for capturing intermediate radicals with TEMPO[21-22]

For aryl radical (5): In a 5 mL snap vial equipped with magnetic stirring bar the catalyst $[Ru(bpy)_3]Cl_2$ (0.2 eq.), aryl diazonium tetrafluoroborate **1a** (0.25 mmol, 1 eq.) and TEMPO (2 eq.) were dissolved in CH_3CN containing 1 eq. of water and the resulting mixture was degassed by three "pump-freeze-thaw" cycles via a syringe needle. The vial was irradiated through the vial's plane bottom side using 440 nm LEDs. After 4 h of irradiation, a TEMPO trapped compound **9** was detected by mass spectra.

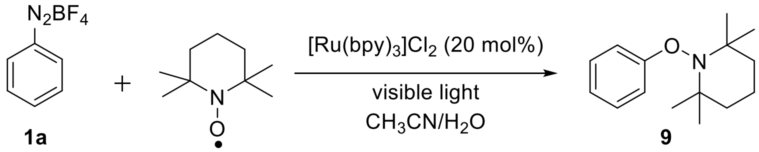

MS (CI): [MH$^+$]: 234.2

For radical 6: In a 5 mL snap vial equipped with magnetic stirring bar the catalyst $[Ru(bpy)_3]Cl_2$ (0.2 eq.), aryl diazonium tetrafluoroborate **1a** (0.25 mmol, 1 eq.), styrene **2a** (2 eq.) and TEMPO (2 eq.) were dissolved in CH_3CN containing 1 eq. of water and the resulting mixture was degassed by three "pump-freeze-thaw" cycles via a syringe needle. The vial was irradiated through the vial's plane bottom side using 440 nm LEDs. After 4 h of irradiation, a TEMPO trapped compound **10** was detected by mass spectra.

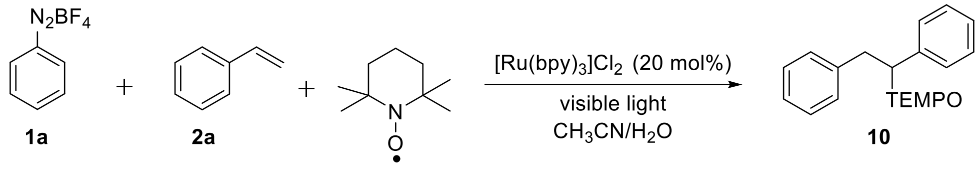

MS (ESI): [MH$^+$]: 338.2

1.4.5. Carbenium Ion Trapping Experiments

Water as the nucleophile: In a 5 mL snap vial equipped with magnetic stirring bar the catalyst [Ru(bpy)$_3$]Cl$_2$ (0.005 eq.), arenediazonium tetrafluoroborate (1 eq., 0.25 mmol), alkene (2 eq.), and water (20 eq.) were dissolved in 1 mL CH$_3$CN, and the resulting reaction mixture was degassed by three “pump-freeze-thaw” cycles via a syringe needle. The vial was irradiated through the vial’s plane bottom side using 440 nm blue LEDs. After 4 h of irradiation, the reaction mixture was transferred to a separating funnel, diluted with dichloromethane and washed with 15 mL of water. The aqueous layer was washed three times (3x 15 mL) with dichloromethane. The combined organic phases were dried over Na$_2$SO$_4$, filtered and concentrated in vacuum.

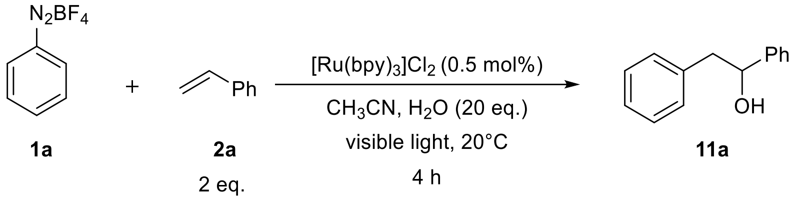

1,2-Diphenylethanol (11a)

^{1}H NMR (300 MHz, CDCl$_3$): δ ppm 7.46 – 7.12 (m, 10H), 4.91 (dd, *J* = 8.3, 5.1 Hz, 1H), 3.15 – 2.81 (m, 2H), 1.89 (s, 1H).

^{13}C NMR (75 MHz, CDCl$_3$): δ ppm 143.9, 138.7, 129.6, 128.7, 128.6, 127.8, 126.8, 126.0, 75.5, 46.2.

Methanol as the nucleophile: In a 5 mL snap vial equipped with magnetic stirring bar the catalyst [Ru(bpy)$_3$]Cl$_2$ (0.005 eq.), arenediazonium tetrafluoroborate (1 eq., 0.25 mmol), alkene (2 eq.), were dissolved in 1 mL CH$_3$OH, and the resulting reaction mixture was degassed by three “pump-freeze-thaw” cycles via a syringe needle. The vial was irradiated through the vial’s plane bottom side using 440 nm blue LEDs. After 4 h of irradiation, the reaction mixture was transferred to a separating funnel, diluted with dichloromethane and washed with 15 mL of water. The aqueous layer was washed three times (3 x 15 mL) with dichloromethane. The combined organic phases were dried over Na$_2$SO$_4$, filtered and concentrated in vacuum.

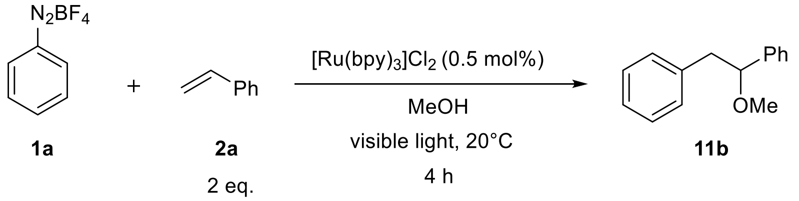

(1-Methoxyethane-1,2-diyl)dibenzene[15, 22] (11b)

^{1}H NMR (300 MHz, CDCl$_3$): δ ppm 7.34 – 7.14 (m, 10H), 4.32 (dd, *J* = 6.5, 5.9 Hz, 1H), 3.19 (s, 3H), 3.10 (dd, *J* = 13.9, 6.3 Hz, 1H), 2.89 (dd, *J* = 13.8, 5.8 Hz, 1H).

^{13}C NMR (75 MHz, CDCl$_3$):δ ppm 141.8, 138.6, 129.6, 128.5, 128.2, 127.8, 126.9, 126.2, 85.2, 56.9, 44.9.

1.4.6. ^{1}H and ^{13}C NMR Spectra of Selected Compounds

^{1}H NMR (300 MHz, CDCl$_3$)

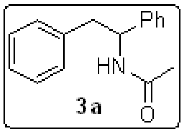

3a

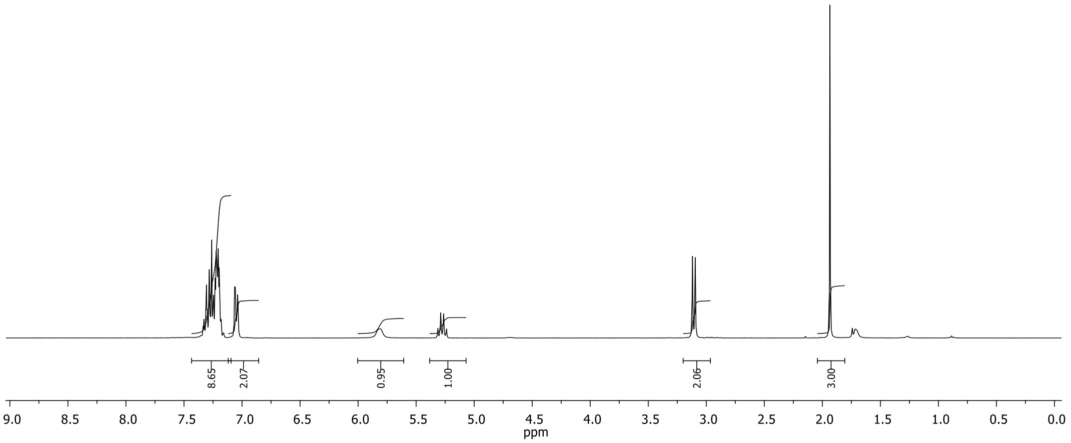

^{13}C NMR (75 MHz, $CDCl_3$)

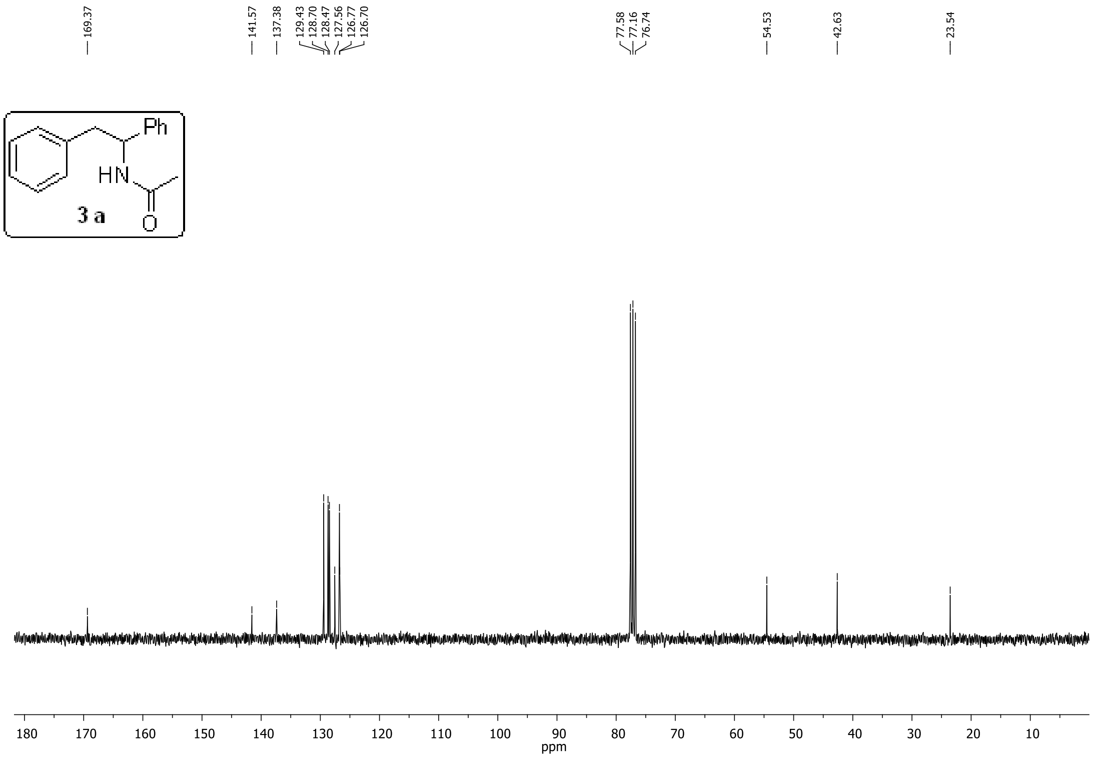

^{1}H NMR (300 MHz, $CDCl_3$)

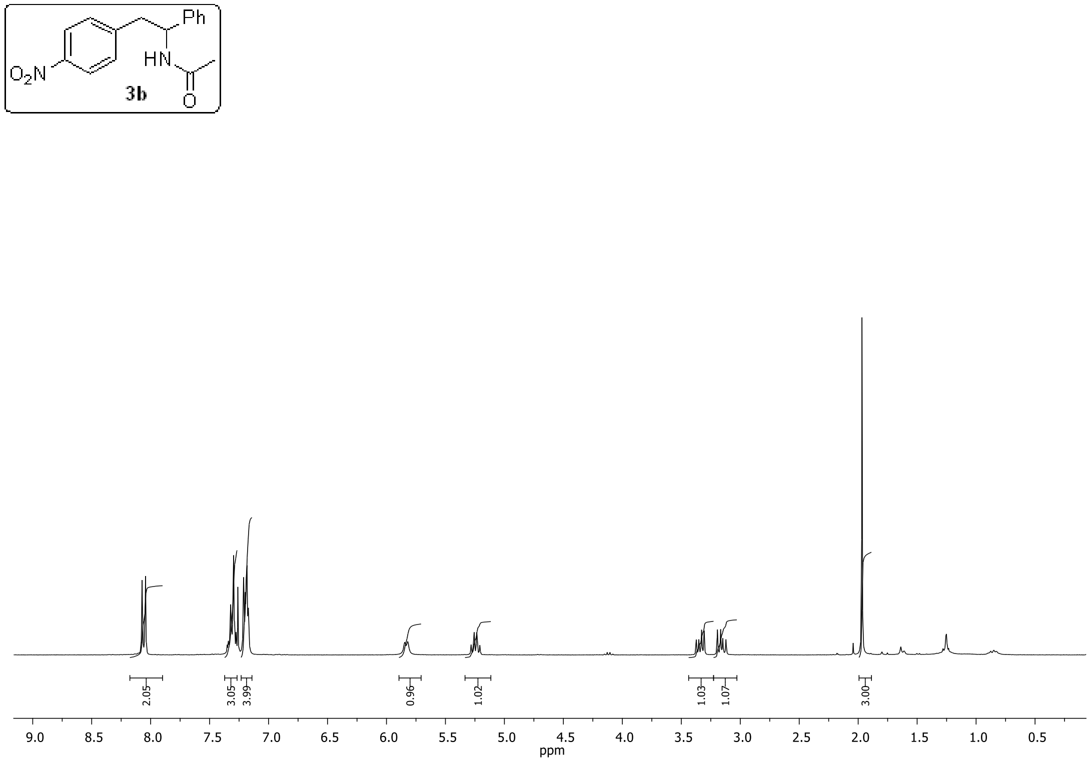

^{13}C NMR (75 MHz, $CDCl_3$)

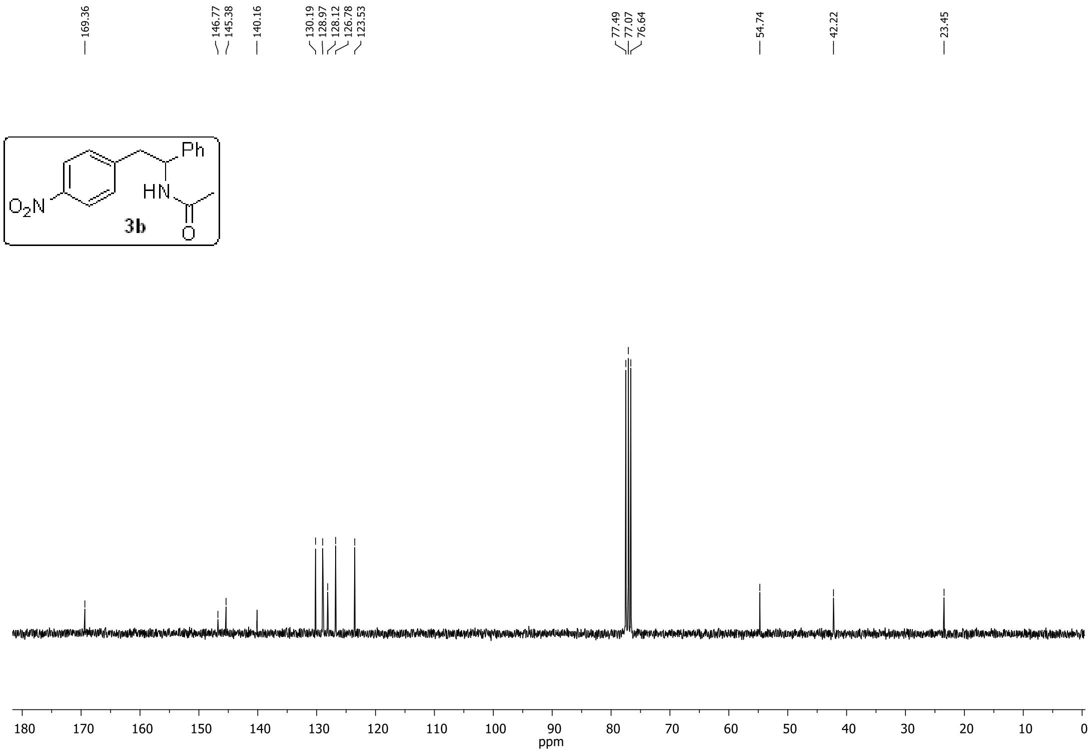

^1H NMR (300 MHz, $CDCl_3$)

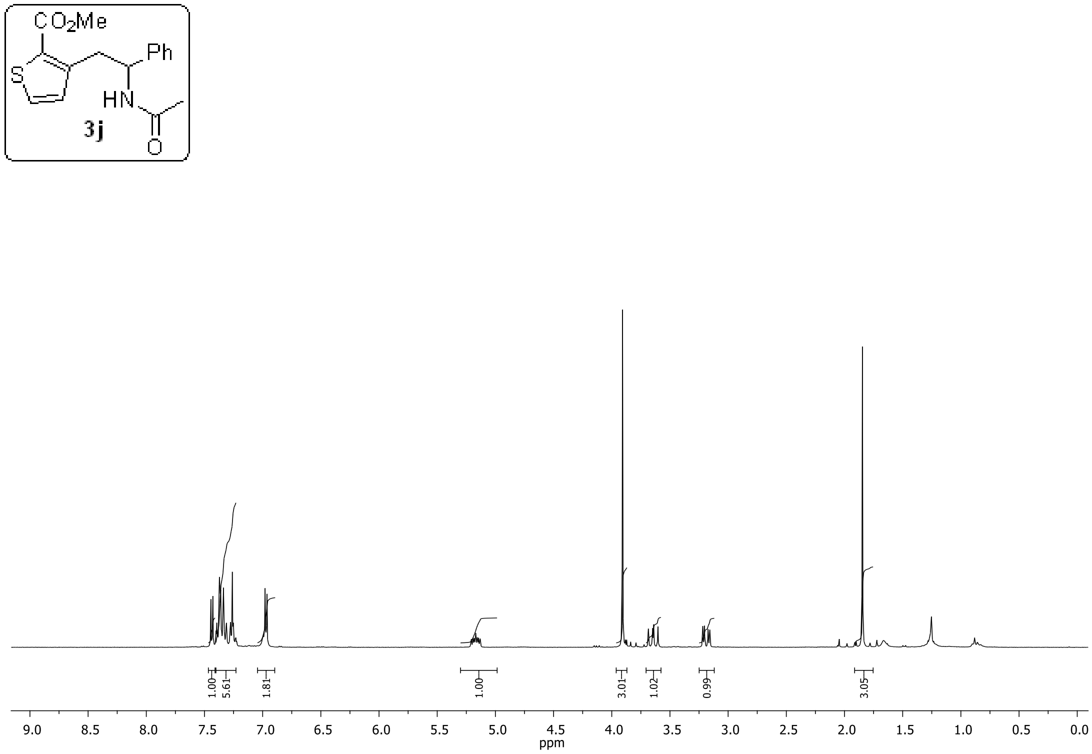

^{13}C NMR (75 MHz, CDCl$_3$)

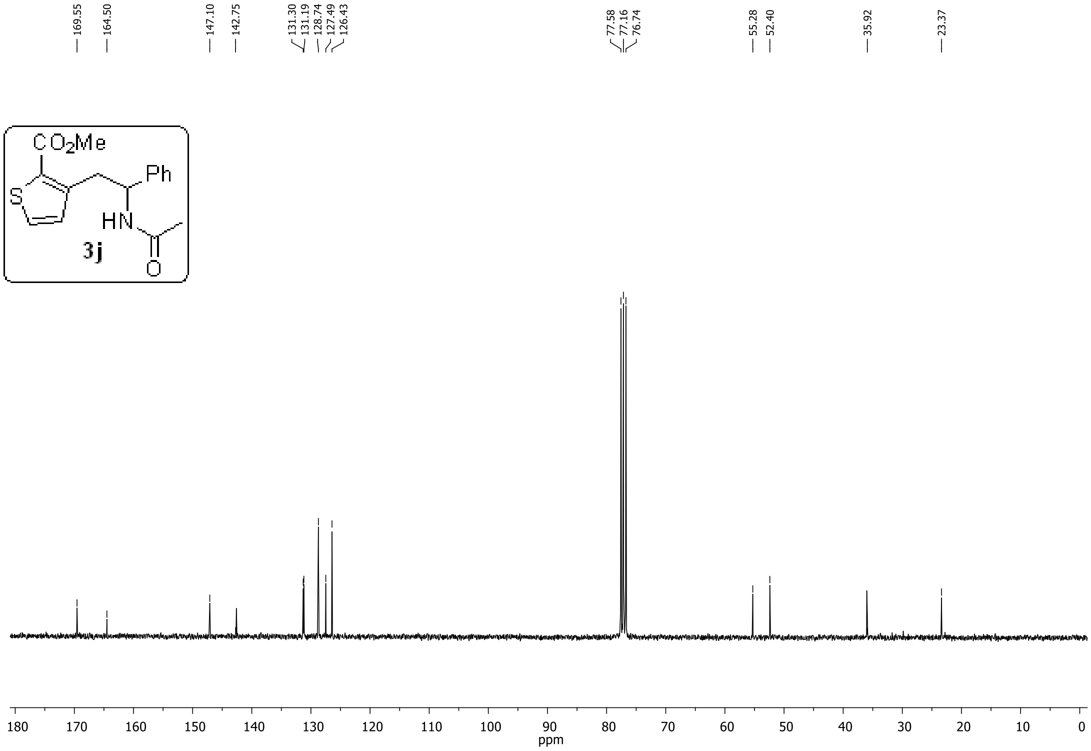

^{1}H NMR (300 MHz, CDCl$_3$)

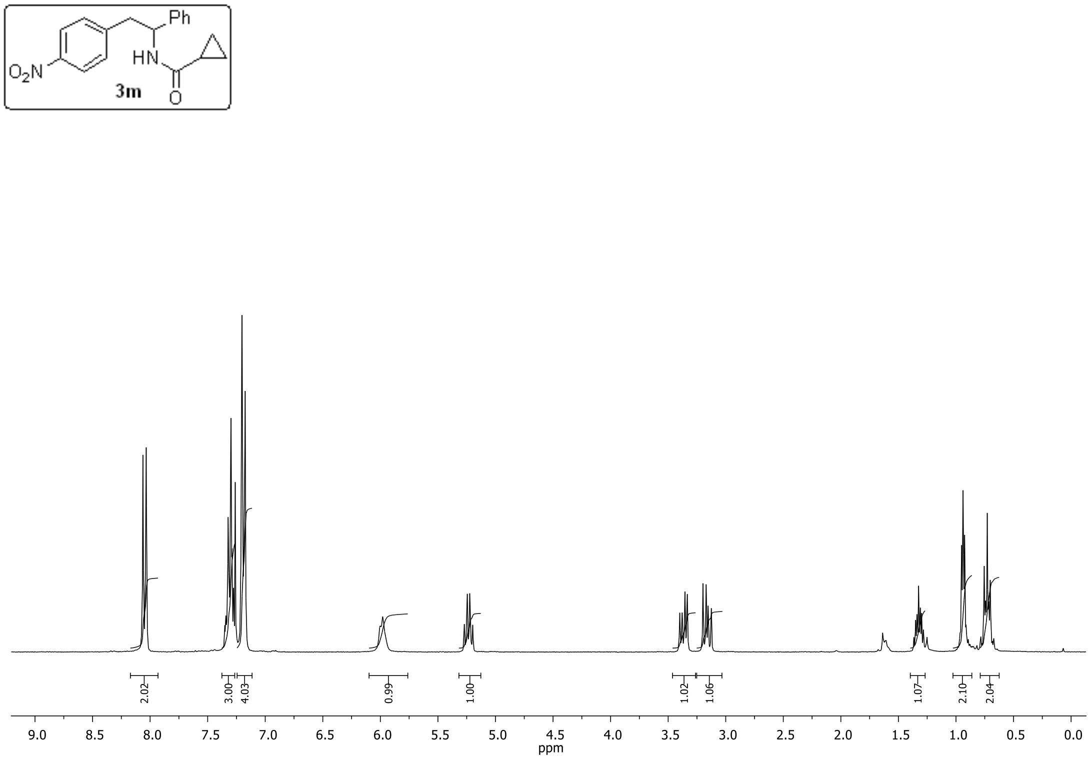

^{13}C NMR (75 MHz, CDCl$_3$)

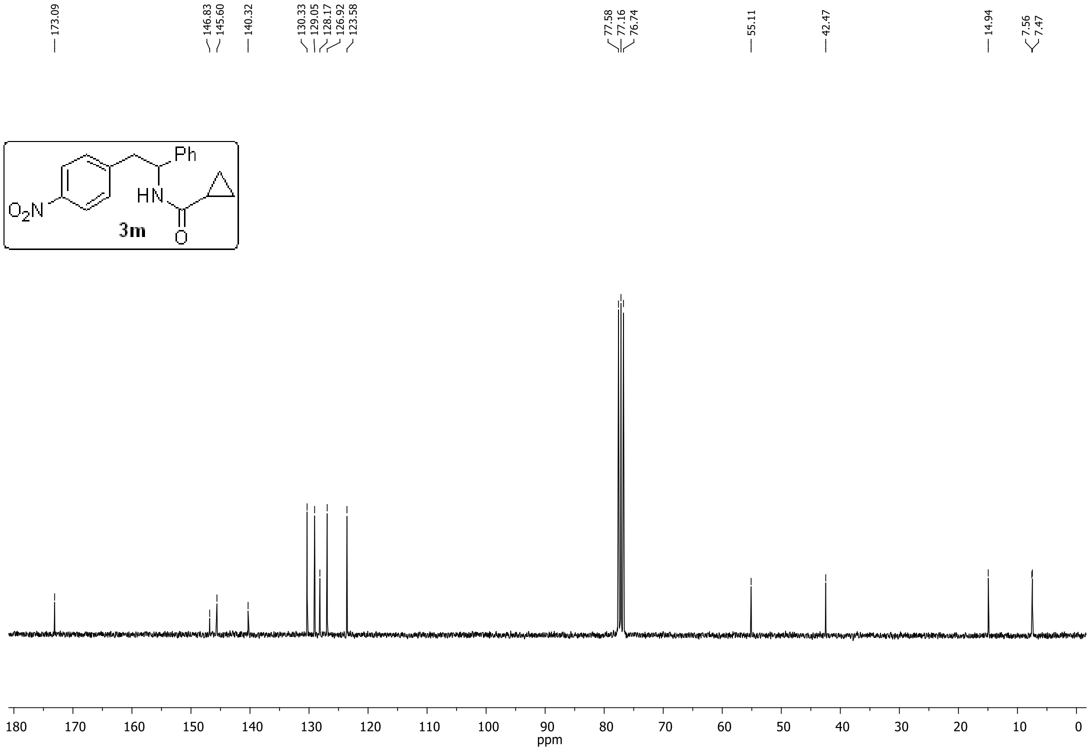

^{1}H NMR (300 MHz, CDCl$_3$)

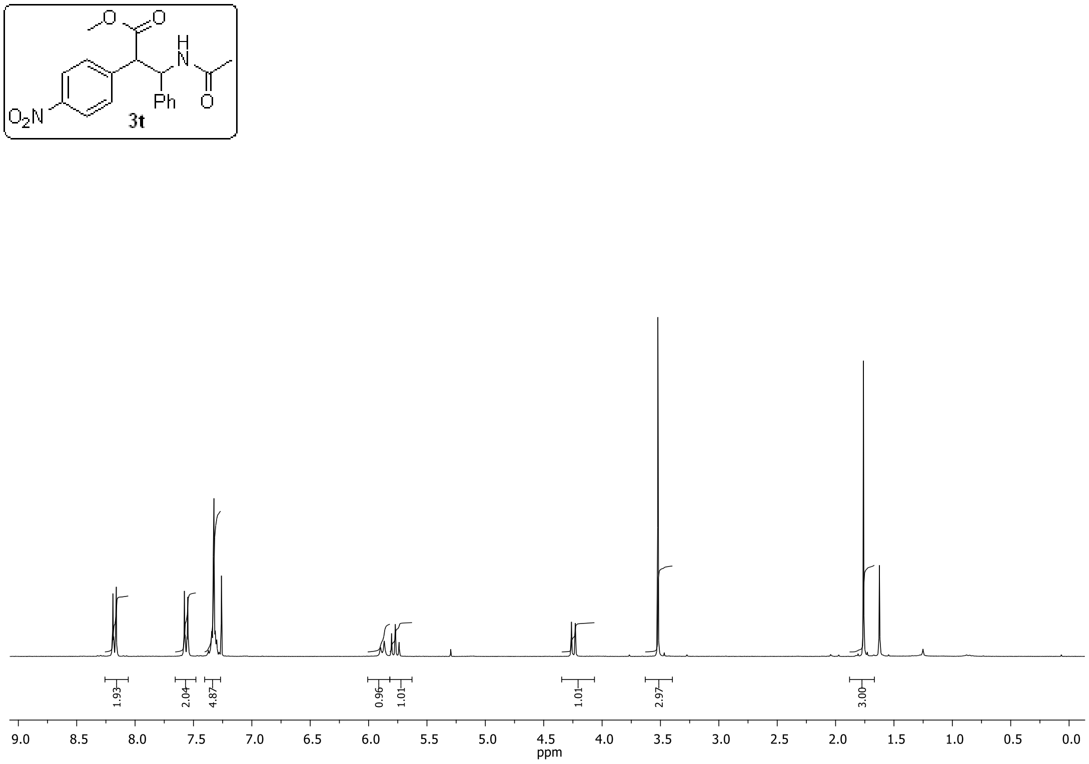

^{13}C NMR (75 MHz, $CDCl_3$)

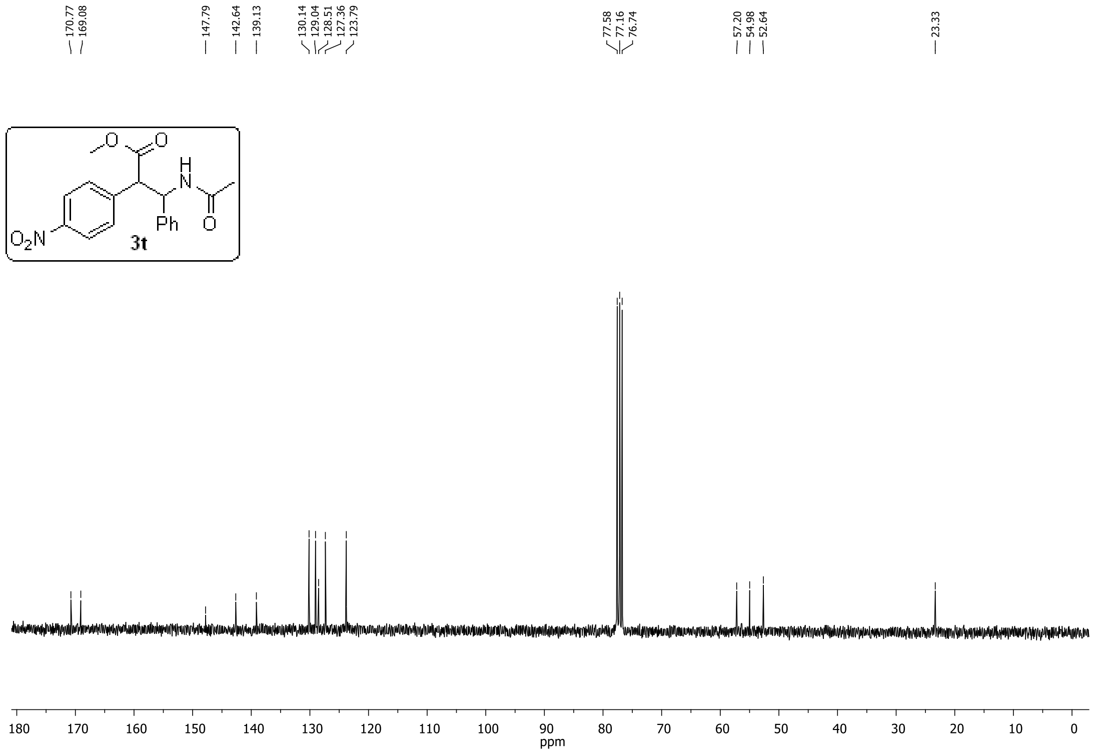

1.5. References

[1] H. Meerwein, E. Büchner, K. van Emster, *Journal für Praktische Chemie* **1939**, *152*, 237-266.

[2] M. R. Heinrich, *Chem.- Eur. J.* **2009**, *15*, 820-833.

[3] M. R. Heinrich, O. Blank, D. Ullrich, M. Kirschstein, *J. Org. Chem.* **2007**, *72*, 9609-9616.

[4] M. R. Heinrich, O. Blank, S. Wölfel, *Org. Lett.* **2006**, *8*, 3323-3325.

[5] S. B. Höfling, A. L. Bartuschat, M. R. Heinrich, *Angew. Chem., Int. Ed.* **2010**, *49*, 9769-9772.

[6] M. R. Heinrich, A. Wetzel, M. Kirschstein, *Org. Lett.* **2007**, *9*, 3833-3835.

[7] G. Pratsch, C. A. Anger, K. Ritter, M. R. Heinrich, *Chem.- Eur. J.* **2011**, *17*, 4104-4108.

[8] G. Pratsch, M. Heinrich, in *Radicals in Synthesis III, Vol. 320* (Eds.: M. Heinrich, A. Gansäuer), Springer Berlin Heidelberg, **2012**, pp. 33-59.

[9] A. Wetzel, G. Pratsch, R. Kolb, M. R. Heinrich, *Chem.- Eur. J.* **2010**, *16*, 2547-2556.

[10] H. Zollinger, *Acc. Chem. Res.* **1973**, *6*, 335-341.

[11] M. K. Staples, R. L. Grange, J. A. Angus, J. Ziogas, N. P. H. Tan, M. K. Taylor, C. H. Schiesser, *Org. Biomol. Chem.* **2011**, *9*, 473-479.

[12] R. Leardini, G. F. Pedulli, A. Tundo, G. Zanardi, *J. Chem. Soc., Chem. Commun.* **1985**, 1390-1391.

[13] M. Mahesh, J. A. Murphy, F. LeStrat, H. P. Wessel, *Beilstein J. Org. Chem.* **2009**, *5*, 1.

[14] S. Donck, A. Baroudi, L. Fensterbank, J.-P. Goddard, C. Ollivier, *Adv. Synth. Catal.* **2013**, *355*, 1477-1482.

[15] G. Fumagalli, S. Boyd, M. F. Greaney, *Org. Lett.* **2013**, *15*, 4398-4401.

[16] Y. Yasu, T. Koike, M. Akita, *Adv. Synth. Catal.* **2012**, *354*, 3414-3420.

[17] Y. Yasu, T. Koike, M. Akita, *Org. Lett.* **2013**, *15*, 2136-2139.

[18] D. P. Hari, B. Konig, *Angew. Chem., Int. Ed.* **2013**, *52*, 4734-4743.

[19] D. P. Hari, T. Hering, B. Konig, *Chimica Oggi-Chemistry Today* **2013**, *31*, 59-62.

[20] D. P. Hari, T. Hering, B. König, *Org. Lett.* **2012**, *14*, 5334-5337.

[21] D. P. Hari, P. Schroll, B. König, *J. Am. Chem. Soc.* **2012**, *134*, 2958-2961.

[22] P. Schroll, D. P. Hari, B. König, *ChemistryOpen* **2012**, *1*, 130-133.

[23] T. Hering, D. P. Hari, B. König, *J. Org. Chem.* **2012**, *77*, 10347-10352.

[24] F. Mo, G. Dong, Y. Zhang, J. Wang, *Org. Biomol. Chem.* **2013**, *11*, 1582-1593.

[25] D. Kalyani, K. B. McMurtrey, S. R. Neufeldt, M. S. Sanford, *J. Am. Chem. Soc.* **2011**, *133*, 18566-18569.

[26] D. P. Hari, B. König, *Angew. Chem.* **2013**, *125*, 4832-4842.

[27] J. J. Ritter, P. P. Minieri, *J. Am. Chem. Soc.* **1948**, *70*, 4045-4048.

[28] J. J. Ritter, J. Kalish, *J. Am. Chem. Soc.* **1948**, *70*, 4048-4050.

[29] J. Clayden, N. Greeves, S. Warren, P. Wothers, *Organic Chemistry, Oxford Press: New York* **2011**.

[30] R. Vardanyan, V. J. Hruby, *Synthesis of Essential Drugs, 1st Ed. Amsterdam: Elsevier* **2006**.

[31] L. Kurti, B. Czako, *Strategic Applications of Named Reactions in Organic Synthesis. Burlington, MA Elsevier Academic Press* **2005**.

[32] M. Y. Lebedev, M. B. Erman, *Tetrahedron Lett.* **2002**, *43*, 1397-1399.

[33] H. Fernholz, H. J. Schmidt, *Angew. Chem., Int. Ed. Engl.* **1969**, *8*, 521-521.

[34] L. I. Krimen, D. J. Cota, in *Organic Reactions*, John Wiley & Sons, Inc., **2004**.

[35] A. García Martínez, R. Martínez Alvarez, E. Teso Vilar, A. García Fraile, M. Hanack, L. R. Subramanian, *Tetrahedron Lett.* **1989**, *30*, 581-582.

[36] F. Neufingerl, *Allgemeine und anorganische Chemie*, Jugend und Volk, Wien, **2006**.

[37] R. D. Larsen, R. A. Reamer, E. G. Corley, P. Davis, E. J. J. Grabowski, P. J. Reider, I. Shinkai, *J. Org. Chem.* **1991**, *56*, 6034-6038.

[38] M. Movassaghi, M. D. Hill, *Org. Lett.* **2008**, *10*, 3485-3488.

[39] C. K. Prier, D. A. Rankic, D. W. Macmillan, *Chem Rev* **2013**, *113*, 5322-5363.

[40] J. M. R. Narayanam, C. R. J. Stephenson, *Chem. Soc. Rev.* **2011**, *40*, 102-113.

[41] J. Xuan, W.-J. Xiao, *Angew. Chem., Int. Ed.* **2012**, *51*, 6828-6838.

[42] C. Seki, M. Hirama, N. D. M. R. Hutabarat, J. Takada, C. Suttibut, H. Takahashi, T. Takaguchi, Y. Kohari, H. Nakano, K. Uwai, N. Takano, M. Yasui, Y. Okuyama, M. Takeshita, H. Matsuyama, *Tetrahedron* **2012**, *68*, 1774-1781.

[43] Y. Yasu, T. Koike, M. Akita, *Angew. Chem., Int. Ed.* **2012**, *51*, 9567-9571.

[44] E. Kim, S. Choi, H. Kim, E. J. Cho, *Chem.- Eur. J.* **2013**, *19*, 6209-6212.

[45] H. Cano-Yelo, A. Deronzier, *Tetrahedron Lett.* **1984**, *25*, 5517-5520.

[46] H. Cano-Yelo, A. Deronzier, *J. Chem. Soc., Perkin Trans. 2* **1984**, 1093-1098.

[47] H. Cano-Yelo, A. Deronzier, *New J. Chem.* **1987**, *11*, 479-485.

[48] H. Cano-Yelo, A. Deronzier, *J. Chem. Soc., Perkin Trans. 2* **1984**, 1093-1098

[49] P. Hanson, J. R. Jones, A. B. Taylor, P. H. Walton, A. W. Timms, *J. Chem. Soc., Perkin Trans. 2* **2002**, 1135-1150.

Chapter 2

2. Visible Light Photooxidation of Nitrate: The Dawn of a Nocturnal Radical

PC
hν
PC
2 eq
10b
Ph

"Gedankenexperiment"
painting by Julia Leopold within the project "Art meets Science", 2016

This chapter was published in: T. Hering, T. Slanina, A. Hancock, U. Wille and B. König, *Chem. Commun.* **2015**, *51*, 6568-6571. - Published by The Royal Society of Chemistry

TH performed all reactions and wrote the manuscript. TH and TS did the UV/Vis measurements and fluorescence quenching. AH carried out the laser flash photolysis. UW and BK supervised the project and are corresponding authors.

2.1. Introduction

The nitrate radical ($NO_3^{\bullet}$) is the most important nocturnal free radical oxidant in the troposphere and thus accounts for the majority of the oxidative reactions at night-time.[1] In the atmosphere $NO_3^{\bullet}$ oxidizes a broad scope of volatile organic species including alkenes,[2-3] alcohols,[4-5] terpenes,[1] esters,[6] and sulfides.[1] It is a highly reactive and chemically versatile *O*-centered radical [7] with an oxidation potential of +2.00 V (vs. SCE in MeCN).[a][8] Apart from electron transfer (ET)[9-10] $NO_3^{\bullet}$ also reacts by addition to π systems[1, 11] and by hydrogen atom abstraction (HAT).[8, 12-13] Overall, the reactivity of $NO_3^{\bullet}$ with organic molecules can be seen in between that of hydroxyl radicals ($OH^{\bullet}$) and sulfate radical anions ($SO_4^{\bullet -}$).[14]

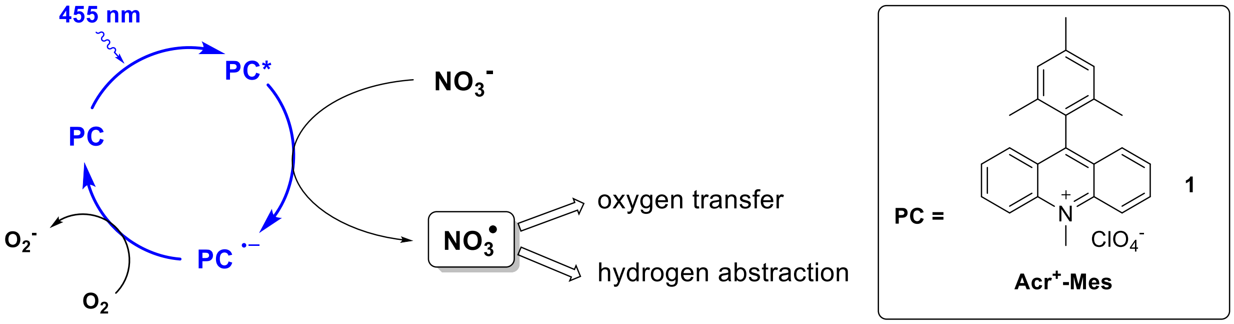

Scheme 2-1. Generation of $NO_3^{\bullet}$ by visible light photoredox catalysis using **Acr$^+$-Mes** (**1**) as the photocatalyst.

Despite its high chemical versatility, it is surprising that only limited synthetic applications of $NO_3^{\bullet}$ are available so far. In 1994, Shono *et al.* reported the addition of electrochemically generated $NO_3^{\bullet}$ to alkenes leading to nitrate esters, which were directly converted into the corresponding alcohols or iodoalkanes.[11] The reaction of $NO_3^{\bullet}$ with cyclic alkynes and alkynones was employed to obtain *cis*-fused bicyclic ketones in self-terminating oxidative radical cyclizations.[15-16] This concept was later extended to open-chain alkyne ethers to produce tetrasubstituted tetrahydrofurans with good diastereoselectivity.[17-18] One reason for the limited use of $NO_3^{\bullet}$ as a reagent in organic transformations is its rather difficult accessibility. Common methods for $NO_3^{\bullet}$ generation on preparative scale in solution are the reaction of nitrogen dioxide and ozone,[1, 19] electrooxidation of nitrate anions [11] or the photolysis of $(NH_4)_2Ce(NO_3)_6$ (CAN) with UV light (λ = 350 nm).[14, 20] However, the use of toxic gases, high electrode potentials,[8] or UV irradiation are limiting the applications and may lead to undesired side reactions. The generation of $NO_3^\bullet$ by visible light photoredox catalysis using readily available inorganic nitrate salts as radical precursor, as depicted in Scheme 2-1, should overcome some of these drawbacks and would also allow the use of oxygen as the terminal oxidant.

---

[a] Potential measured for $NO_3^{\bullet}/NO_3^{-}$: E_0= 2.0 V vs. SCE (in MeCN).

2.2. Results and Discussion

We were pleased to observe that, upon excitation of the organic photocatalyst 9-mesityl-10-methylacridinium perchlorate (**1**) with blue light, oxidation of nitrate anions to $NO_3^\bullet$, readily occurs, thus providing a convenient access to $NO_3^\bullet$ on a preparative scale. 9-mesityl-10-methylacridinium perchlorate (**1**) a catalyst developed by Fukuzumi *et al.* was chosen because it is known to have a strong oxidizing capacity in the excited state.[21-22] To the best of our knowledge, this is the first visible light mediated generation of these radicals.

In order to elucidate the mechanism of the $NO_3^\bullet$ formation, we monitored generation of the reduced catalyst **Acr$^\bullet$-Mes** in the presence of $LiNO_3$ upon continuous irradiation of a 5 µM solution of **Acr$^+$-Mes** (**1**) in MeCN with 455 nm light under anaerobic conditions. The differential absorption spectrum shows the appearance of **Acr$^\bullet$-Mes** with a maximum at 520 nm[21, 23] after irradiation for 120 s and 240 s (Figure 2-1). This observation suggests a direct oxidation of NO_3^- by the excited catalyst and demonstrates that NO_3^- can act as an electron donor to the excited catalyst. The reduced catalyst **Acr$^\bullet$-Mes** is stable under argon, however, the signal vanishes completely after aeration of the reaction mixture due to reoxidation of **Acr$^\bullet$-Mes** to the ground state catalyst **Acr$^+$-Mes** by oxygen (see Scheme 2-1).[24] The negative signal at $\lambda < 460$ nm in the differential absorption spectrum is caused mainly by the decrease of the ground state absorption of **Acr$^+$-Mes** as a result of the formation of **Acr$^\bullet$-Mes** and partial photobleaching of **Acr$^+$-Mes**.[b]

---

[b] After aeration the ground state absorption of **Acr$^+$-Mes** cannot be fully recovered (see Experimental Section, Figure 2-5).

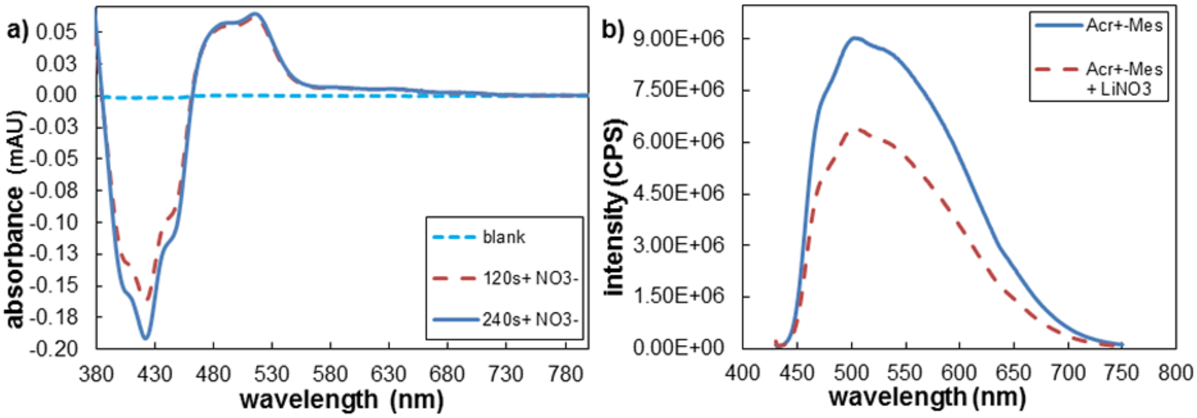

Figure 2-1. (a) Formation of the reduced catalyst **Acr$^{\bullet}$-Mes** in the presence of LiNO$_3$ under anaerobic conditions after 120 s and 240 s of continuous irradiation. (b) Quenching of the fluorescence of excited **Acr^{+}-Mes** by LiNO$_3$ indicating a reaction from the singlet state.

The long-lived triplet state with a microsecond lifetime is generally discussed as the reactive state in most oxidative reactions.[25-26] The exact nature of this state is controversial and could be both a CT^{T} state with an oxidation potential of +1.88 V vs. SCE, as reported by Fukuzumi [25] or a locally excited triplet state, LE^{T}, with an oxidation potential of +1.45 V vs. SCE as reported by Verhoeven.[26] However, neither would have the oxidative capacity to oxidize NO$_3^{–}$. Recent detailed mechanistic investigations by the group of Nicewicz *et al.* revealed that for substrates with oxidation potentials exceeding +1.88 V (vs. SCE), a reaction should occur out of the short-lived excited singlet state (mainly CT^{S}), which has an estimated oxidation potentials of 2.08 V (Scheme 2-2).[23] Since both singlet states are fluorescent (ϕ_F~8%), whereas the triplet states do not emit,[23] we performed fluorescence quenching experiments to explore the nature of the reactive state involved in NO$_3^{–}$ oxidation. Figure 2-1b shows a clear quenching of the fluorescence by LiNO$_3$, which confirms that oxidation of NO$_3^{–}$ occurs from the singlet excited state of **1**. It should be noted that the fluorescence spectrum in Figure 2-1 is a combination of the emissions by both CT^{S} and LE^{S}, which are reported to be in thermal equilibrium. However, the LE^{S} is reported to be inactive in oxidation reactions.[23] Moreover, laser flash photolysis experiments confirmed that no interaction of the long lived triplet state and NO$_3^{–}$ can be observed (see Experimental Section, Figure 2-7). Based on these findings, we suggest that the reaction proceeds *via* a singlet excited state as depicted in Scheme 2-2.

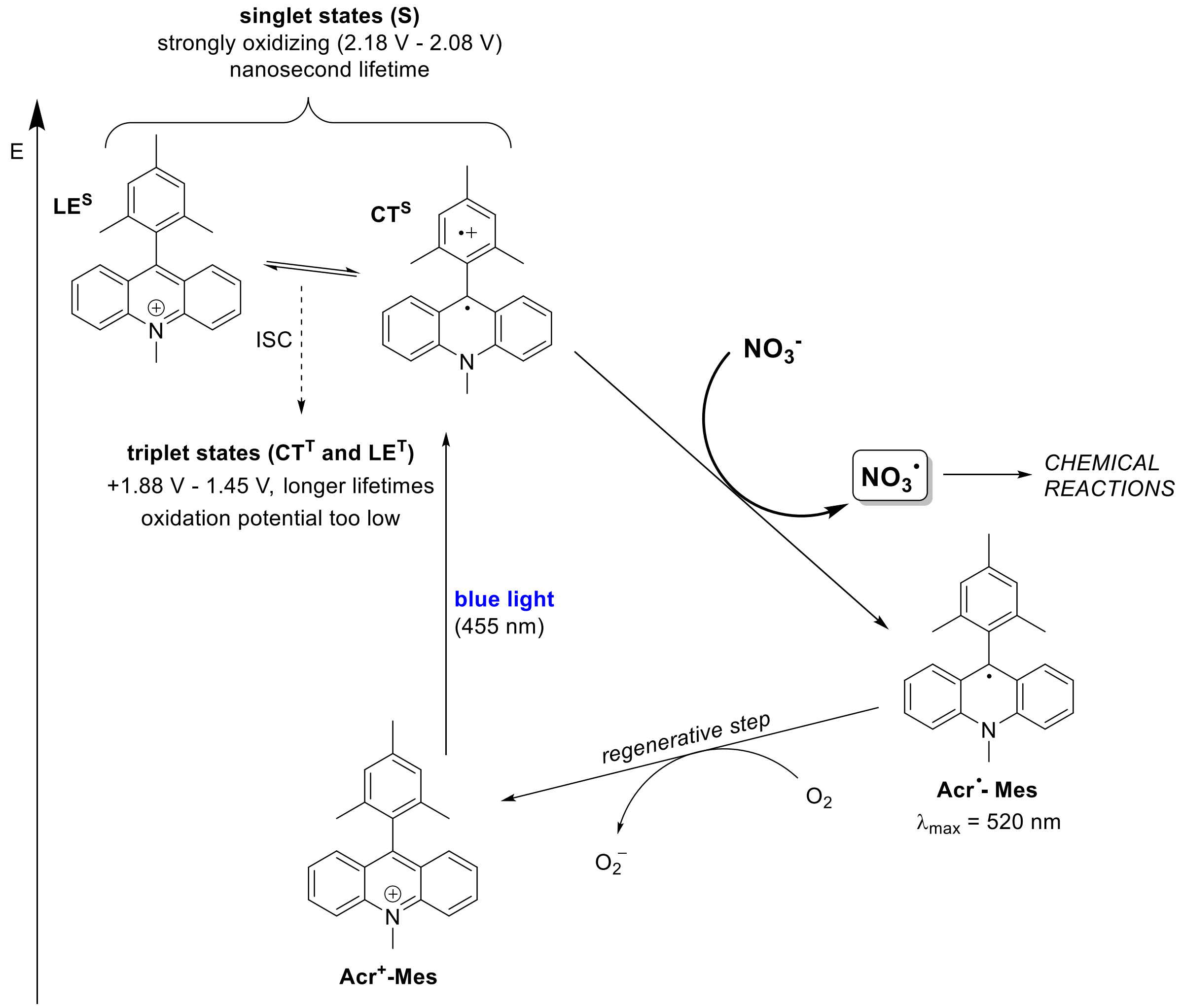
singlet states (S)
strongly oxidizing (2.18 V - 2.08 V)
nanosecond lifetime
E
LE^S
CT^S
ISC
triplet states (CT^T and LE^T)
+1.88 V - 1.45 V, longer lifetimes
oxidation potential too low
blue light
(455 nm)
NO3-
NO3•
CHEMICAL REACTIONS
regenerative step
O2
O2−
Acr•- Mes
λmax = 520 nm
Acr+-Mes

Scheme 2-2. Proposed mechanism of visible light mediated generation of $NO_3^{\bullet}$ via photocatalytic oxidation by **Acr⁺-Mes**. The electron transfer from NO_3^{-} occurs with a short-lived singlet state (LE^S or CT^S) with sufficient oxidative capacity to generate the reduced catalyst **Acr•-Mes** and $NO_3^{\bullet}$, the longer lived transient triplet species (CT^T or LE^T) is not reactive towards NO_3^{-}. The reduced catalyst **Acr•-Mes** is regenerated by oxygen. (All oxidation potentials are given vs. SCE in MeCN or PhCN).[23, 25-26]

Having demonstrated the pathway for photocatalytic $NO_3^{\bullet}$ generation, we selected the well-studied reaction of $NO_3^{\bullet}$ with diphenylacetylene (**2**) yielding benzil (**3**) and benzophenone (**4**) to explore the synthetic application of this new method and to compare it with the previously reported methods. The results are compiled in Table 2-1. Under photocatalytic conditions using 5 mol% of **Acr⁺-Mes** (**1**), 0.25 mmol of alkyne **2** and 2 eq. of $LiNO_3$, diketone **3** and ketone **4** were obtained after 2 h of irradiation with blue light (λ_{max} = 455 nm) with yields comparable to previous methods.[27] When oxygen was replaced by ammonium persulfate as the electron acceptor in a degassed system, the yield and product ratio was not changed significantly (entry 5). This shows that potential interfering reactions by singlet oxygen could be excluded. In the absence of light or catalyst no reaction occurred (entries 7, 9). However, small amounts of diketone **3** were formed in the direct reaction of **2** with the excited catalyst in the absence of nitrate ions (entry 8). According to computational studies, the mechanism for the $NO_3^{\bullet}$ induced oxidation of diphenylacetylene, diketone **3** and benzophenone (**4**) are formed through competing pathways in the initial vinyl radical adduct **5** (Scheme 2-3). While diketone **3** results from a 5-*endo* cyclization, followed by loss of $NO^{\bullet}$, the key-step in the formation of benzophenone (**4**) is γ-fragmentation with elimination of $NO_2^{\bullet}$, and subsequent Wolff-rearrangement of the carbene intermediate **7** followed by oxidative decarboxylation.[27]

Table 2-1. Oxidation of diphenylacetylene **2** by $NO_3^{\bullet}$.[a]

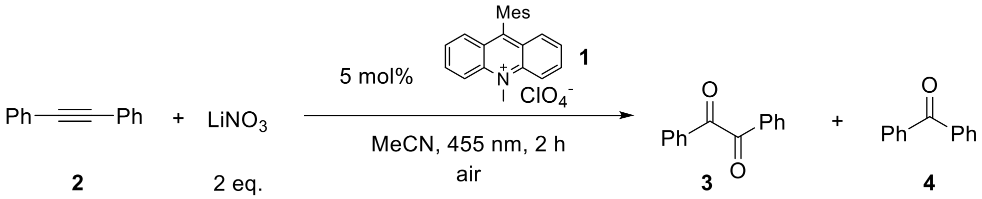

Entry	Conditions	Yield 3+4 (%)[b]
1	5 mol% **1**, air	50 (30+20)
2	5 mol% **1**, O_2	55 (31+24)
3	$NaNO_3$	41 (27+15)
4	10 mol% **1**	38 (24+14)
5	$(NH_4)_2S_2O_8$, N_2 atmosphere	46 (27+19)
6	DCM	52 (32+20)
7	without light	0
8	without NO_3^-	13 (**3** only)
9	without **1**	0

[a] Reactions were carried out using diphenylacetylene (**2**, 0.25 mmol) and the respective amount of 9-mesityl-10-methylacridinium perchlorate (**1**) in 1 mL of MeCN unless otherwise noted with an irradiation time of 2 h. [b] Quantitative GC yields using acetophenone as internal standard.

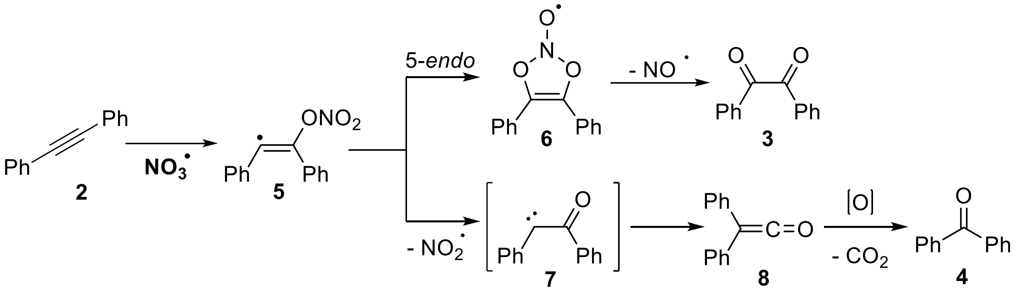

Scheme 2-3. Proposed mechanism for the oxidation of aromatic alkynes by $NO_3^\bullet$.[27]

Next, we applied the photocatalytic $NO_3^\bullet$ formation to the synthesis of tetrasubstituted tetrahydrofurans, which proceeds *via* a self-terminating radical cascade that is initiated by $NO_3^\bullet$ addition to the triple bond in alkyne **9**. The reaction was described previously using either anodic oxidation of lithium nitrate or CAN photolysis.[17-18] The starting material **9** (Scheme 2-4) contains an aliphatic alkyne, which is more difficult to oxidize compared to **2** and thus decreases the background reaction that is caused by direct oxidation of **9** by the photocatalyst. The reaction of **9b** with 2 eq. of $LiNO_3$ and 5 mol% **1** gave the anticipated product **10b** in a yield of 37% (67% based on conversion), with 45% of the starting material **9b** being recovered. Methyl ether **9a** gave lower yields and an incomplete conversion, which can be rationalized by a non-regioselective addition of $NO_3^\bullet$ to both ends of the alkyne (see Experimental Section, Scheme 2-7), in accordance with previous reports. The low conversion (and resulting low product yield) is likely due to the fact that $NO_3^\bullet$ leads to degradation of catalyst **1**. This effect could also be observed in UV/Vis measurements of the reaction mixture, which showed severe photobleaching of the ground state during irradiation (see Experimental Section, Figure 2-6). It is likely that the observed degradation proceeds *via* oxidation of the methyl groups on the mesityl moiety of the catalyst,[8] which is a known degradation pathway that leads to loss of catalytic activity.[28] The problem of low conversion could be partly overcome through slow addition of the catalyst *via* syringe pump.

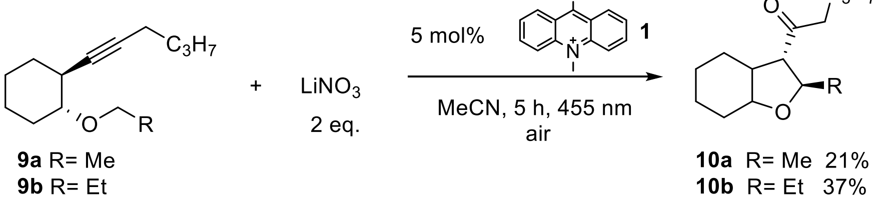

9a R= Me
9b R= Et

10a R= Me 21%
10b R= Et 37%

Scheme 2-4. Self-terminating radical oxidative cyclization to tetrasubstituted tetrahydrofurans **10**.[17-18]

As mentioned before, apart from addition to π systems, $NO_3^\bullet$ also reacts through hydrogen atom abstraction,[8, 12-13] which was explored in the catalytic oxidation of non-activated alcohols (Scheme 2-5). In this reaction, $NO_3^\bullet$ acts as a redox mediator, which is regenerated during the catalytic cycle, according to the mechanism in Scheme 2-5. Initial HAT from the alcohol carbon by $NO_3^\bullet$ [29] leads to the regeneration of NO_3^- as nitric acid and formation of radical **12**. The latter is subsequently oxidized by either $NO_3^\bullet$ or oxygen to give cationic intermediate **13**, which deprotonates to yield ketone **14**. The mechanism is similar to the indirect anodic oxidation of alcohols by nitrate.[30] Donaldson and Styler reported the enhanced gas phase oxidation of propanol under UV irradiation using TiO_2 co-embedded with KNO_3. The finding was explained by formation of $NO_3^\bullet$ and its ability to abstract hydrogen atoms from the alcohol carbon atom.[31]

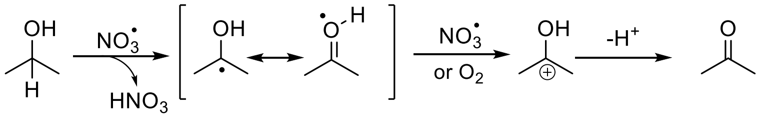

11 **12** **13** **14**

Scheme 2-5. General mechanism of the nitrate mediated alcohol oxidation via initial hydrogen abstraction followed by oxidation and loss of a proton.

The reaction was explored using *tert*-butyl cyclohexanol (**11a**) and the results are compiled in Scheme 2-6. To our delight, oxidation into the corresponding ketone **14a** occurred upon irradiation with blue light in the presence of $LiNO_3$ using 5 mol% of **1** in acetonitrile. No reaction was observed in the absence of nitrate, which clearly confirms the role of $NO_3^\bullet$ in this reaction. Stepwise reduction of the amount of $LiNO_3$ from 2 eq. to 20 mol% did not affect the outcome, showing that $NO_3^\bullet$ can act as mediator in this reaction (Scheme 2-6). An acidification of the solution due to formation of nitric acid was observed, but no apparent influence on the reaction or the stability of the catalyst was found. The addition of different bases (Li_2CO_3, LiOAc, pyridine, lutidine) did not influence the outcome of the reaction or the stability of the catalyst.

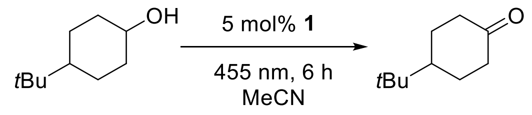

11a **14a**

$LiNO_3$	**14a**
2 eq.	45 %
1 eq.	41 %
0.5 eq.	39 %
0.2 eq.	42 %
0 eq.	0 %

Scheme 2-6. Experimental conditions and results for the $NO_3^\bullet$ mediated oxidation of alcohols.

The scope of this method was explored towards other non-activated alcohols and electron deficient benzyl alcohols. All reactions were carried out by two sequential additions of 5 mol% of **1** in order to counteract the loss of catalytic activity caused by degradation of the catalyst. The reactions proceed with good selectivity (Table 2-2, entries 1, 2, 4), but the conversion was incomplete and unreacted starting material was recovered. Aliphatic (entries 1, 2, 3) and benzylic alcohols (entries 4, 6) were converted. In the oxidation of isomenthol (**11b**) (entry 2) the configuration of the stereocenter remained unchanged, while the basic substrate **11e** gave no product, which is most likely due to an acid/base reaction of pyridine with nitric acid that is generated during this reaction[c] by the H-abstraction by $NO_3^•$ or a possible direct oxidation of the nitrogen of pyridine by the photocatalyst or possibly $NO_3^•$ (entry 5).[32]

Table 2-2. Experimental conditions and results for the $NO_3^•$ mediated oxidation of alcohols.[a]

entry	alcohol	product	yield product (%)[b]	recovered starting material (%)[b]
1	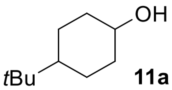 **11a**	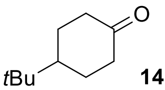 **14a**	45 (79)	44
2	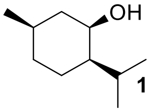 **11b**	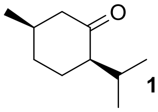 **14b**	42 (95)	56
3	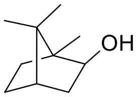 **11c**	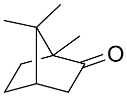 **14c**	40 (40)	--
4[c]	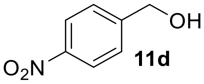 **11d**	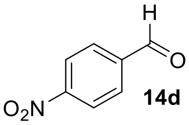 **14d**	55 (100)	45
5[d]	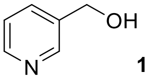 **11e**	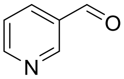 **14e**	--[d]	--[d]
6	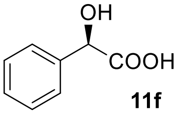 **11f**	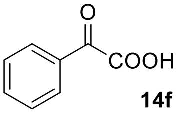 **14f**	13 (38)	66

[a] Reactions carried out using 0.25 mmol of the alcohol **11**, 1 eq. of $LiNO_3$ and 10 mol% of **1** (two subsequent additions of 5 mol%) in 1 mL of MeCN with an irradiation time of 6 h. [b] Isolated yields, in brackets yield based on conversion. [c] Background reaction without $LiNO_3$ is 9%. d) Decomposition of substrate **11e**.

---

[c] Based on the assumption that both the initial hydrogen abstraction and the oxidation of **12** are done by nitrate radicals.

2.3. Conclusion

In conclusion, we described a new and simple access to highly reactive nitrate radicals using visible light photocatalysis with an organic dye as the photoredox catalyst. This method avoids the use of toxic compounds, or high electrochemical potentials and is, to the best of our knowledge, the first method yielding $NO_3^\bullet$ in a catalytic process using in visible light. We verified the formation of nitrate radicals by observation of the reduced catalyst **Acr$^\bullet$-Mes** and showed that the mechanism is proceeding via the singlet excited state of the catalyst. By investigating the addition to aromatic alkynes, a previously well studied model reaction of $NO_3^\bullet$, we showed that the photocatalytic procedure is as efficient as the previously employed methods.

2.4. Experimental Section

2.4.1. General Information

NMR Spectroscopy: NMR spectroscopy was carried out on either a Bruker Avance 400 (^{1}H: 400.13 MHz, ^{13}C: 101 MHz, T = 300 K) or a Bruker Avance 300 (^{1}H: 300.13 MHz,^{13}C: 75 MHz, T = 295 K). The solvent residual peak (δ ($CDCl_3$): H 7.26; C 77.0) was used as an internal reference, chemical shifts were reported in δ [ppm], resonance multiplicities as s (singlet), d (doublet), t (triplet), m (multiplet) and coupling constants *J* in Hertz [Hz]. The spectrometer is given for each spectrum.

Thin Layer Chromatography (TLC): For monitoring the reactions pre-coated TLC-sheets ALUGRAM Xtra SIL G/UV254 from Macherey-Nagel were used. The visualization was done by UV light (254 nm or 366 nm) or staining with $CeSO_4$/ $H_3Mo_{12}O_{40}P$.

Flash Column Chromatography: Standard flash chromatography was performed on an Isolera™ Spektra Systems automated with high performance flash purification system. Macherey-Nagel silica gel 60 M (230-440 mesh) was used for column chromatography.

Photochemical set-up, LEDs: Photocatalytic reactions were performed with 455 nm LEDs (OSRAM Oslon SSL 80 royal-blue LEDs, λ_{em} = 455 nm (± 15 nm), 3.5 V, 700 mA). Reaction vials (5 mL crimp cap vials) were illuminated from the bottom with LEDs and cooled from the side using custom made aluminum cooling block connected to a thermostat (Figure 2-2).

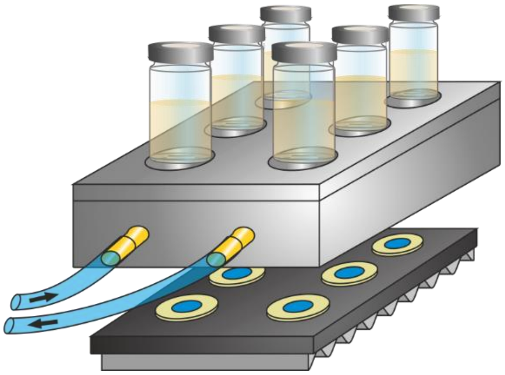

Figure 2-2. Photochemical set-up.

2.4.2. CV- Measurement

CV measurement was performed with the three-electrode potentiostat galvanostat PGSTAT302N from Metrohm Autolab using a glassy carbon working electrode, a platinum counter electrode and a silver wire as a reference electrode. The potential was achieved relative to the Fc/Fc$^+$ redox couple (set by external reference). The control of the measurement instrument, the acquisition and processing of the cyclic voltammetric data were performed with the software Metrohm Autolab NOVA 1.6.013. The measurements were carried out as follows: a 0.1 M solution of TBATFB in MeCN was placed in the measuring cell and the solution was degassed by a stream of argon for 5 min. After measuring of the baseline $LiNO_3$ was added (1 mL, 0.01 M in MeCN) and the solution was degassed by Argon purge for 5 min. The cyclic voltammogram was recorded with a single scan with a scan rate of 50 mV/s (using Fc/Fc$^+$ as external standard). The potentials were converted to SCE according to V. V. Pavlishchuk and A. W. Addison.[33]

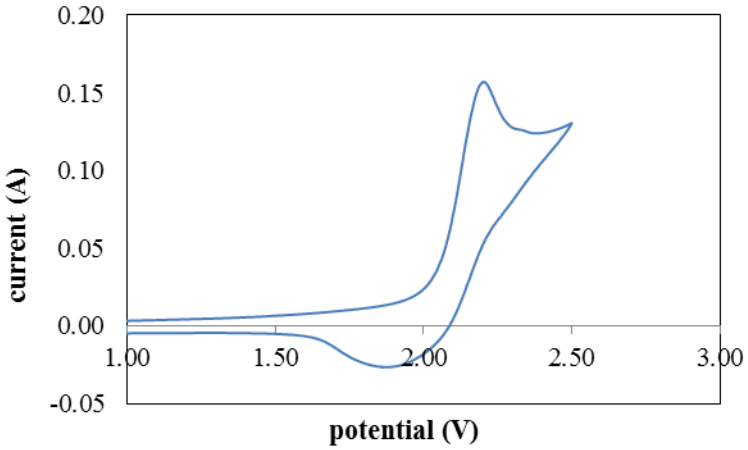

Figure 2-3. Cyclovoltammogram of $LiNO_3$ in MeCN at 25°C.

2.4.3. Spectroscopic Investigations

UV/VIS and emission spectroscopy

The UV-Vis measurements with online irradiation were performed on a self-made apparatus using a fluorescence cuvette in a fluorescence cuvette holder, LED (Cree-XP, royal blue, 455 nm) placed perpendicular to the optical pathway of the Agilent 8453 UV-Vis Spectrometer (Figure 2-4). The measurement was performed in 10 mm Hellma fluorescence quartz cuvettes (117.100F-QS) with a screw cap with PTFE-coated silicon septum. To obtain differential spectra the measured solution in darkness without LED irradiation was used as blank reference.

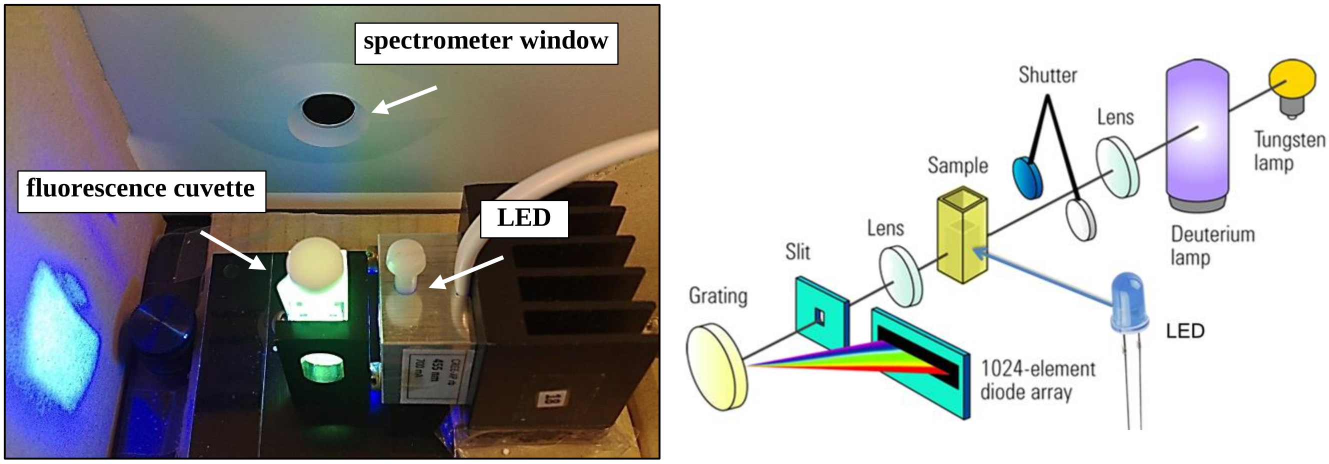
spectrometer window
fluorescence cuvette
LED
Shutter
Lens
Tungsten lamp
Sample
Lens
Deuterium lamp
Slit
Grating
LED
1024-element diode array

Figure 2-4. Setup for UV-Vis measurement with online irradiation.

The measurement was performed with a solution of 9-mesityl-10-methylacridinium perchlorate (**1**) (c= 5 µM) and $LiNO_3$ (c= 0,5 x 10^{-3} M) in MeCN under argon atmosphere. The spectra were taken online during irradiation. The aerated spectrum was taken after opening the cuvette and shaking the sample under continuous irradiation (Figure 2-5, green curve). The ground state absorption of the catalyst cannot be fully recovered due to photobleaching of the catalyst.

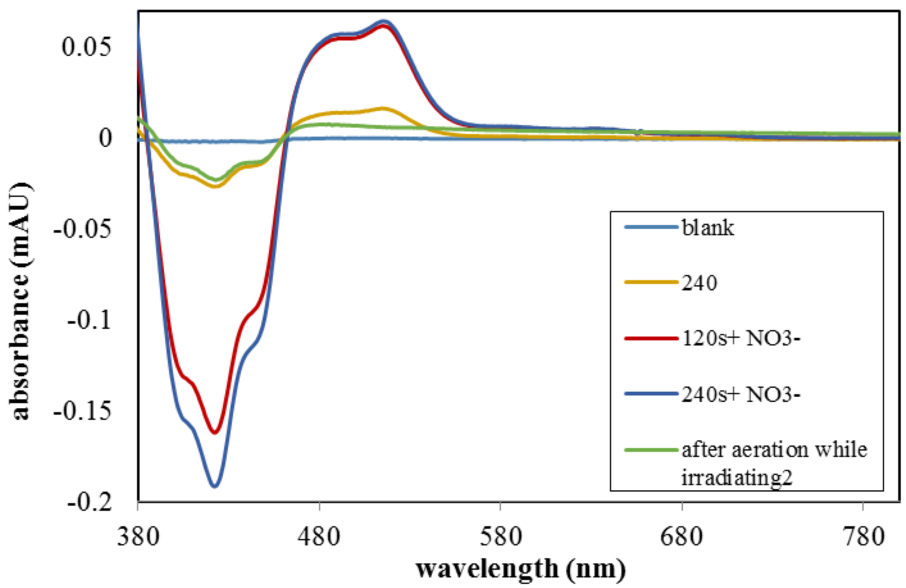

Figure 2-5. Spectra of the reduced catalyst **Acr$^{•}$-Mes** formed upon irradiation in the presence of LiNO$_3$ under inert atmosphere after 120 s (red) and 240 s (blue). The orange curve shows the catalyst after 240 s of irradiation without LiNO$_3$. The green curve shows the irradiated sample after exposure to air.

Fluorescence quenching

Fluorescence measurements were performed with Horiba FluoroMax-4 fluorimeter, 10 mm Hellma fluorescence quartz cuvettes (117.100F-QS) with a screw cap with PTFE-coated silicon septum was used. The quenching experiment was performed with a 5 µM solution of **Acr^{+}-Mes** in MeCN in open air with 50 eq. LiNO$_3$ (excitation wavelength: 420 nm).

UV/VIS

UV/Vis analyses were performed with Varian Cary 50 UV/Vis spectrophotometer and Agilent 8453 UV/Vis Spectrometer. To observe the photostability of the catalyst **1** (**Acr^{+}¬Mes**) during the reaction we measured a UV/Vis spectrum of the reaction mixture before the irradiation and after 1 h of irradiation. The reaction mixture contained *tert*-butylcyclohexanol (0.25 mmol), **1** (5 mol%) and LiNO$_3$ (0.5 mmol, 2 eq.) in 1 mL MeCN in open air, for UV/Vis measurements the solution was diluted 1:10 with pure MeCN. Figure 2-6 shows a strong photobleach of the catalyst **1** after 1 h of irradiation. This degradation of **1** is likely due to oxidation of the mesityl-moiety by NO$_3^{•}$.

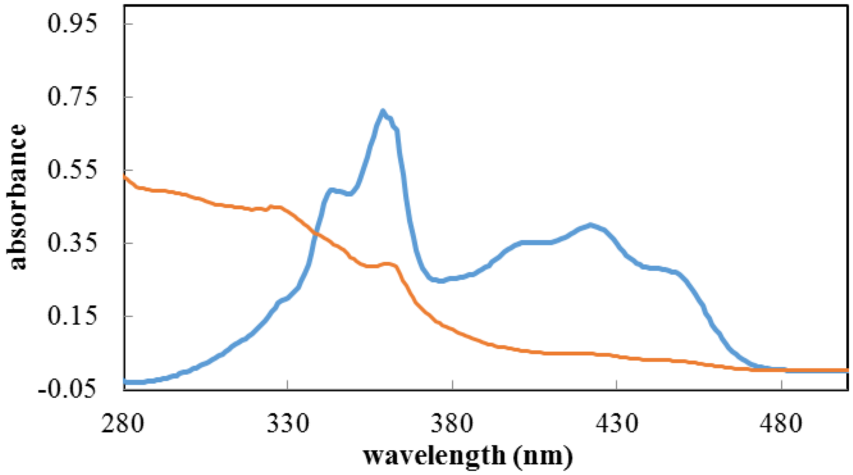

Figure 2-6. Absorption spectra of the reaction mixture before irradiation (blue curve) and after 1h of irradiation with 455 nm (red curve).

Laser flash photolysis

Materials. Burdick and Jackson HPLC grade acetonitrile and Aldrich tetrabutylammonium nitrate were sourced commercially and used as received. 9-Mesityl-10-methylacridinium Perchlorate was purchased from TCI chemicals and was recrystallized from MeOH/MeCN and ether prior to use.[26]

Laser Flash Photolysis studies were conducted on an Edinburgh Instruments LP920 spectrometer using the third harmonic of a Quantel Brilliant B Nd:YAG LASER (6 ns pulse, 355 nm) as the excitation source. All experiments were performed with the laser operating at a nominal power rating of 20-30 mJ per pulse. The detection system employs a Hammamatsu R2856 photomultiplier tube interfaced with a Tektroniz TDS 3012C Digital Phosphor oscilloscope for transient absorption spectra; wavelength resolved spectra were collected using an ANDOR DH720 ICCD camera. Measurements of the photochemical reactions of **Acr$^+$-Mes** with $NO_3^{\bullet}$ were performed according to the following procedure. MeCN solutions of **Acr$^+$-Mes** ClO_4 (1 x 10 $^{-4}$ M) were sparged with nitrogen alone or in the presence of $(Bu_4N)NO_3$ (1 x 10 $^{-3}$ M). Each individual transient and spectra represents 15-100 averages.

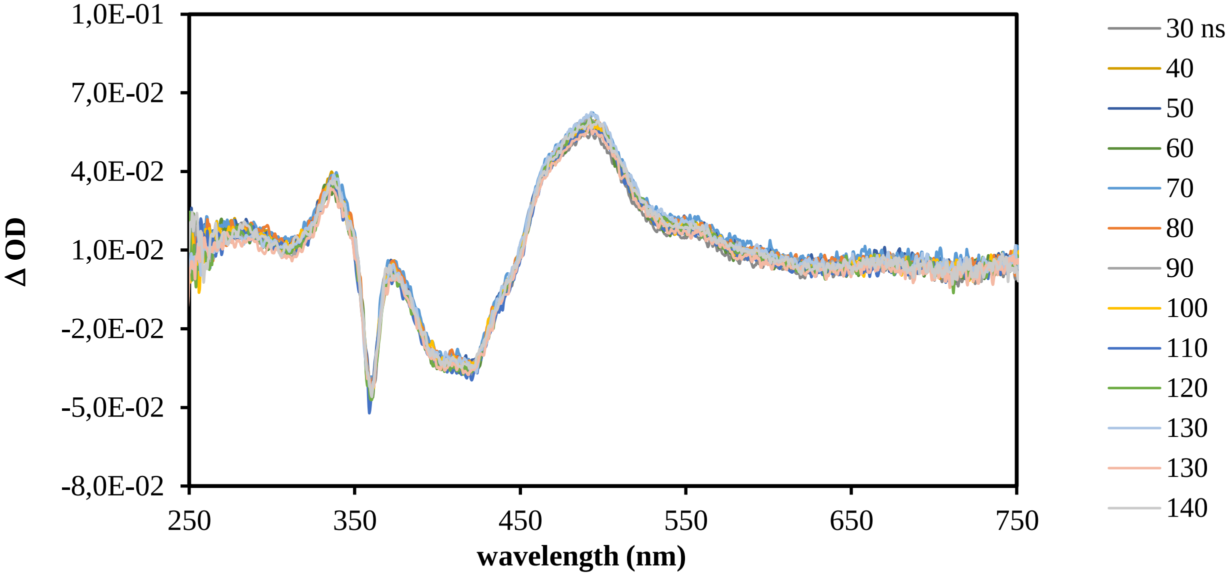

Figure 2-7. Laser flash photolysis of **Acr$^+$-Mes** and LiNO$_3$ under N$_2$-atmosphere.

As depicted in Figure 2-7 LFP measurements showed that no quenching of the observed excited triplet state (CT^T or LE^T) by NO$_3^-$ occurs. This supports a reaction from a short-lived singlet excited state as proposed in the mechanism. The singlet excited state has already decayed after 30 ns and thus cannot be observed. Figure 2-8 shows that in the measurements after 10 ns and 20 ns some contribution from the fluorescence of the singlet state can still be detected. The calculated differential spectra (red curve) of the measurement after 10 ns and 30 ns match with the reported fluorescence spectra.[23]

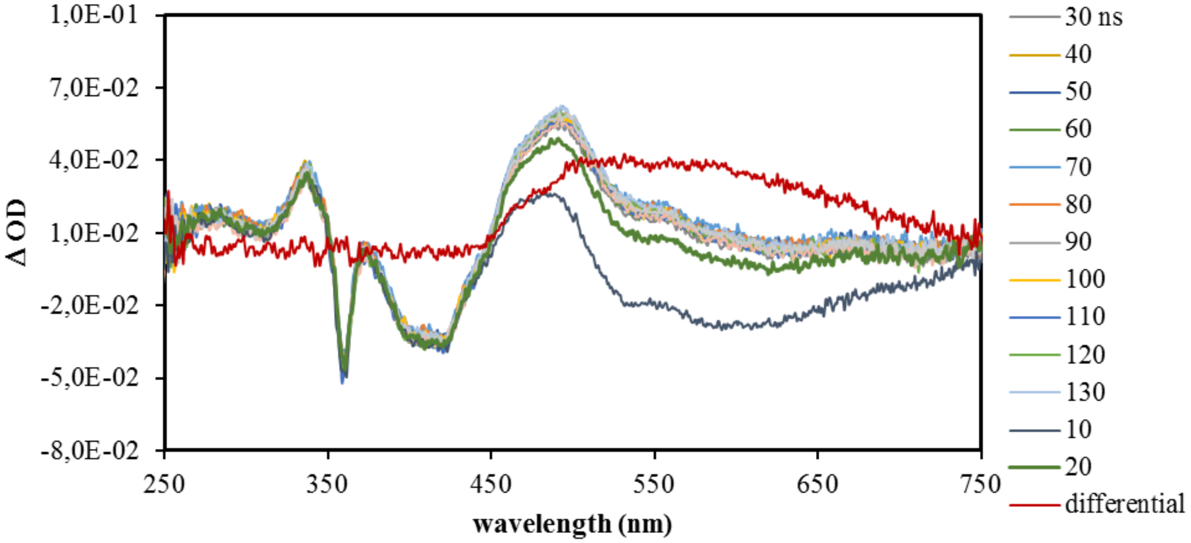

Figure 2-8. Measurements after 10 ns and 20 ns still show some contributions from the singlet state emission.

2.4.4. Synthetic Procedures

General procedure A: Photocatalytic oxidation of diphenylacetylene (2)

In a 5 mL crimp cap vial 45 mg (0.25 mmol, 1 eq.) diphenylacetylene (**2**), the respective amount of $LiNO_3$, and 5 mg (5 mol%) 9-mesityl-10-methylacridinium perchlorate (**1**) were dissolved in 1 mL MeCN, equipped with stirring bar and irradiated for 2 h with high power LEDs (λ_{max}= 455 nm) in open air. The temperature was kept constant at 22 °C. After the irradiation period 0.1 mmol of the GC-standard acetophenone (100 µL of a 1.0 M stock solution) was added to the reaction mixture. The mixture was filtered and submitted to GC analysis without further work-up.

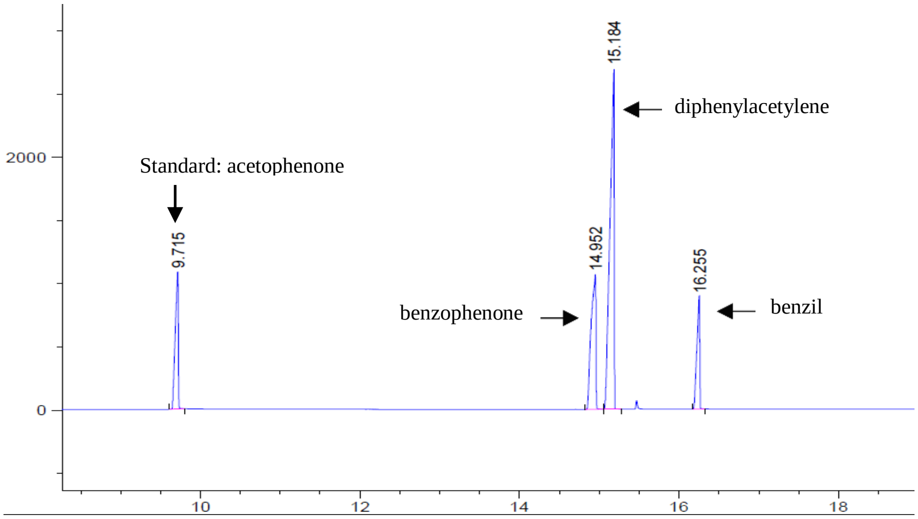

Figure 2-9. Example of the GC spectra obtained from the oxidation of compound **2**.

GC was calibrated using a three-point calibration; the calibration curve for benzil is shown as an example (Figure 2-10). The GC oven temperature program was adjusted as follows: initial temperature 40 °C was kept for 3 minutes, the temperature was increased at a rate of 15 °C/min over a period of 16 minutes until the final temperature (280 °C) was reached and kept for 5 minutes.

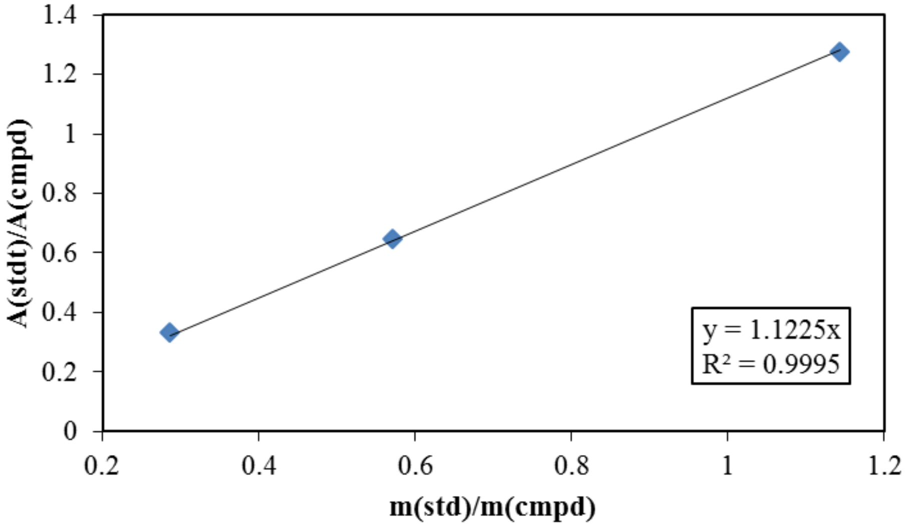

Figure 2-10. Exemplary calibration curve for benzil (**3**).

Photooxidation of Compound 9

Synthesis of starting materials **9a** and **9b** was performed according to literature known procedures.[17]

Two vials each with 52 mg (0.25 mmol, 1 eq.) of the alkyne ether **9** and 35 mg $LiNO_3$ (2 eq., 0.5 mmol) suspended in 0.5 mL of MeCN were irradiated with LEDs (λ=455 nm). To this mixture a solution of 5 mg (5 mol%) catalyst **1** was added via a syringe pump (rate: 0.5 mL/h). The total irradiation time was 6 h. After irradiation the two reaction mixtures were combined, diluted with water and extracted three times with diethyl ether. The combined organic layers were dried over Na_2SO_4, filtered and concentrated in vacuum. The resulting crude product was further purified by column chromatography using diethyl ether in pentane (2:10) as an eluent.

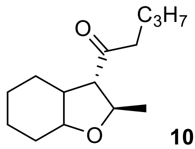

10a Yield: 21% (0.11 mmol)

NMR data is in accordance with literature.[27]

^{1}H NMR (300 MHz, $CDCl_3$) δ 4.36 (dq, *J* = 9.6, 6.4 Hz, 1H), 3.09 (td, *J* = 10.4, 3.8 Hz, 1H), 2.94 (dd, *J* = 11.1, 9.6 Hz, 1H), 2.34 (t, *J* = 7.4 Hz, 2H), 2.05 (dt, *J* = 7.0, 3.0 Hz, 1H), 1.80 (ddd, *J* = 12.2, 8.7, 3.1 Hz, 3H), 1.64 (dt, *J* = 19.1, 7.8 Hz, 2H), 1.57 – 1.42 (m, 2H), 1.41 – 1.08 (m, 7H), 0.98 (d, *J* = 6.4 Hz, 3H), 0.85 (t, *J* = 7.3 Hz, 3H).

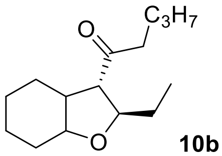

10b

Yield: 37% (0.19 mmol)

NMR data is in accordance with literature.[27]

^{1}H NMR (400 MHz, CDCl$_3$) δ 4.12 (td, *J* = 9.5, 3.8 Hz, 1H), 3.12 (td, *J* = 10.5, 3.8 Hz, 1H), 2.98 (dd, *J* = 10.9, 9.7 Hz, 1H), 2.39 (t, *J* = 7.4 Hz, 2H), 2.14 – 2.06 (m, 1H), 1.85 – 1.75 (m, 3H), 1.72 – 1.64 (m, 2H), 1.58 – 1.48 (m, 2H), 1.41 – 1.21 (m, 6H), 1.07 – 0.95 (m, 1H), 0.90 (m, 6H).
^{13}C NMR (75 MHz, CDCl$_3$) δ 210.0 (C$_{carbonyl}$), 82.5 (-(CH$_2$)$_2$-*CH*-O), 80.0 (-(CH$_2$)$_2$-*CH*-O), 58.9 (-CH-), 47.3 (-CH-), 45.2 (-CH$_2$-), 31.4 (-CH$_2$-), 28.2 (-CH$_2$-), 26.2 (-CH$_2$-), 25.6 (-CH$_2$-), 25.5 (-CH$_2$-), 24.2 (-CH$_2$-), 22.3 (-CH$_2$), 13.9 (-CH$_3$), 10.8 (-CH$_3$).

General Procedure B: Nitrate mediated alcohol oxidation

In a 5 mL crimp cap vial 0.25 mmol (1 eq.) of the alcohol, 17 mg (0.25 mmol, 1 eq.) LiNO$_3$, and 5 mg (5 mol%) 9-mesityl-10-methylacridinium perchlorate (**1**) were dissolved in 1 mL MeCN, equipped with stirring bar and irradiated with high power LEDs (λ= 455 nm) in open air until complete bleaching of the yellow color of catalyst **1** (ca. 2-3 h depending on the substrate). Then another 5 mg (5 mol%) of **1** was added to the reaction mixture and irradiated to a total time of 6 h. The temperature was kept constant at 22 °C. After the irradiation period the mixture was diluted with water and extracted three times with diethylether. The combined organic phases were dried over Na$_2$SO$_4$, filtered and concentrated in vacuum. The resulting crude product was further purified by column chromatography using petroleum ether/ ethyl acetate as the eluent (20-40 % ethyl acetate in petroleum ether).

4-(*tert*-Butyl)cyclohexan-1-one (14a)[34]

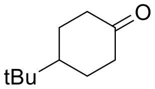

^{1}H NMR (300 MHz, CDCl$_3$) δ 2.42 – 2.27 (m, 4H), 2.12 – 2.05 (m, 2H), 1.50 – 1.39 (m, 3H), 0.92 (s, 9H).

Isomenthon (14b)[35]

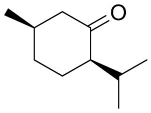

^{1}H NMR (300 MHz, CDCl$_3$) δ 2.35 – 2.25 (m, 1H), 2.15 – 2.06 (m, 1H), 2.05 – 1.89 (m, 3H), 1.78-1.63 (m, 2H), 1.54 – 1.38 (m, 2H), 0.99 (d, *J* = 6.5 Hz, 3H), 0.93 (d, *J* = 6.4 Hz, 3H), 0.84 (d, *J* = 6.5 Hz, 3H).

^{13}C NMR (75 MHz, CDCl$_3$) δ 213.8, 56.2, 47.0, 33.4, 28.4, 26.8, 25.9, 20.5, 19.9, 18.9.

(1S,4S)-1,7,7-Trimethylbicyclo[2.2.1]heptan-2-one (Camphor) (14c)[36]

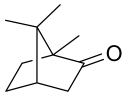

^{1}H NMR (300 MHz, CDCl$_3$) δ 2.40 – 2.27 (m, 1H), 2.08 (t, J = 4.5 Hz, 1H), 2.02 – 1.87 (m, 1H), 1.84 (d, *J* = 18.2 Hz, 1H), 1.74 – 1.57 (m, 2H), 1.46 – 1.26 (m, 2H), 0.95 (s, 3H), 0.90 (s, 3H), 0.83 (s, 3H).

4-Nitrobenzaldehyde (14d)[37]

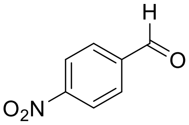

^{1}H NMR (300 MHz, CDCl$_3$) δ 10.16 (s, 1H), 8.40 (d, *J* = 8.7 Hz, 2H), 8.08 (d, *J* = 8.8 Hz, 2H).

Methyl 2-oxo-2-phenylacetate (14f)[38]

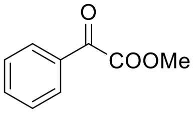

^{1}H NMR (300 MHz, CDCl$_3$) δ 8.05 – 7.99 (m, 2H), 7.67 (m, 1H), 7.56 – 7.47 (m, 2H), 3.98 (s, 3H).

^{13}C NMR (75 MHz, CDCl$_3$) δ 186.1, 164.1, 135.0, 132.4, 130.1, 128.9, 52.8.

2.4.5. Proposed Mechanism for the Photooxidation of Compound 9

Scheme 2-7 shows the mechanism of the cyclization as proposed in previous reports.[15, 17] In the first step a nitrate radical adds to the triple bond of alkyne-ether **9** which leads to a vinylic radical. Subsequent hydrogen abstraction of the H-atom in α-position of the ether leads to radical intermediate which cyclizes to product **10**. A crucial step which could account for lower yields is the non-regioselective first step, the addition of the nitrate radical to the alkyne **9**, if the opposite side of the triple bond is attacked, no product will be formed.

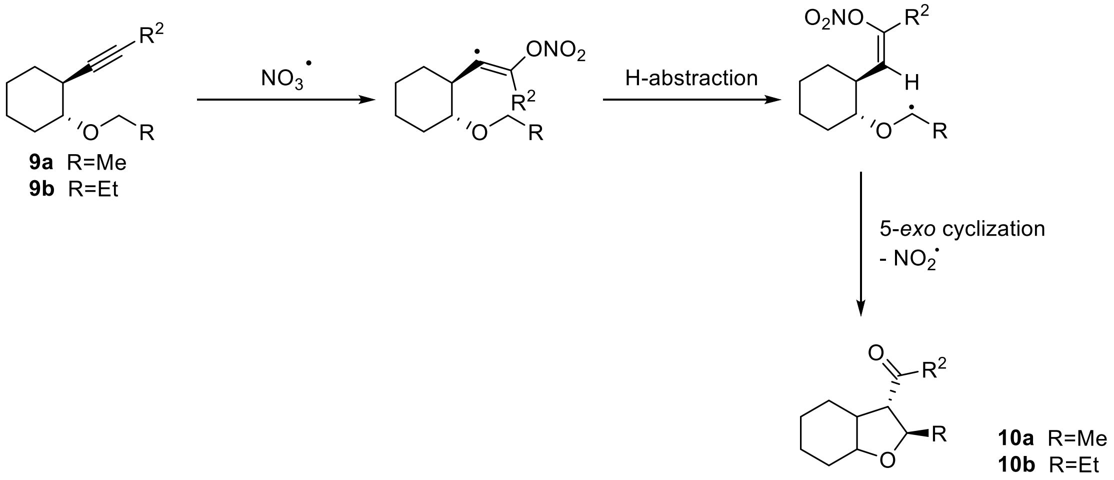

Scheme 2-7. Proposed mechanism for the self-terminating radical cyclization of **9** by $NO_3^{\bullet}$.

2.5. References

[1] R. P. Wayne, I. Barnes, P. Biggs, J. P. Burrows, C. E. Canosa-Mas, J. Hjorth, G. Le Bras, G. K. Moortgat, D. Perner, G. Poulet, G. Restelli, H. Sidebottom, *Atmospheric Environment. Part A. General Topics* **1991**, *25*, 1-203.

[2] M. P. Pérez-Casany, I. Nebot-Gil, J. Sánchez-Marín, F. Tomás-Vert, E. Martínez-Ataz, B. Cabañas-Galán, A. Aranda-Rubio, *J. Org. Chem.* **1998**, *63*, 6978-6983.

[3] H. Gong, A. Matsunaga, P. J. Ziemann, *J. Phys. Chem. A* **2005**, *109*, 4312-4324.

[4] J. C. Harrison, J. R. Wells, *Int. J. Chem. Kinet.* **2012**, *44*, 778-788.

[5] D. Rousse, C. George, *Phys. Chem. Chem. Phys.* **2004**, *6*, 3408-3414.

[6] S. Langer, E. Ljungstrom, I. Wangberg, *J. Chem. Soc., Faraday Trans.* **1993**, *89*, 425-431.

[7] O. Ito, S. Akiho, M. Iino, *J. Phys. Chem.* **1989**, *93*, 4079-4083.

[8] E. Baciocchi, T. D. Giacco, S. M. Murgia, G. V. Sebastiani, *J. Chem. Soc., Chem. Commun.* **1987**, 1246-1248.

[9] H. Suzuki, T. Mori, *J. Chem. Soc., Perkin Trans. 2* **1996**, 677-683.

[10] E. Baciocchi, I. Del Giacco, C. Rol, G. V. Sebastiani, *Tetrahedron Lett.* **1985**, *26*, 541-544.

[11] T. Shono, M. Chuankamnerdkarn, H. Maekawa, M. Ishifune, S. Kashimura, *Synthesis* **1994**, *1994*, 895-897.

[12] Andrey A. Fokin, Sergey A. Peleshanko, Pavel A. Gunchenko, Dmitriy V. Gusev, Peter R. Schreiner, *Eur. J. Org. Chem.* **2000**, *2000*, 3357-3362.

[13] M. Mella, M. Freccero, T. Soldi, E. Fasani, A. Albini, *J. Org. Chem.* **1996**, *61*, 1413-1422.

[14] U. Wille, *Chem. - Eur. J.* **2002**, *8*, 340-347.

[15] U. Wille, *J. Am. Chem. Soc.* **2001**, *124*, 14-15.

[16] U. Wille, *Chem. Rev.* **2012**, *113*, 813-853.

[17] U. Wille, L. Lietzau, *Tetrahedron* **1999**, *55*, 11465-11474.

[18] U. Wille, L. Lietzau, *Tetrahedron* **1999**, *55*, 10119-10134.

[19] L. F. Gamon, J. M. White, U. Wille, *Org. Biomol. Chem.* **2014**, *12*, 8280-8287.

[20] D. C. E. Sigmund, U. Wille, *Chem. Commun.* **2008**, 2121-2123.

[21] S. Fukuzumi, H. Kotani, K. Ohkubo, S. Ogo, N. V. Tkachenko, H. Lemmetyinen, *J. Am. Chem. Soc.* **2004**, *126*, 1600-1601.

[22] K. Ohkubo, K. Mizushima, R. Iwata, K. Souma, N. Suzuki, S. Fukuzumi, *Chem. Commun.* **2010**, *46*, 601-603.

[23] N. A. Romero, D. A. Nicewicz*, J. Am. Chem. Soc.* **2014**.

[24] K. Ohkubo, K. Mizushima, S. Fukuzumi, *Res. Chem. Intermed.* **2013**, *39*, 205-220.

[25] S. Fukuzumi, K. Ohkubo, T. Suenobu, *Acc. Chem. Res.* **2014**, *47*, 1455-1464.

[26] A. C. Benniston, A. Harriman, P. Li, J. P. Rostron, H. J. van Ramesdonk, M. M. Groeneveld, H. Zhang, J. W. Verhoeven, *J. Am. Chem. Soc.* **2005**, *127*, 16054-16064.

[27] U. Wille, J. Andropof*, Aust. J. Chem.* **2007**, *60*, 420-428.

[28] A. C. Benniston, K. J. Elliott, R. W. Harrington, W. Clegg, *Eur. J. Org. Chem.* **2009**, *2009*, 253-258.

[29] S. Langer, E. Ljungstrom, *J. Chem. Soc., Faraday Trans.* **1995**, *91*, 405-410.

[30] D. Kyriacou, *Modern Electroorganic Chemistry*, Springer-Verlag, Berlin, Heidelberg, **1994**.

[31] S. A. Styler, D. J. Donaldson, *Environmental Science & Technology* **2011**, *45*, 10004-10012.

[32] A. Thellend, P. Battioni, W. Sanderson, D. Mansuy, *Synthesis* **1997**, *1997*, 1387-1388.

[33] V. V. Pavlishchuk, A. W. Addison, *Inorg. Chim. Acta* **2000**, *298*, 97-102.

[34] B. Guan, D. Xing, G. Cai, X. Wan, N. Yu, Z. Fang, L. Yang, Z. Shi, *J. Am. Chem. Soc.* **2005**, *127*, 18004-18005.

[35] D. A. Lanfranchi, M.-C. Blanc, M. Vellutini, P. Bradesi, J. Casanova, F. Tomi, *Magn. Reson. Chem.* **2008**, *46*, 1188-1194.

[36] E. M. Elgendy, S. A. Khayyat, *Russ. J. Org. Chem.* **2008**, *44*, 814-822.

[37] Y. Yuan, X. Shi, W. Liu, *Synlett* **2011**, *2011*, 559-564.

[38] S. B. Salunke, N. S. Babu, C.-T. Chen, *Adv. Synth. Catal.* **2011**, *353*, 1234-1240.

CHAPTER 3

3. Halogenase Inspired Oxidative Chlorination Using Flavin Photocatalysis

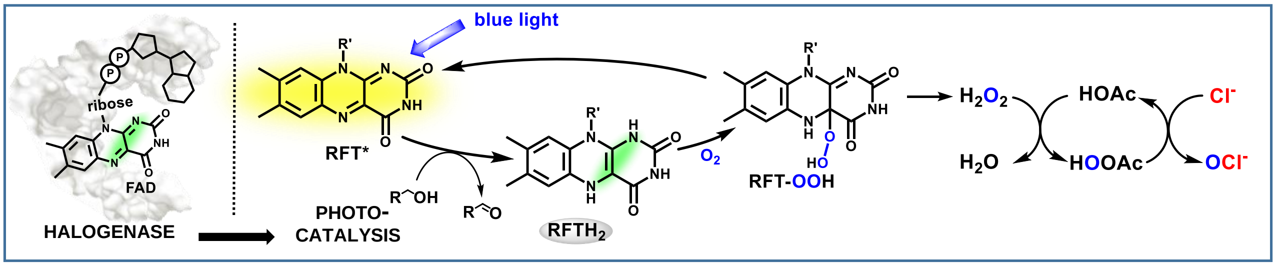
blue light
ribose
P
FAD
HALOGENASE
R'
RFT*
PHOTO-CATALYSIS
R OH
R O
RFTH$_2$
O$_2$
RFT-OOH
H$_2$O$_2$
H$_2$O
HOAc
HOOAc
Cl$^-$
OCl$^-$

This chapter was published in: T. Hering, B. Mühldorf, R. Wolf, B, König, *Angew. Chem. Int. Ed.* **2016**, *55*, 5342-5345.

TH performed the photocatalytic reactions and the synthesis of the chlorinated products. BM also performed photocatalytic reactions and carried out the GC-FID analysis. TH wrote the manuscript with contributions from BM. RW and BK supervised the project and are corresponding authors.

3.1. Introduction

Chlorinated aromatic compounds are ubiquitous in organic chemistry. They serve as key precursors for metal-catalyzed cross couplings and are widely employed in natural products, pharmaceuticals and material science to tune biological or electronic properties.[1-5] While traditional chemistry mostly relies on the use of hazardous and toxic chlorine gas or synthetic equivalents such as NCS and ^{t}BuOCl as the source of electrophilic chlorine, nature has developed a more elegant strategy based on the enzymatically catalyzed oxidation of abundant and non-toxic chloride ions in an oxidative chlorination.[6-7] Halogenases efficiently yield aryl halides from halide ions and aromatic compounds using either O_2 or hydrogen peroxide (haloperoxidases) as the oxidant.[8-10] With respect to environmental factors, these are the ideal oxidants as only water is produced as a by-product. For this reason a variety of chemical oxidative halogenations have been developed.[6-7] However, while great progress has been made in the area of oxidative bromination, oxidative chlorination remains challenging. The few examples known suffer from drastic conditions and low selectivity[6-7, 11-12] or rely on stronger or metal based stoichiometric oxidants.[13-22] Over the last years, halogenases have been successfully isolated and used for the halogenation (mostly bromination) of aromatic compounds.[23-32] These reactions show high selectivity and have also been scaled up to gram amounts,[24] but as the enzymes are naturally substrate specific the scope of accessible products is limited, and the isolation and handling of the enzymes is difficult.

We aimed to develop a biomimetic system inspired by flavin adenine dinucleotide (FAD)-dependent halogenases, which represent one of the main families of this enzyme group.[8] The FAD dependent system combines several advantages: O_2 is used as oxidant avoiding the separate addition of H_2O_2 as required for heme and vanadate dependent haloperoxidases. The cofactor FAD is a purely organic, metal-free catalyst, and simple flavin derivatives are known to act as oxidative photocatalysts.[33-34] The enzymatic mechanism (Scheme 3-1) involves the reduction of FAD by $NADH_2$ to yield a reduced $FADH_2$, which reacts with oxygen to form a peroxo species FAD-OOH that is subsequently attacked by chloride ions to form the "Cl^+" equivalent HOCl.[35] Our system replaces FAD by the cheap dye riboflavin tetraacetate (RFT), which is known to form reduced $RFTH_2$ upon excitation with visible light in the presence of benzyl alcohols (Scheme 3-1).[33-34] This allows us to replace the biomolecules FAD and $NADH_2$ and to perform the reactions in organic solvents using a stable and inexpensive catalyst.

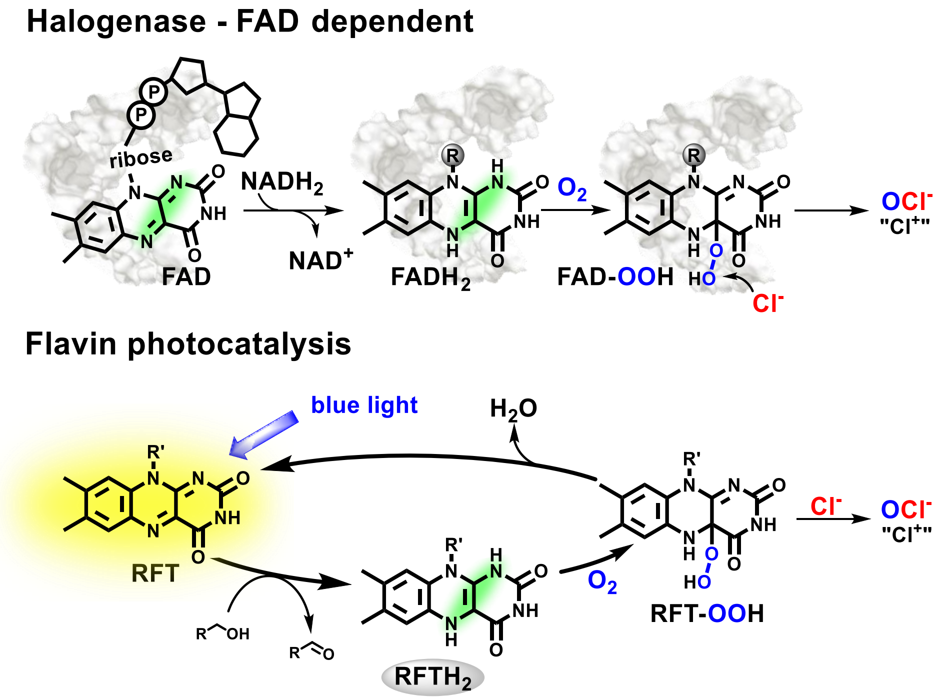

Halogenase - FAD dependent

Flavin photocatalysis

Scheme 3-1. Analogy of the mechanistic model of chloride oxidation by FAD-dependent halogenases (top) and the proposed photocatalytic halogenase mimetic system (bottom); R'=$CH_2(CHOAc)_3CH_2OAc$.

A key challenge in developing a photocatalytic halogenase mimetic system is the efficient generation of electrophilic hypochlorite. In analogy to the enzymatic system, $RFTH_2$ forms a short-lived flavin-peroxo species RFT-OOH, which should oxidize chloride ions to OCl^- (Scheme 3-1). However, in the enzyme the reaction of the flavin peroxide to form hypochlorite and the subsequent chlorination of the substrate are catalyzed by the complex enzyme environment. For some enzymes as RebH the mediation by a lysine residue in the active center is crucial for the reactivity and selectivity of the reaction. Moreover, X-ray studies of halogenases have shown that the substrate and the flavin peroxide (FAD-OOH) are brought in very close proximity (~10 Å) before a reaction takes place.[8, 36] This is also the reason why the simple chemical system, using anisole (**1**) as the substrate, 10 mol% RFT as the photocatalyst under aerobic conditions and irradiation with blue light (λ_{max} = 455 nm) in the presence of HCl as the chloride source and *p*-methoxy benzyl alcohol (*p*MBA) as a replacement for $NADH_2$ in 2 mL acetonitrile, did not yield any chlorination product of anisole (Scheme 3-2).

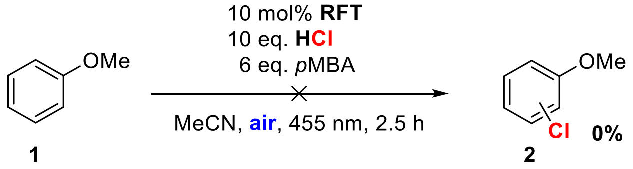

Scheme 3-2. Test reaction for the chlorination of anisole (**1**) with the photocatalytic system using 20 µmol of **1** in 2 mL acetonitrile.

In order to chemically mimic the enzymatic system, a mediator is needed, which is sufficiently long lived in order to enable the formation of perchloric acid. During the course of our investigations we discovered that peracetic acid can oxidize chloride ions and is able to perform oxidative chlorination of aromatic compounds (Experimental Section, Table 3-3).[37-38] Peracetic acid is highly explosive when isolated, but it can be formed in equilibrium with acetic acid and H_2O_2.[39-40] As it is known that RFT−OOH formed in the photocatalytic oxidation quickly releases one equivalent of H_2O_2,[33] we added 10 eq. of acetic acid to the system described above and, to our delight, observed the chlorination of anisole (**1**).

Control reactions showed that all reaction components are essential to observe the chlorination reaction (Experimental Section, Table 3-2). Based on this we propose an *in situ* formation of peracetic acid as depicted in Figure 1, which acts as the described mediator and enables the chlorination via the following reaction cycle. In the first step, the photocatalyst RFT is excited by visible light irradiation (λ_{max}= 455 nm) to RFT* and reduced to $RFTH_2$ by oxidation of the benzylic alcohol (*p*MBA). $RFTH_2$ is re-oxidized by air forming H_2O_2, which does not directly oxidize chloride, but forms peracetic acid (HOOAc) in an equilibrium with acetic acid (HOAc). The hereby *in situ* generated HOOAc subsequently reacts with chloride to form the electrophilic chlorine species HOCl, which attacks anisole (**1**) in an electrophilic aromatic substitution reaction. However, we cannot exclude other electrophilic chlorine species in equilibrium with HOCl, e.g. Cl_2O, ClOAc, Cl_2 and H_2OCl^+, be involved.[12, 41-42]

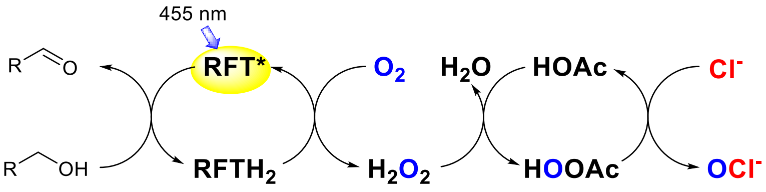

Figure 3-1. Proposed mechanistic scheme of the peracetic acid mediated oxidation of chloride by flavin photocatalysis.

With this mechanistic model in hand we optimized the reaction conditions for the highest formation of peracetic acid (see Experimental Section). The equilibrium of H_2O_2 and acetic acid is known to be shifted towards the side of peracetic acid by strong acids.[39] Therefore, hydrochloric acid proved to be the ideal chloride source as it dissolved well in acetonitrile and is a strong acid at the same time. The reaction with triethylammonium chloride (TEACl) and 20 mol% H_2SO_4 also led to product formation, but with a slightly lower yield. No chlorination was observed with any of the tested chloride salts (TEACl, NaCl, KCl, and NH_4Cl) in the absence of added acid. Furthermore, elevated temperatures are known to be beneficial for peracetic acid formation.[40] An increase of the reaction temperature from 25 °C to 45 °C improved the yield of chloroanisole (**2**) from 28% to 66% (p:o 5:1); a further increase to 60 °C led to decomposition of the photocatalyst (Experimental Section, Table 3-5). We also varied the peracid and replaced acetic acid by the stronger acids formic acid and triflic acid (Experimental Section, Table 3-4). Formic acid showed significantly lower yields than acetic acid, while triflic acid with 5 eq. TEACl and 5 eq. HCl gave a comparable yield of the chlorinated anisole. Alternative reagents for the generation of peracetic acid such as acetic anhydride or acetyl chloride enabled product formation, but were less efficient than acetic acid.

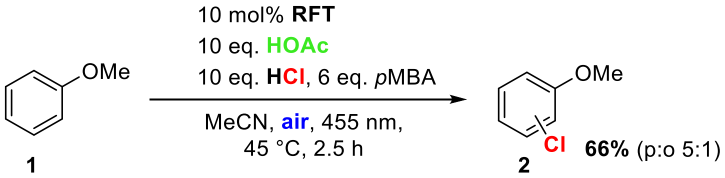

Scheme 3-3. Oxidative chlorination of anisole (**1**) with the photocatalytic halogenase mimetic system.

The optimized conditions depicted in Scheme 3-3 were used to investigate the substrate scope. While an enzyme usually has a highly specific binding pocket and thus a narrow substrate scope, but high selectivity, our system does not bind the substrate and should allow a broader substrate scope. The results are summarized in Table 3-1. The system works excellently for arenes with nitrogen +M substituents such as *N*,*N*-dimethylaniline (entry 1) or amides (entries 2,3). Substrates with an alkoxy group, such as anisole (entry 4) or diphenylether (entry 5), can also be successfully chlorinated in good to moderate yields. When the arene is too electron rich, as for example in dimethoxybenzene carrying two +M-substituents, the yield decreases due to the unselective direct oxidation of the substrate by the photocatalyst (entry 6). The acidic conditions lead to a protonation of RFT observable by UV/VIS measurements (Experimental Section, Figure 3-5, 3-6). In its protonated form RFT is known to have a high oxidative power.[43] Substrates, which are too electron poor, e.g. trifluoromethoxybenzene (entry 7), are not attacked by hypochlorite and do not give chlorination products neither in the photocatalytic system nor if peracetic acid is added directly (Experimental Section, Table 3-3). Acetophenones (entries 9, 10) are mono-chlorinated in the α-position. The reaction proceeds via the enol form and therefore works better when the stronger triflic acid is used instead of acetic acid.[a] It is worth noting that aromatic amines (entries 1, 8) show *ortho* selectivity for the chlorination. This may be explained by the intermediate formation of an *N*-chloramine. This selectivity is not observed with amides (entries 2, 3).

For comparison, Table 3-1 also shows the yields of chlorination obtained by adding 6 eq. of H_2O_2 directly to the reaction mixture instead of being generated by the photocatalytic process (reaction contained no RFT and *p*MBA). Even though the direct addition of H_2O_2 always gave full conversion of the substrate, the yields were considerably lower for most substrates than in the photocatalytic system. The slow generation of peroxide by the flavin-catalyzed process is beneficial for the reaction as it circumvents the problem of unselective side reactions and over-chlorination often observed for H_2O_2-based systems. The same observation was made for haloperoxidase-catalyzed reactions.[27]

---

[a] Incomplete conversion is observed as the required keto-enol equilibrium slows down the reaction. If the reaction of the substrate and the peracetic acid is not fast enough, a Bayer-Villiger type background reaction of the benzaldehyde consumes the peracid, see M. Matsumoto, K. Kobayashi, Y. Hotta, *J. Org. Chem.* **1984**, *49*, 4740-4741.

Table 3-1. Scope of the flavin-catalyzed oxidative chlorination and results obtained by direct addition of H_2O_2.[a]

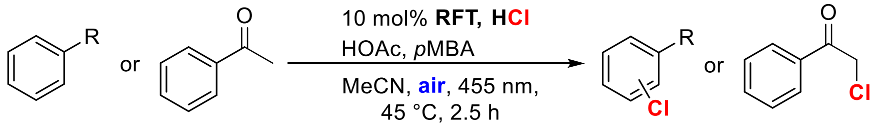

entry	substrate	product	conv./ %^{b}	yield/ %^{b,c}	H_2O_2^{d}
1	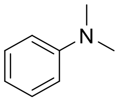 **3**	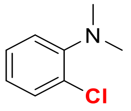 **4**	100	**96** (o:di 2:1)	14 (o:di 1:0)
2[e]	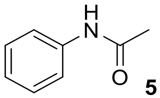 **5**	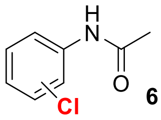 **6**	100	**97** (p:o 3:1)	37 (p:o 1:0)
3[e]	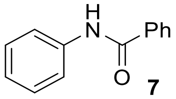 **7**	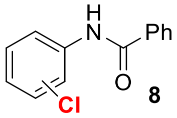 **8**	96	**98** (p:o 5: 1)	24
4	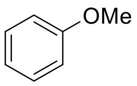 **9**	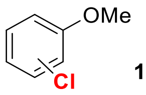 **10**	100	**66** (p:o 5:1)	17
5	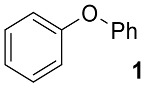 **11**	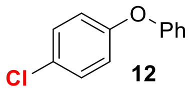 **12**	79	**80**	55
6	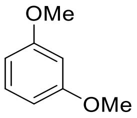 **13**	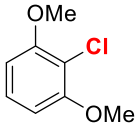 **14**	100	**40**	23
7	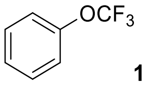 **15**	--	0	--	--
8	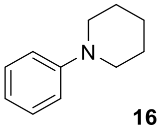 **16**	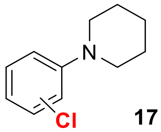 **17**	70	**64**	68
9[f]	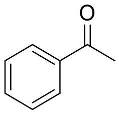 **18**	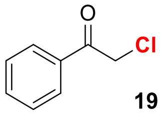 **19**	76	**63**	11
10[f]	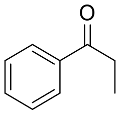 **20**	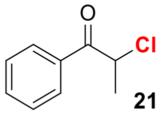 **21**	49	**64**	84

[a] Reactions were performed with 0.02 mmol of the substrate, 10 eq. HCl, 10 eq. HOAc, 6 eq. *p*MBA and 10 mol% RFT in 2.0 mL MeCN. The reaction mixtures were irradiated for 2.5 h at 45 °C. [b] determined by GC-FID using an internal standard [c] based on conversion [d] 6 eq. H_2O_2 10 eq. HOAc and 10 eq. HCl in 2 mL MeCN [e] with KCl addition [f] with TFA.

3.2. Conclusion

In conclusion, visible light flavin photocatalysis allows the oxidative chlorination of arenes inspired by FAD-dependent halogenases. The biomolecules FAD and $NADH_2$ were replaced by the cheap organic dye riboflavin tetraacetate and methoxy benzyl alcohol as the reducing agent. As a result, the reaction can be performed in organic media. Acetic acid was added to the system forming peracetic acid *in situ*, which acts as a mediator to activate the peroxide for chloride oxidation. Compared to the specific binding pocket of an enzyme, the activation by peracetic acid is a more general strategy and thus allows a broader substrate scope. The developed system allows the chlorination of electron rich arenes, e.g. anisole, methylanilines, diphenyl ether and amides, as well as the α-chlorination of acetophenones.

3.3. Experimental Section

3.3.1. General Information

Chemicals: RFT was prepared according to a known literature procedure.[44] All other chemicals were obtained commercially (Sigma Aldrich, VWR or TCI) or synthesized according to known literature procedures; **4**,[45] **8**,[46] and **17**,[47]. Compounds **12** and **21** were synthesized using a scaled up reaction of peracetic acid described in the general procedure for reactions with peracetic acid.

Photochemical set-up, LEDs: Photocatalytic reactions were performed with 455 nm LEDs (OSRAM Oslon SSL 80 royal-blue LEDs, λ_{em} = 455 nm (± 15 nm), 3.5 V, 700 mA). Reaction vials (5 mL crimp cap vials, no cap) were illuminated from the bottom with LEDs and cooled or heated from the side using custom made aluminum cooling block connected to a thermostat. A magnetic stirrer is placed below the LED array.

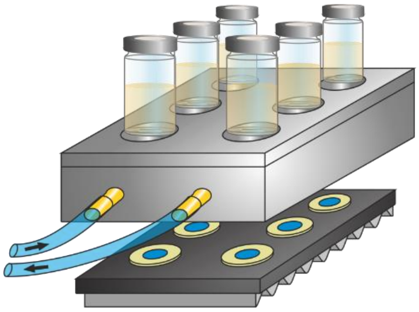

Figure 3-2. Photochemical reaction set-up.

3.3.2. General Procedure for the Photocatalytic Chlorination

In a vial 0.02 mmol of the respective substrate, together with 10 mol% (0.002 mmol) RFT, 0.2 mmol (10 eq.) HCl, 0.2 mmol (10 eq.) HOAc (or TFA) and 0.12 mmol (6 eq.) *p*-methoxy benzylalcohol were dissolved in 2 mL of dry acetonitrile. The reaction mixture was irradiated under stirring for 2.5 h using the set-up depicted in Figure 3-2. After the irradiation the internal standard (0.01 mmol *n*-pentadecane) was added to the reaction and the reaction was immediately quenched with sat. Na_2CO_3-solution and brine. The mixture was extracted with ethyl acetate and subjected to GC-FID analysis.

3.3.3. GC-FID Measurements

The GC oven temperature program was adjusted as follows: The initial temperature of 60 °C was kept for 3 minutes, the temperature was increased at a rate of 20 °C/min until the final temperature (290 °C) was reached and kept for 2 minutes; internal standard: *n*-pentadecane.

For substrates with lower boiling points a slightly different method was applied: The initial temperature of 60 °C was kept for 3 minutes, the temperature was increased at a rate of 25 °C/min until the final temperature (160 °C) was reached and kept for 5 minutes; internal standard: *n*-pentadecane

GC was calibrated using a six-point calibration; the calibration curve for *o*-chloranisole is shown as an example. Authentic samples of each compound were used for calibration.

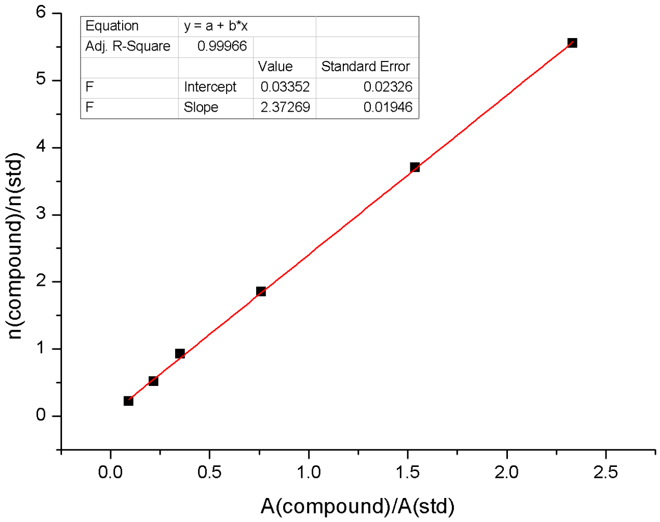

Figure 3-3. Exemplary calibration curve for *o*-chloranisole.

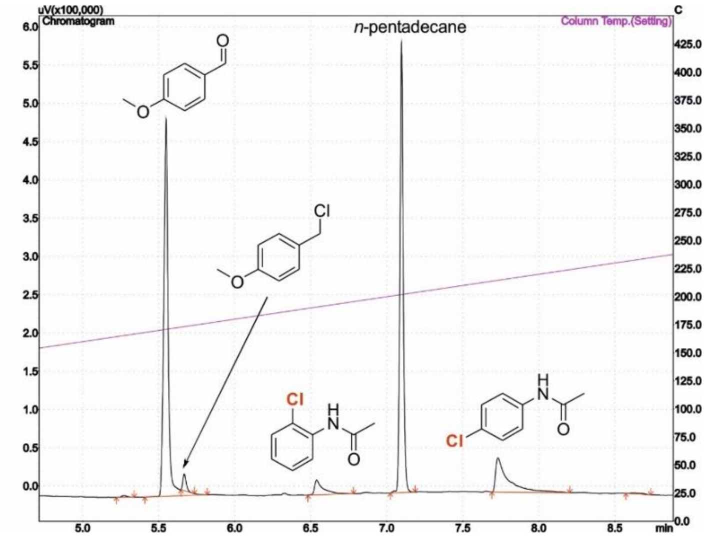

Figure 3-4. Example of the GC spectra obtained from the chlorination of acetanilide (**5**).

3.3.4. Control Reactions

Control reactions were performed using equal amounts of the respective compounds as described in the general procedure. Work-up and analysis was done accordingly. No chlorination product was observed, when any of the components was omitted or the reaction was kept in the dark (entry 9). As described in the manuscript an unproductive background reaction occurred with protonated RFT.

Table 3-2. Control reactions.

entry	condition	conversion/ %[a]	yield/ %[a]
1	RFT, anisole	17	0
2	RFT, anisole, HCl	100	0
3	RFT, anisole, HCl, HOAc	100	0
4	RFT, anisole, *p*MBA	24	0
5	RFT, anisole, *p*MBA, HOAc	100	0
6	RFT, anisole, *p*MBA, HCl	100	0
7	anisole, HCl	0	0
8	anisole, HOAc, HCl	0	0
9	no light	28	0

[a] Determined by GC-FID using an internal standard.

3.3.5. Reactions with Peracetic Acid

Peracetic acid can be used as a stoichiometric oxidant in oxidative chlorination. Table 3-3 shows the yields of oxidative chlorination obtained for the substrates described in the manuscript. The results were obtained using the following procedure.

General procedure for the reaction with peracetic acid

In a vial 0.02 mmol of the respective substrate, 10 eq. HCl and 0.024 mmol (1.2 eq) peracetic acid were dissolved in 2.5 mL MeCN. The reaction mixture was stirred for 2.5 h at r.t.. Afterwards the internal standard (0.01 mmol *n*-pentadecane) was added to the reaction and the reaction was immediately quenched with sat. Na_2CO_3-solution and brine. The mixture was extracted with ethyl acetate and subjected to GC-FID analysis.

For all substrates except for the electron poor compound **15** the corresponding chlorinated product was obtained. This observation proves that peracetic acid induces oxidative chlorination. However, for most substrates the use of peracetic acid employed directly will lead to an undesired double chlorination. The high reactivity of peracetic acid leads to overchlorination if used as a reagent directly, but is beneficial for the use as a mediator generated slowly in small amount as in the flavin photocatalysis.

Table 3-3. Oxidative chlorination using peracetic acid as the stoichiometric oxidant.

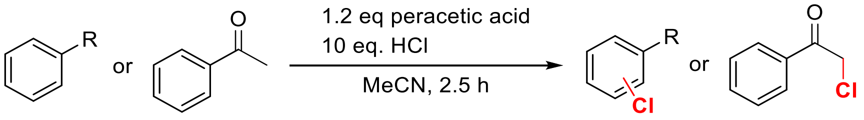

entry	substrate	yield/ %[a]	double chlorination/ %[a]
1	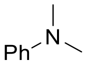 **3**	50 (p:o 0:100)	32
2	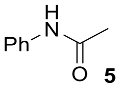 **5**	68 (p:o 5:1)	--
3	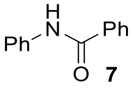 **7**	>99	0
4	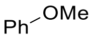 **9**	65 (p:o 15:1)	13
5[b]	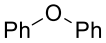 **11**	46	48[b]
6	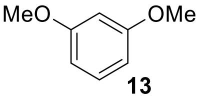 **13**	82	0
7	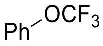 **15**	--	--
8[b]	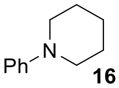 **16**	64 (p:o 1:11)	25
9	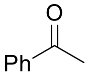 **18**	64	8
10[b]	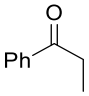 **20**	84	18

[a] Obtained by GC-FID analysis using *n*-petadecane as the internal standard. [b] Calibration factor for the monochlorinated product was used for estimation of the double chlorination.

3.3.6. Optimization of the Reaction Conditions

As described in the manuscript Table 3-4 summarized the results of the screening of different routes for the generation of peracetic acid (entries 1-6) and the variation of the peracid (entries 7-11). The most efficient generation of peracetic acid was achieved by a combination of acetic acid and hydrochloric acid (entry 1), even though acetic anhydride and acetyl chloride showed formation of chloroanisol, but in significantly lower yields. Triflic acid yielded the best results when a combination of hydrochloric acid and TEACl was used as the chloride source (entry 8).

Table 3-4. Variation of the peracid and chloride source.

entry	system	conv. /%[a]	yield /%[a]
1	**HOAc (10 eq.), HCl (10 eq.)**	**100**	**66**
2	HOAc (10 eq.), KCl	97	0
3	HOAc (10 eq.), TEACl (10 eq.), 20 mol% H_2SO_4	100	34
4	Ac_2O (10 eq.), HCl (10 eq.)	86	28
5	acetyl chloride (10 eq.)	100	17
6	acetyl chloride (10 eq.), HCl (5 eq.)	85	15
7	TFA (10 eq.), HCl (10 eq.)	65	27
8	**TFA (10 eq.), HCl (5 eq.), TEACl (5 eq.)**	**100**	**57**
9	TFA (10 eq.), KCl	100	30
10	HCOOH (10 eq.), HCl (10 eq.)	86	42
11	HCOOH (10 eq.), TEACl (10 eq.)	40	0

[a] Determined by GC-FID using an internal standard.

The temperature dependence of the reaction is shown in Table 3-5.

Table 3-5. Temperature dependence of the reaction.

entry	temperature	yield/ %[a]	conv. anisole/ %[a]
1	25 °C	28	98
2	35 °C	35	64
3	**45 °C**	**66**	**100**
4	45 °C (5 mol% RFT)	46	62
5	60 °C	0	16

[a] Determined by GC-FID using an internal standard.

Table 3-6 shows the screening of solvents known to lead to an efficient photooxidation of *p*MBA and hence formation of H_2O_2. Except for MeCN, none of the investigated solvents led to formation of the chlorinated product. Even though water is reported to be beneficial for the oxidation of *p*MBA, it prevents productive formation of peracetic acid as it shifts the equilibrium (equ. 1) to the side of acetic acid.

$$\mathrm{HOAc} + \mathrm{H_2O_2} \rightleftharpoons \mathrm{HOOAc} + \mathrm{H_2O} \qquad \text{(equ. 1)}$$

Table 3-6. Solvent screening at 45 °C.[a]

entry	solvent	yield/ %[b]	conv. anisole/ %[b]
1	MeOH	0	9
2	MeOH/MeCN 1:1	0	64
3	DMSO	0	10
4	MeCN/H_2O 2:1	0	56
5	**MeCN, dry**	**66**	**95**

[a] Average over 2 reactions [b] Yields determined by GC-FID analysis.

3.3.7. UV/VIS Spectroscopy

The UV-Vis measurements with online irradiation were performed on a self-made apparatus using a fluorescence cuvette in a fluorescence cuvette holder, LED (Cree-XP, royal blue, 455 nm) placed perpendicular to the optical pathway of the Agilent 8453 UV-Vis Spectrometer. The measurement was performed in 10 mm Hellma fluorescence quartz cuvettes (117.100F-QS).

First, we monitored the change of the absorption bands of RFT in the presence of HCl in MeCN (Figure 3-5). The formation of an absorption band is observed at λ_{max} = 390 nm, which is assigned to the protonated species $RFTH^+$.[43] We irradiated a degassed mixture of RFT and *p*MBA in MeCN in the presence of HCl and HOAc (Figure 3-6). The absorption band at λ_{max} = 390 nm decreases under irradiation, whereas the formation of a distinct broad band at λ_{max} = 460-530 nm is observed. This broad band is characteristic for $^2RFTH_2^{\bullet+}$, which is generated by protonation of the reduced flavin species $^2RFTH^{\bullet}$ under acid conditions.[43]

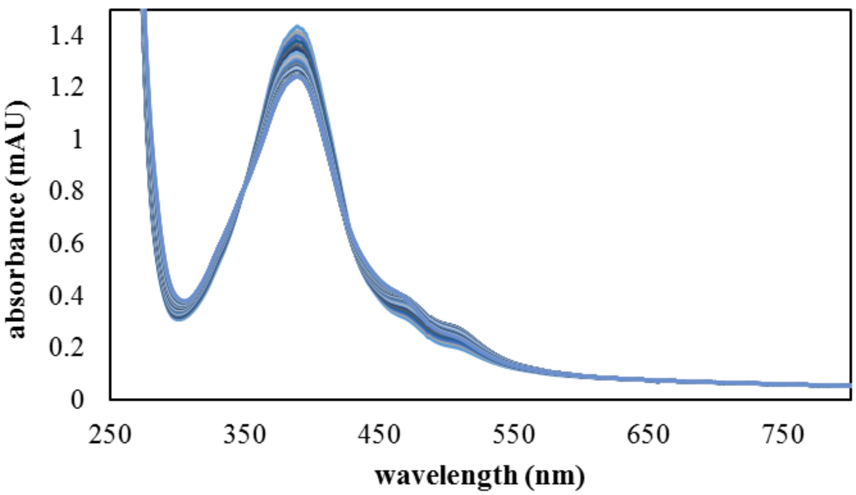

Figure 3-5. Electronic absorption spectra of RFT (0.1 mM, blue) in the presence of HCl in MeCN at 298 K. The spectra were measured over 6 min recording one spectra every 10 s.

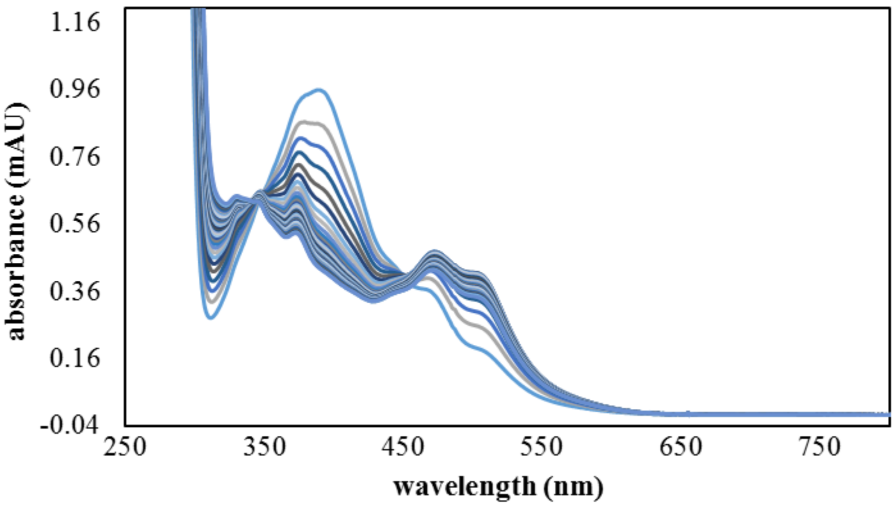

Figure 3-6. Electronic absorption spectra of *p*MBA (6.7 mM) and RFT (0.1 mM) in the presence of HCl while irradiating with blue light in MeCN at 298 K. The spectra were measured over 6 min recording one spectra every 10 s.

3.4. References

[1] J. Fauvarque, *Pure Appl. Chem.* **1996**, *68*, 1713-1720.

[2] A. F. Littke, G. C. Fu, *Angew. Chem., Int. Ed.* **2002**, *41*, 4176-4211.

[3] A. F. Littke, G. C. Fu, *Angew. Chem.* **2002**, *114*, 4350-4386.

[4] G. W. Gribble, *J. Chem. Educ.* **2004**, *81*, 1441-1449.

[5] H. Liu, X. Cao, Y. Wu, Q. Liao, A. J. Jimenez, F. Würthner, H. Fu, *Chem. Commun.* **2014**, *50*, 4620-4623.

[6] A. Podgoršek, M. Zupan, J. Iskra, *Angew. Chem., Int. Ed.* **2009**, *48*, 8424-8450.

[7] A. Podgoršek, M. Zupan, J. Iskra, *Angew. Chem.* **2009**, *121*, 8576-8603.

[8] F. H. Vaillancourt, E. Yeh, D. A. Vosburg, S. Garneau-Tsodikova, C. T. Walsh, *Chem. Rev.* **2006**, *106*, 3364-3378.

[9] A. Butler, M. Sandy, *Nature* **2009**, *460*, 848-854.

[10] J. M. Winter, B. S. Moore, *J. Biol. Chem.* **2009**, *284*, 18577-18581.

[11] A. O. Terent'ev, S. V. Khodykin, N. A. Troitskii, Y. N. Ogibin, G. I. Nikishin, *Synthesis* **2004**, *2004*, 2845-2848.

[12] R. Ben-Daniel, S. P. de Visser, S. Shaik, R. Neumann, *J. Am. Chem. Soc.* **2003**, *125*, 12116-12117.

[13] L. Gu, T. Lu, M. Zhang, L. Tou, Y. Zhang, *Adv. Synth. Catal.* **2013**, *355*, 1077-1082.

[14] K.-D. Umland, C. Mayer, S. F. Kirsch, *Synlett* **2014**, *25*, 813-816.

[15] J.-Y. Wang, Q. Jiang, C.-C. Guo, *Synth. Commun.* **2014**, *44*, 3130-3138.

[16] Z. Cong, T. Kurahashi, H. Fujii, *Angew. Chem., Int. Ed.* **2011**, *50*, 9935-9939.

[17] Z. Cong, T. Kurahashi, H. Fujii, *Angew. Chem.* **2011**, *123*, 10109-10113.

[18] A. K. Vardhaman, P. Barman, S. Kumar, C. V. Sastri, D. Kumar, S. P. de Visser, *Chem. Commun.* **2013**, *49*, 10926-10928.

[19] P. J. Hansen, J. H. Espenson, *Inorg. Chem.* **1995**, *34*, 5839-5844.

[20] R. Prebil, S. Stavber, *Adv. Synth. Catal.* **2014**, *356*, 1266-1274.

[21] P. Pandit, K. S. Gayen, S. Khamarui, N. Chatterjee, D. K. Maiti, *Chem. Commun.* **2011**, *47*, 6933-6935.

[22] P. B. Thorat, B. Y. Bhong, N. N. Karade, *Synlett* **2013**, *24*, 2061-2066.

[23] S. A. Shepherd, C. Karthikeyan, J. Latham, A.-W. Struck, M. L. Thompson, B. R. K. Menon, M. Q. Styles, C. Levy, D. Leys, J. Micklefield, *Chem. Sci.* **2015**, *6*, 3454-3460.

[24] M. Frese, N. Sewald, *Angew. Chem., Int. Ed.* **2015**, *54*, 298-301.

[25] M. Frese, N. Sewald, *Angew. Chem.* **2015**, *127*, 302-305.

[26] D. R. M. Smith, S. Grüschow, R. J. M. Goss, *Curr. Opin. Chem. Biol.* **2013**, *17*, 276-283.

[27] F. Sabuzi, E. Churakova, P. Galloni, R. Wever, F. Hollmann, B. Floris, V. Conte, *Eur. J. Inorg. Chem.* **2015**, *2015*, 3519-3525.

[28] E. Fernández-Fueyo, M. van Wingerden, R. Renirie, R. Wever, Y. Ni, D. Holtmann, F. Hollmann, *ChemCatChem* **2015**, *7*, 4035-4038.

[29] J. T. Payne, M. C. Andorfer, J. C. Lewis, *Angew. Chem., Int. Ed.* **2013**, *52*, 5271-5274.

[30] J. T. Payne, M. C. Andorfer, J. C. Lewis, *Angew. Chem.* **2013**, *125*, 5379-5382.

[31] J. T. Payne, C. B. Poor, J. C. Lewis, *Angew. Chem., Int. Ed.* **2015**, *54*, 4226-4230.

[32] J. T. Payne, C. B. Poor, J. C. Lewis, *Angew. Chem.* **2015**, *127*, 4300-4304.

[33] U. Megerle, M. Wenninger, R.-J. Kutta, R. Lechner, B. König, B. Dick, E. Riedle, *Phys. Chem. Chem. Phys.* **2011**, *13*, 8869-8880.

[34] R. Lechner, S. Kümmel, B. König, *Photochem. Photobiol. Sci.* **2010**, *9*, 1367-1377.

[35] E. Yeh, L. J. Cole, E. W. Barr, J. M. Bollinger, D. P. Ballou, C. T. Walsh, *Biochemistry* **2006**, *45*, 7904-7912.

[36] E. Yeh, L. C. Blasiak, A. Koglin, C. L. Drennan, C. T. Walsh, *Biochemistry* **2007**, *46*, 1284-1292.

[37] Y. He, C. R. Goldsmith, *Synlett* **2010**, 1377-1380.

[38] Peracetic acid itself has not been extensively used for oxidative chlorination. However, we noticed that a number of oxidative chlorination reactions with hydrogen peroxide were performed in acetic acid as the solvent. We assume also that in these cases an in situ formation of peracetic acid might be responsible for the reactivity, see: a) references in A. Podgoršek, M. Zupan, J. Iskra, *Angew. Chem., Int. Ed.* **2009**, *48*, 8424-8450. b) N. I. Rudakova, Y. G. Erykalov, *Russ. J. Gen.Chem.* **2005**, *75*, 748-750. c) G. Jerzy, Ż. Slawomir, *Synth. Commun.* **1997**, *27*, 3291-3299.

[39] H. Klenk, P. H. Götz, R. Siegmeier, W. Mayr, in *Ullmann's Encyclopedia of Industrial Chemistry*, Wiley-VCH Verlag GmbH & Co. KGaA, **2000**.

[40] X. Zhao, T. Zhang, Y. Zhou, D. Liu, *J. Mol. Catal. A: Chem.* **2007**, *271*, 246-252.

[41] C. G. Swain, D. R. Crist, *J. Am. Chem. Soc.* **1972**, *94*, 3195-3200.

[42] P. B. D. de la Mare, I. C. Hilton, C. A. Vernon, *Journal of the Chemical Society (Resumed)* **1960**, 4039-4044.

[43] S. Fukuzumi, S. Kuroda, *Res. Chem. Intermed.* **1999**, *25*, 789-811.

[44] S. Alagaratnam, N. J. Meeuwenoord, J. A. Navarro, M. Hervás, M. A. De la Rosa, M. Hoffmann, O. Einsle, M. Ubbink, G. W. Canters, *FEBS J.* **2011**, *278*, 1506-1521.

[45] Y. Lv, Y. Zheng, Y. Li, T. Xiong, J. Zhang, Q. Liu, Q. Zhang, *Chem. Commun.* **2013**, *49*, 8866-8868.

[46] A. M. C. H. van den Nieuwendijk, D. Pietra, L. Heitman, A. Göblyös, A. P. Ijzerman, *J. Med. Chem.* **2004**, *47*, 663-672.

[47] X.-Z. Shu, X.-F. Xia, Y.-F. Yang, K.-G. Ji, X.-Y. Liu, Y.-M. Liang, *J. Org. Chem.* **2009**, *74*, 7464-7469.

CHAPTER 4

---

4. Photocatalytic Activation of *N*−Chloro Compounds for the Chlorination of Arenes

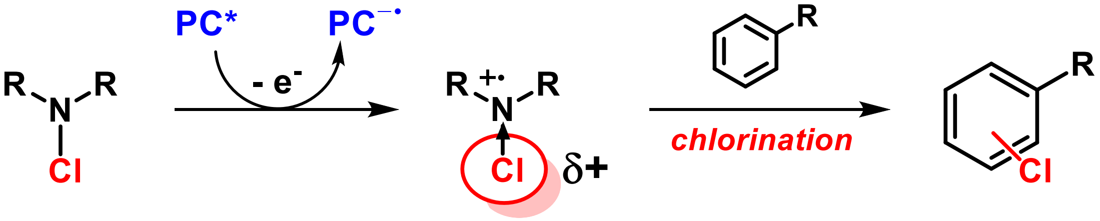

This chapter was submitted for publication: T. Hering, B. König, **2016**, *submitted*.

TH carried out all reactions and wrote the chapter. Bernd Mühldorf performed the GC analysis of Table 4-4 and 4-5. BK supervised the project.

4.1. Introduction

Chlorinated aromatic compounds can be found in many pharmaceuticals, agrochemicals, and polymers and serve as starting materials for the synthesis of organometallic reagents. Moreover, they are versatile synthetic precursors for metal catalyzed cross-couplings.[1-4] Due to the importance of aromatic chlorides the development of efficient strategies for the electrophilic chlorination of arenes under mild conditions is still of great interest. Since chloride usually does not undergo electrophilic aromatic substitution but rather reacts as a nucleophile these transformations require the use of a “Cl^+” reagent. Traditional electrophilic chlorination reagents as Cl_2, SO_2Cl_2 and *t*BuOCl have a high reactivity, but are also very aggressive and hence relatively unselective.[1, 5-6] Their hazardous properties make them difficult to handle and limit their practical application. *N*−Chloro compounds, such as *N*−chlorosuccinimide (NCS), *N*−chloramines or modern guanidine based reagents (Palau’chlor)[7] are valuable alternatives as they contain positively polarized chlorine atoms and are inexpensive and easy to handle. However, except for Palau’chlor, which requires a multi-step synthesis, they show only moderate reactivity and often need activation by redox active metals,[8-10] Lewis[11-13] or Brønsted acids[14-15] or radical initiators.[16] Most of these activations rely on an increase of the N−Cl bond polarization by decreasing the electron density on the nitrogen e.g. by coordination of a Lewis acid or protonation of the nitrogen. An analogous effect can be achieved by photocatalytic oxidation of the nitrogen atom to a radical cation **2** as depicted in Scheme 4-1. The resulting radical cation **2** should have a significantly enhanced reactivity compared to the neutral *N*−chloro compound **1** since the positive charge on the nitrogen pulls electron density from the chlorine and induces a strong positive polarization (δ+).

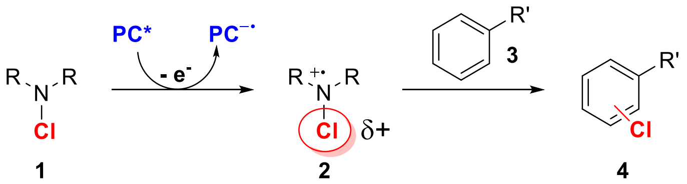

Scheme 4-1. General Scheme of the oxidative activation of *N*−chloro compounds by photoredox catalysis (PC= photocatalyst).

The use of photoredox catalysis to oxidize **1** would offer a mild way to catalytically activate *N*−chloramines/−amides by visible light at room temperature. This strategy could be a practical alternative to conventional activation pathways.

4.2. Activation of *N*−Chloramines

There are few reports known using *N*−chloramines as starting materials in photoredox catalysis. However, these examples are not based on the oxidation of *N*−chloramines to activate them for electrophilic chlorination, but rather on the reduction to induce a cleavage of Cl^- yielding a nitrogen centered radical, which reacts further to form a C−N-bond.[17-18] Even though in some examples chloride is later incorporated into the product, it always reacts as a nucleophile and not as an electrophile. To investigate whether *N*−chloramines (**1**) can also be activated by photocatalytic oxidation to undergo electrophilic aromatic substitution (S_EAr), we chose the chlorination of an electron rich arene, namely dimethoxybenzene (**3a**) as a model reaction: A solution of **3a** (0.25 mmol), the *N*−chloramine **1a** (1.2 eq.), the photocatalyst $[Ru(bpy)_3]Cl_2$ (5 mol%) and ammonium peroxodisulfate (1.2 eq.) to reoxidize the photocatalyst in MeCN was irradiated under N_2-atmosphere over night with blue LEDs (λ_{max}= 455 nm). The photocatalytic reaction yielded 13% of the chlorinated arene **4a** whereas without irradiation no chlorination was observed.

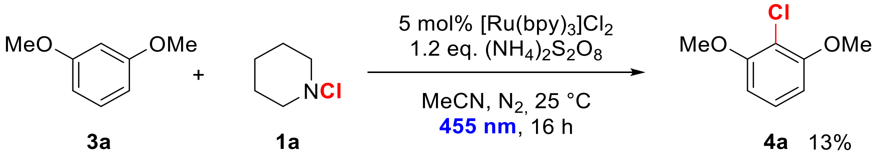

Scheme 4-2. Test reaction for the photocatalytic chlorination of dimethoxybenzene (**3a**) with 1-chlororpiperidine (**1a**).

Even though the yield of chlorination was low, these initial results showed that *N*−chloramines can be activated for S_EAr by photocatalytic oxidation. Thereupon we aimed to optimize the reaction conditions. First we investigated whether the metal based photocatalyst $[Ru(bpy)_3]Cl_2$ can be replaced by cheap organic dyes such as eosin Y or 9-mesityl-10-methylacridinium perchlorate (Acr^+-Mes) (Figure 4-1). The redox properties of eosin Y ($E^0_{(EY*/EY^{\bullet-})}$ = 0.79 V vs. SCE) are similar to $[Ru(bpy)_3]Cl_2$ ($E^0_{(Ru(II)*/Ru(I))}$= 0.77 V vs. SCE),[19] nevertheless only traces of chlorination could be obtained when using 10 mol% eosin Y instead of $[Ru(bpy)_3]Cl_2$ (yield **4a** <5%). Next we tested Acr^+-Mes which is a very strong oxidant in its excited state ($E^0_{(MA^+*/MA^\bullet)}$ = 2.08 V vs. SCE)[20] but despite this high oxidative power the catalyst was less efficient in this transformation than $[Ru(bpy)_3]Cl_2$ (yield **4a** 7%). A possible complication with this catalyst could be that its oxidation potential is sufficiently high to oxidize dimethoxybenzene (**3a**) directly and thus leads to undesired side reactions.[21]

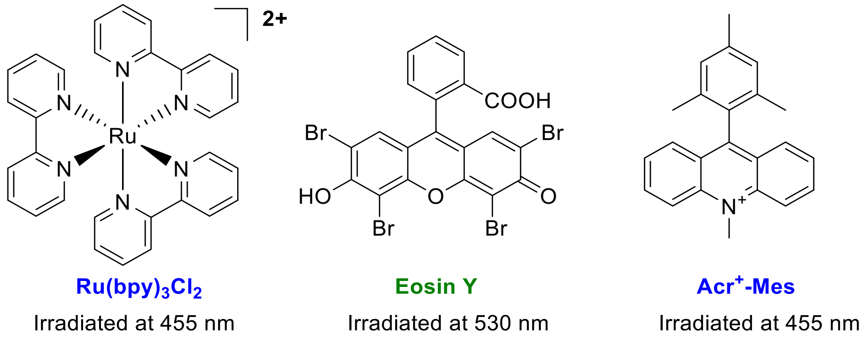

Figure 4-1. Employed photocatalyst and the wavelength used for irradiation.

Next, we varied the *N*−chloramine to investigate the influence of the substituents on the nitrogen. The results of this screening are depicted in Table 4-1. The highest yields of chlorinated dimethoxybenzene **4a** were obtained using 1-chloromorpholine (**1b**) (74%, entry 2), which is except for the heteroatom structurally very similar to the previously employed piperidine derivative (**1a**, entry 1). The *N*−chloro compounds with benzyl groups **1c** and with “push-pull” substituents **1d** (entries 3, 4) gave comparable yields, but are unfavorable with respect to atom economy. Further optimization of the reaction was therefore carried out using 1-chloromorpholine (**1b**).

Table 4-1. Variation of the *N*−chloro compound using the reaction conditions depicted in Scheme 4-2.[a]

entry	*N*−chloro compound	yield (%)[b]	conversion (%)[b]
1	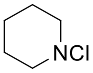 **1a**	13	26
2	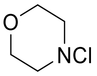 **1b**	**74**	**>99**
3	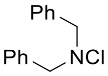 **1c**	62	>99
4	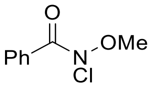 **1d**	61	>99

[a] Reactions were carried out using 0.25 mmol **3a**, 1.2 eq of the respective *N*−chloro compound, 1.2 eq $(NH_4)_2S_2O_8$, and 5 mol% $[Ru(bpy)_3]Cl_2$ x 6 H_2O in 1.5 mL MeCN. The irradiation time (λ_{max}= 455 nm) was 16 h. [b] Determined by GC analysis using anisole as the internal standard.

Having identified the suitable *N*−chloramine, we continued with varying the solvent of the reaction (Table 4-2). All polar solvents and DCM (entries 1-4) showed conversion to the desired product **4b**, whereas the non-polar solvents toluene and 1,2-dichloroethane (1,2-DCE) gave only minor product formation (entries 5, 6). This observation can be explained by the different solubility of the photocatalyst, which poorly dissolves in non-polar solvents. The reaction was most efficient in a mixture of MeCN and water (entry 4), which even led to double chlorination. The enhanced reactivity when water is added to the reaction presumably results from a higher solubility of peroxodisulfate ensuring a quicker regeneration of the photocatalyst.

Table 4-2. Results of the solvent screening.[a]

entry	solvent	yield (%)[b]	conversion (%)[b]
1	MeCN	74	>99
2	MeOH	42	60
3	DCM	45	45
4	MeCN/H_2O 3:1	**48** **+ double chlorin.**	**>99**
5	toluene	<5	<5
6	1,2-DCE	7	22

[a] Reactions were carried out using 0.25 mmol **3a**, 1.2 eq **1b**, 1.2 eq $(NH_4)_2S_2O_8$, and 5 mol% $[Ru(bpy)_3]Cl_2$ x 6 H_2O in 1.5 mL of the respective solvent. The irradiation time (λ_{max}= 455 nm) was 16 h. [b] Determined by GC analysis using anisole as the internal standard.

For further studies the substrate was changed from dimethoxybenzene (**3a**) to the less electron rich anisole (**3b**) since this will circumvent the problem of double chlorination. Table 4-3 summarizes the main results of the reaction optimization. First, we continued the solvent screening and tested different MeCN/H_2O ratios (Table 4-3, entries 1-3). The reaction using a 4:1 mixture of MeCN and H_2O showed an excellent yield of 95%. Using this solvent mixture the catalyst loading could be lowered to 2 mol% without a change in the yield. A further decrease to 1 mol% showed a slightly decreased yield of 80% (entries 2, 4, 5). Neither the addition of base (entries 6, 7) nor acid (entry 8) or a higher amount of the *N*−chloramine **1b** (entry 9) improved the yield further. The conducted control reactions (entries 10-12) showed that no efficient reaction is observed without light, without the catalyst or without $(NH_4)_2S_2O_8$ respectively. Low amounts of product obtained in the reaction without light and without the catalyst (entries 11, 12) indicate that $(NH_4)_2S_2O_8$ is to some extend able to oxidize the *N*−chloramine **1b**. The *N*−chloro compound **1b** itself cannot chlorinate anisole directly (entry 10).

Table 4-3. Reaction optimization with anisole (**3b**) as the substrate.

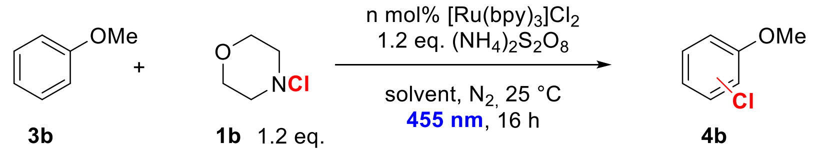

entry	reaction condition	yield (%)[a]	p/o ratio (p:o)	conversion (%)[a]
1[b]	5 mol% $Ru(bpy)_3Cl_2$, MeCN	26	(11:1)	46
2[b]	5 mol% $Ru(bpy)_3Cl_2$, MeCN/H_2O 9:1	88	(5:1)	>99
3	5 mol% $Ru(bpy)_3Cl_2$, MeCN/H_2O 4:1	95	(5:1)	95
4[b]	2 mol% $Ru(bpy)_3Cl_2$, MeCN/H_2O 9:1	90	(5:1)	90
5[b]	1 mol% $Ru(bpy)_3Cl_2$, MeCN/H_2O 9:1	80	(5:1)	83
6	5 mol% $Ru(bpy)_3Cl_2$, MeCN, NaOAc	70	(6:1)	83
7	5 mol% $Ru(bpy)_3Cl_2$, MeCN, pyridine	13	(5:1)	32
8	5 mol% $Ru(bpy)_3Cl_2$, MeCN, HCl 2 M	76	(6:1)	88
9	5 mol% $Ru(bpy)_3Cl_2$, MeCN/H_2O 9:1, 2 eq. **1b**	76	(5:1)	>99
10	5 mol% $Ru(bpy)_3Cl_2$, MeCN/H_2O 9:1, **no $(NH_4)_2S_2O_8$**	0	--	0
11	**no $Ru(bpy)_3Cl_2$**, MeCN/H_2O 9:1	27	(4:1)	48
12	5 mol% $Ru(bpy)_3Cl_2$, MeCN/H_2O 9:1, **no light**	18	(3:1)	33

[a] Determined by GC analysis using toluene as the internal standard. [b] Average over two reactions.

Having optimized the reaction conditions we explored the scope of the reaction towards different arenes (Table 4-4). Electron rich substrates with a +M-substituent such as anisole, dimethoxybenzene, phenol and acetanilide can be chlorinated in good yields (entries 1-5). The aromatic amine **3f** (entry 6) showed only a moderate yield of 39%. The chlorination yield is probably diminished by an unproductive direct oxidation of the amine by the excited photocatalyst.[22] Unfortunately, the reaction is limited to electron rich arenes with +M-substituents, arenes with +I-substituents such as xylene and toluene gave only little chlorinated product (entries 8, 9). No chlorination could be observed for more electron poor substrates as chlorobenzene (entry 10). This suggests that the polarization of the N−Cl-bond induced by photocatalytic oxidation of the nitrogen atom is not strong enough to obtain highly electrophilic chlorine. Hence, the reaction only proceeds with very electron rich substrates. Furthermore, we tried to use the developed method for the α-chlorination of acetophenone, but could only detect traces of chloracetophenone (entry 11).

Table 4-4. Scope of the visible light mediated chlorination of arenes with *N*−chloramines.[a]

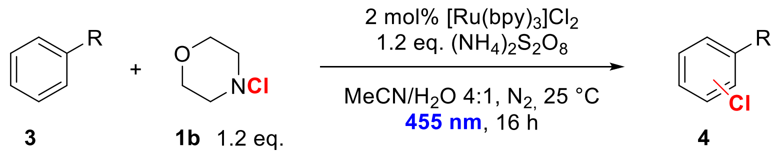

entry	substrate	conversion/ %[b]	yield/ %[b]	selectivity (p/o)
1	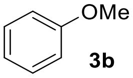 **3b**	95	95	5:1
2[c]	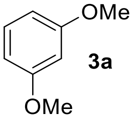 **3a**	>99	74	100:0
3[d]	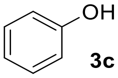 **3c**	100	66	2:1
4	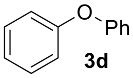 **3d**	55	41	13:1
5	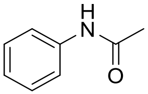 **3e**	83	75	2:1
6	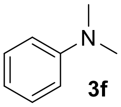 **3f**	100	39	1:1
7	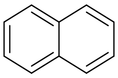 **3g**	20	20	100:0[e]
8	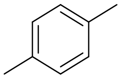 **3h**	24	9	2:1[f]
9	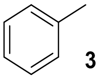 **3i**	23	<5	--
10	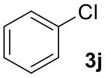 **3j**	0	0	--
11	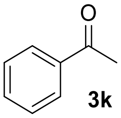 **3k**	14	<5	--

[a] Reactions were carried out using 0.25 mmol of the arene **3**, 1.2 eq **1b**, 1.2 eq $(NH_4)_2S_2O_8$, and 2 mol% $[Ru(bpy)_3]Cl_2$ x 6 H_2O in 1.5 mL MeCN/H_2O 4:1. The irradiation time (λ_{max}= 455 nm) was 16 h. [b] Determined by GC analysis. [c] In MeCN [d] 3 mL solvent [e] 1-chloronaphthalenen [f] 2-chloroxylene:α-chloroxylene.

Despite the limitation concerning the substrate scope, we were able to show that photoredox catalysis is suitable for activating *N*−chloramines for electrophilic aromatic chlorination and can serve as an alternative to existing activation methods.

From a synthetic point it would be very interesting to incorporate both the chlorine as well as the amine part into the product to obtain an amino-chlorination (Scheme 4-3, compound 8).

Therefore we applied our reaction conditions for the chlorination of styrene (**5**) to obtain the aminochlorinated product **8**. A similar reaction has been described for styrene using chloramine T as the *N*−chloro compound and CO_2 as the oxidant.[23] However, in our case no aminochlorination could be observed. Instead only 1,2-dichlorethylbenzene (**7**) and the chlorohydrin **6** formed by attack of water was obtained.

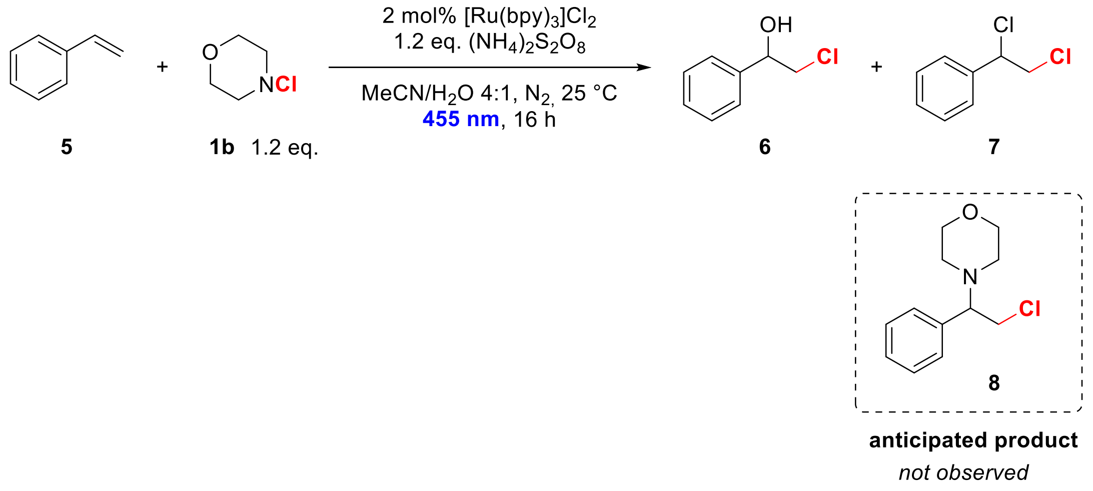

Scheme 4-3. Chlorination of styrene (**5**) by the photocatalytic reaction using 1-chloromorpholine (**1b**) as the chlorine source. The anticipated product **8** with incorporation of the amine moiety is depicted in the dashed box.

4.3. Activation of NCS

N−Chlorosuccinimide (NCS) is a well-known and widely used chlorination reagent, generally requires activation. The electron density on the nitrogen atom is significantly reduced by two electron withdrawing groups compared to *N*−chloramines. Accordingly the chlorine atom on NCS is more electrophilic leading to a higher reactivity in S_EAr. With photocatalytically activated NCS it should therefore be possible to chlorinate also less electron rich substrates as xylene and toluene, which were not accessible by *N*−chloramines. On the other hand the electron withdrawing groups make the oxidative activation of NCS more challenging as they increase the oxidation potential significantly. To investigate whether the oxidation potential is still within the range of the photocatalyst $[Ru(bpy)_3]Cl_2$, cyclic voltammetry was measured (see Experimental Part, Figure 4-3). The obtained potential for the oxidation of NCS of 1.10 V vs. SCE would be too high for an oxidation from the excited state of the photocatalyst (Scheme 4-4) as proposed in the previous paragraph for *N*−chloramines. However, the potential of Ru(III) which can be accessed by oxidative quenching of the excited catalyst Ru(II)* would be sufficient to perform the oxidation of NCS. Ru(II)* can be oxidized to Ru(III) by $(NH_4)_2S_2O_8$[24] which was also employed in the reactions with *N*−chloramines to reoxidize Ru(I).

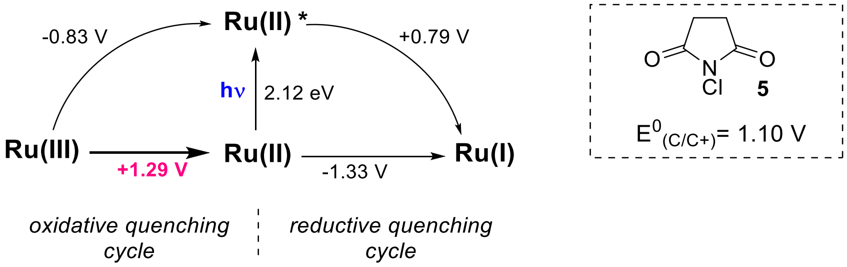

Scheme 4-4. Redox properties of the photocatalyst $[Ru(bpy)_3]Cl_2$ and oxidation potential of NCS. Potentials are given vs. SCE.[24]

Based on the redox potentials it is likely that the previously described photocatalytic activation of the easily oxidizable *N*−chloramines proceeds via the reductive quenching of Ru(II)* (reductive quenching cycle) while the more challenging oxidation of NCS has to proceed via the oxidative quenching cycle where Ru(II)* is first quenched by $(NH_4)_2S_2O_8$ to give the strongly oxidizing Ru(III). From a thermodynamic point the photocatalytic activation of NCS by the developed system is therefore feasible. This would be, to the best of our knowledge, the first photocatalytic activation of NCS for S_NAr. Cho *et al.* recently reported visible light mediated *in situ* formation of acid chlorides using NCS as a reagent.[25] However, this reaction proceeds via the transfer of a chlorine radical to a photocatalytically formed acyl radical and does not involve a direct interaction of the photocatalyst and NCS.

To test whether the developed reaction conditions indeed lead to an enhanced activity of NCS for electrophilic chlorination of arenes, we monitored the reaction of NCS with anisole with and without the activation by photoredox catalysis over a period of 180 min. The results are summarized in Figure 4-2. For the photocatalytic reaction a solution of anisole (**3b**), NCS (**5**, 1.2 eq.), $(NH_4)_2S_2O_8$ (1.2 eq.) and 2 mol% of the photocatalyst in 2 mL MeCN/water 4:1 was irradiated with 455 nm under N_2-atmosphere. Samples were taken after 30 min, 75 min, 120 min and 180 min. For comparison a parallel reaction with only anisole (**3b**) and NCS (1.2 eq.) in 2 mL MeCN/water 4:1 was performed and samples were taken at the same time intervals. Figure 4-2 shows a clear enhancement of the chlorination yield in the photocatalytic reaction (blue curve) compared to the non-catalyzed reaction (red curve). Thereby we could show that NCS is activated for electrophilic chlorination by photocatalytic oxidation at room temperature.

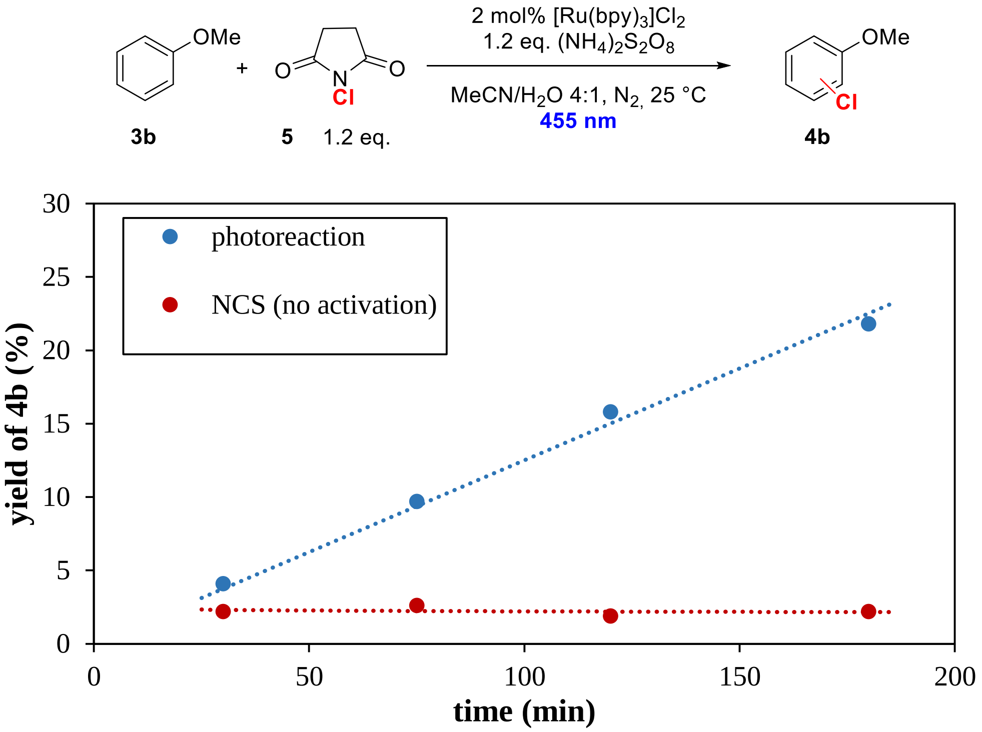

Figure 4-2. Monitoring of the chlorination of anisole (**3b**) by NCS without any activation (red curve) and using the photocatalytic activation shown above (blue curve).

As it has been successfully demonstrated that the reactivity of NCS in the electrophilic aromatic chlorination of anisole is significantly enhanced by photoredox catalysis, we next aimed to explore the effect on a variety of different arenes. To quantify the effect we compared the yields of chlorination obtained with just NCS to the yields obtained using the photocatalytic activation. The results are compiled in Table 4-5. For almost all tested arenes the photocatalytic system enabled reactions, which failed to deliver any notable amount of product in the absence of the photocatalyst under the tested reaction conditions. Only for aromatic amines or amides (entries 7, 8) the reactivity of NCS could not be increased. Xylene and toluene which were inaccessible using *N*−chloramines can be chlorinated as well (entries 5, 6). The yields are, however, moderate.

Table 4-5. Comparison of the electrophilic chlorination using NCS with and without photocatalytic activation.[a]

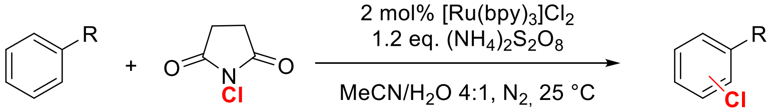

3 **5** 1.2 eq. **4**

entry	substrate	conv. (%)[b]	yield (%)[b,c]	selectivity	NCS, no photocatalyst (%)[a,d]
1	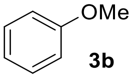 **3b**	100	92	100:0	<5
2	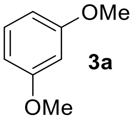 **3a**	96	69	100:0	8 (57)
3	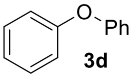 **3d**	58	79	14:1	0
4	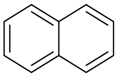 **3g**	100	44	100:0[e]	<1
5	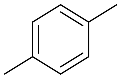 **3h**	85	59	6:1[f]	0
6	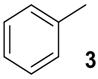 **3i**	29	38	1:1	0
7	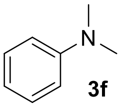 **3f**	100	21	1:1	44 (44)
8	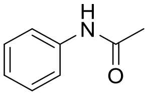 **3e**	93	25	2:1	23 (25)
9	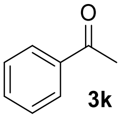 **3k**	13	<5	--	0

[a] Photocatalytic reactions were carried out using 0.25 mmol of substrate, 1.2 eq. NCS, 1.2 eq. $(NH_4)_2S_2O_8$ and 2 mol% $[Ru(bpy)_3]Cl_2$ in 1.5 mL solvent under N_2 atmosphere. The reactions were irradiated for 16 h. [b] Determined by quantitative GC analysis using an internal standard. [c] Yields based on conversion. [d] Yields in brackets are based on conversion. [e] 1-chloronaphthalenen [f] 2-chloroxylene:α-chloroxylene

4.4. Conclusion

In conclusion we demonstrated the applicability of visible light photoredox catalysis to activate *N*−chloramines and NCS for electrophilic aromatic chlorination of arenes. The activation proceeds as proposed by oxidation of the nitrogen atom of the *N*−chloro compound inducing a positive polarization on the chlorine atom. The method was applied for the chlorination of a variety of electron rich arenes. While a +M substituent on the aromatic substrate was necessary to observe chlorination with the *N*−chloramine, the stronger chlorination reagent NCS also allowed the use of less electron rich substrates as xylene and toluene. Despite the limitation regarding the scope, the photocatalytic activation can serve as a valuable catalytic alternative to conventional activation pathways.

4.5. Experimental Section

4.5.1. General Information

NMR Spectroscopy: NMR spectroscopy was carried out on either a Bruker Avance 400 (^{1}H: 400.13 MHz, ^{13}C: 101 MHz, T = 300 K) or a Bruker Avance 300 (^{1}H: 300.13 MHz, ^{13}C: 75 MHz, T = 295 K). The solvent residual peak (δ ($CDCl_3$): H 7.26; C 77.0) was used as an internal reference, chemical shifts are reported in δ [ppm], resonance multiplicities as s (singlet), d (doublet), t (triplet), m (multiplet), b (broad) and coupling constants *J* in Hertz [Hz]. The spectrometer is given for each spectrum.

Thin Layer Chromatography (TLC): For monitoring the reactions pre-coated TLC-sheets ALUGRAM Xtra SIL G/UV254 from Macherey-Nagel were used. The visualization was done by UV light (254 nm or 366 nm).

Flash Column Chromatography: Standard flash chromatography was performed on an Isolera™ Spektra Systems automated with high performance flash purification system. Macherey-Nagel silica gel 60 M (230-440 mesh) was used for column chromatography.

Photochemical set-up, LEDs: Photocatalytic reactions were performed with 455 nm LEDs (OSRAM Oslon SSL 80 royal-blue LEDs, λ_{em} = 455 nm (± 15 nm), 3.5 V, 700 mA). Reaction vials

(5 mL crimp cap vials) were illuminated from the bottom with LEDs and cooled from the side using custom made aluminum cooling block connected to a thermostat.

GC-FID measurements: Reaction optimization**:** The GC oven temperature program was adjusted as follows: initial temperature 40 °C was kept for 3 minutes, the temperature was increased at a rate of 15 °C/min over a period of 16 minutes until the final temperature (280 °C) was reached and kept for 5 minutes.

For Table 4-4 and Table 4-5: The GC oven temperature program was adjusted as follows: The initial temperature of 60 °C was kept for 3 minutes, the temperature was increased at a rate of 20 °C/min until the final temperature (290 °C) was reached and kept for 2 minutes. For substrates with lower boiling points a slightly different method was applied: The initial temperature of 60 °C was kept for 3 minutes, the temperature was increased at a rate of 25 °C/min until the final temperature (160 °C) was reached and kept for 5 minutes; internal standard: *n*-pentadecane.

4.5.2. Synthesis of *N*−Chloramines

All *N*−chloramines were synthesized according to a literature known procedure described by Bella *et. al*.[26]

1-chloropiperidine (1a)
^{1}H NMR (300 MHz, $CDCl_3$) δ 3.14 (bs, 4H), 1.81 – 1.63 (m, 4H), 1.46 (bs, 2H).

4-chloromorpholine (1b)[27]
^{1}H NMR (400 MHz, $CDCl_3$) δ 3.72 (bs, 2H), 3.14 (bs, 2H).

***N*-benzyl-*N*-chloro-1-phenylmethanamine (1c)[28]**
^{1}H NMR (300 MHz, $CDCl_3$) δ 7.45 – 7.27 (m, 5H), 4.16 (s, 2H).

N-chloro-N-methoxybenzamide (1d)[29]
^{1}H-NMR (400MHz, $CDCl_3$): δ 7.83 – 7.74 (m, 2H), 7.63 – 7.52 (m, 1H), 7.49 – 7.41 (m, 2H), 3.88 (s, 3H).

4.5.3. General Procedure for the Photocatalytic Activation of *N*−Chloro Compounds

In a 5 mL crimp cap vial 0.25 mmol of the respective substrate, together with 0.3 mmol (1.2 eq.) of the *N*−chloramine or NCS, 0.3 mmol (1.2 eq.) $(NH_4)_2S_2O_8$, and 2 mol% (0.005 mmol) $[Ru(bpy)_3]Cl_2$ x 6 H_2O were dissolved in 2 mL of MeCN/water 4:1. The reaction mixture was degassed by three cycles of freeze-pump-thaw and irradiated for 16 h with blue LEDs (λ_{max} = 455 nm).

For GC analysis 500 µL of the reaction mixture was added to 500 µL of the Standard solution (0.1 M, anisole for dimethoxybenzene, toluene for anisole, mixed, filtered and submitted to GC analysis.

For Table 4-4 and Table 4-5: After the irradiation the internal standard (0.01 mmol *n*-pentadecane) was added to the reaction and the reaction was immediately quenched with sat. Na_2CO_3-solution and brine. The mixture was extracted with ethyl acetate and subjected to GC-FID analysis.

4.5.4. CV- Measurements

CV measurements were performed with the three-electrode potentiostat galvanostat PGSTAT302N from Metrohm Autolab using a glassy carbon working electrode, a platinum counter electrode and a silver wire as a reference electrode. The potential was achieved relative to the Fc/Fc^+ redox couple (set by internal reference). The control of the measurement instrument, the acquisition and processing of the cyclic voltammetric data were performed with the software Metrohm Autolab NOVA 1.6.013. The measurements were carried out as follows: a 0.1 M solution of TBATFB in MeCN was placed in the measuring cell and the solution was degassed by a stream of argon for 5 min. After measuring of the baseline NCS was added (1 mL, 0.01 M in MeCN) and the solution was degassed by Argon purge for 5 min. The cyclic voltammogram was recorded with two scans with a scan rate of 50 mV/s. Finally ferrocene (2.2 mg, 12 µmol) was added to the solution. The solution was degassed by Argon purge for another 5 min and the measurement was performed with one scan. The potentials were converted to SCE according to V. V. Pavlishchuk and A. W. Addison.[30]

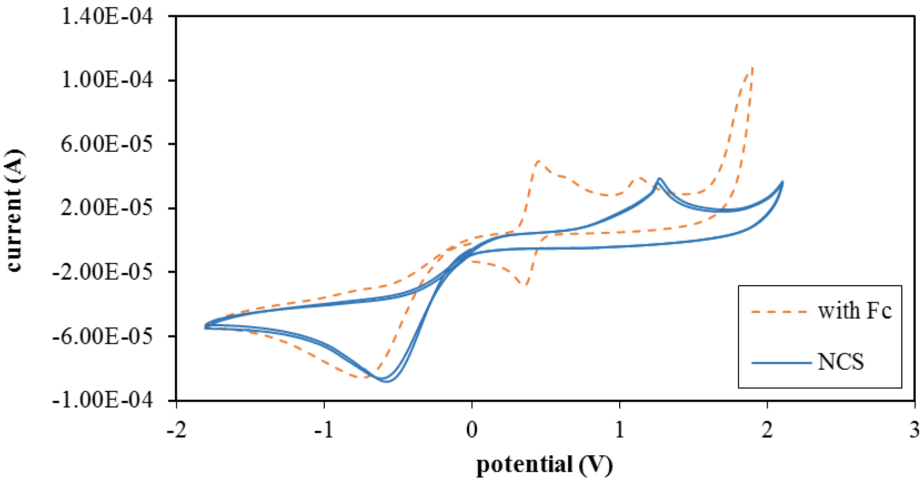

Figure 4-3. Cyclic voltammogram of NCS measured in MeCN, the blue curve shows the spectra of the pure compound, the orange curve is measured after the addition of ferrocene (Fc) as an internal reference. Peak potential was used for the irreversible potential.

4.6. References

[1] J. Fauvarque, *Pure Appl. Chem.* **1996**, *68*, 1713-1720.

[2] A. F. Littke, G. C. Fu, *Angew. Chem., Int. Ed.* **2002**, *41*, 4176-4211.

[3] G. W. Gribble, *J. Chem. Educ.* **2004**, *81*, 1441-1449.

[4] H. Liu, X. Cao, Y. Wu, Q. Liao, A. J. Jimenez, F. Würthner, H. Fu, *Chem. Commun.* **2014**, *50*, 4620-4623.

[5] W. D. Watson, *J. Org. Chem.* **1985**, *50*, 2145-2148.

[6] M. J. Mintz, C. Walling, *Org. Synth.* **1973**, *5*, 184.

[7] R. A. Rodriguez, C.-M. Pan, Y. Yabe, Y. Kawamata, M. D. Eastgate, P. S. Baran, *J. Am. Chem. Soc.* **2014**, *136*, 6908-6911.

[8] D. Qiu, F. Mo, Z. Zheng, Y. Zhang, J. Wang, *Org. Lett.* **2010**, *12*, 5474-5477.

[9] K. Tanemura, T. Suzuki, Y. Nishida, K. Satsumabayashi, T. Horaguchi, *Chem. Lett.* **2003**, *32*, 932-933.

[10] D. Kalyani, A. R. Dick, W. Q. Anani, M. S. Sanford, *Org. Lett.* **2006**, *8*, 2523-2526.

[11] G. K. S. Prakash, T. Mathew, D. Hoole, P. M. Esteves, Q. Wang, G. Rasul, G. A. Olah, *J. Am. Chem. Soc.* **2004**, *126*, 15770-15776.

[12] Y. Zhang, K. Shibatomi, H. Yamamoto, *Synlett* **2005**, *2005*, 2837-2842.

[13] S. M. Maddox, C. J. Nalbandian, D. E. Smith, J. L. Gustafson, *Org. Lett.* **2015**, *17*, 1042-1045.

[14] J. R. L. Smith, L. C. McKeer, J. M. Taylor, *J. Chem. Soc., Perkin Trans. 2* **1989**, 1537-1543.

[15] F. Minisci, E. Vismara, F. Fontana, E. Platone, G. Faraci, *J. Chem. Soc., Perkin Trans. 2* **1989**, 123-126.

[16] I. V. Koval', *Russ. J. Org. Chem.* **2002**, *38*, 301-337.

[17] Q. Qin, D. Ren, S. Yu, *Org. Biomol. Chem.* **2015**, *13*, 10295-10298.

[18] Q. Qin, S. Yu, *Org. Lett.* **2015**, *17*, 1894-1897.

[19] M. Neumann, S. Füldner, B. König, K. Zeitler, *Angew. Chem., Int. Ed.* **2011**, *50*, 951-954.

[20] N. A. Romero, D. A. Nicewicz, *J. Am. Chem. Soc.* **2014**.

[21] K. Ohkubo, K. Mizushima, S. Fukuzumi, *Res. Chem. Intermed.* **2013**, *39*, 205-220.

[22] L. Shi, W. Xia, *Chem. Soc. Rev.* **2012**, *41*, 7687-7697.

[23] S. Minakata, Y. Yoneda, Y. Oderaotoshi, M. Komatsu, *Org. Lett.* **2006**, *8*, 967-969.

[24] F. Teply, *Collect. Czech. Chem. Commun.* **2011**, *76*, 859–917.

[25] N. Iqbal, E. J. Cho, *J. Org. Chem.* **2016**.

[26] M. R. Monaco, P. Renzi, D. M. Scarpino Schietroma, M. Bella, *Org. Lett.* **2011**, *13*, 4546-4549.

[27] T. J. Barker, E. R. Jarvo, *J. Am. Chem. Soc.* **2009**, *131*, 15598-15599.

[28] S. Pandiancherri, D. W. Lupton, *Tetrahedron Lett.* **2011**, *52*, 671-674.

[29] M. Kawase, T. Kitamura, Y. Kikugawa, *J. Org. Chem.* **1989**, *54*, 3394-3403.

[30] V. V. Pavlishchuk, A. W. Addison, *Inorg. Chim. Acta* **2000**, *298*, 97-102.

5. Summary

This thesis presents applications of visible light photoredox catalysis for organic synthesis. Photocatalytic oxidation and reduction is used to generate reactive radical and electrophilic intermediates, which are employed in a variety of organic transformations. The developed reactions include the aminoarylation of alkenes, oxygenation of alkynes, alcohol oxidation and chlorination of arenes.

In **Chapter 1** a variety of amides are efficiently synthesized from alkenes by a photo Meerwein addition reaction. This intermolecular amino-arylation uses diazonium salts as a source of aryl radicals and nitriles to trap a carbenium intermediate in a Ritter reaction. The photocatalytic reaction gives access to different types of amides under mild reaction conditions and tolerates a broad range of functional groups. To demonstrate the applicability of the reaction it was applied as a key step in the synthesis of 3-aryl-3,4-dihydroisoquinolines.

The nitrate radical ($NO_3^\bullet$) is the most important free radical oxidant in the nighttime troposphere, and a unique oxygen-centered radical with high chemical versatility. **Chapter 2** describes an easy access to $NO_3^\bullet$ from readily available nitrate salts by visible light photoredox catalysis using a purely organic dye as the catalyst and oxygen as the terminal oxidant. The interaction of the excited catalyst and nitrate anions was studied by spectroscopic methods to elucidate the mechanism. A short-lived excited singlet state was identified as the reactive state in this transformation. The developed method was applied to the $NO_3^\bullet$ induced oxygenation of alkynes as well as the oxidation of alcohols.

Chapter 3 presents a flavin catalyzed oxidative chlorination of arenes inspired by FAD-dependent halogenases. In the photocatalytic system the biomolecules FAD and $NADH_2$ were replaced by the cheap organic dye riboflavin tetraacetate and methoxy benzyl alcohol as the reducing agent. While an enzyme has a highly selective binding pocket and thus a narrow substrate scope, the photocatalytic system uses *in situ* formed peracetic acid to activate chloride oxidation. This general activation strategy allows a broader substrate scope and has been applied for the chlorination of aromatic amides, anisole, aniline derivatives as well as for the α-chlorination of acetophenone.

In **Chapter 4** photoredox catalysis was used to activate *N*−chloramines and *N*−chlorosuccinimide (NCS) for the electrophilic chlorination of arenes. The photooxidation of the nitrogen atom to a radical cation induces a positive polarization on the chlorine atom which results in a higher reactivity in electrophilic aromatic chlorination reactions. In the case of *N*−chloramines a +M substituent on the aromatic substrate is necessary to observe a productive reaction, the stronger chlorination reagent NCS also allows the use of less electron rich substrates as xylene and toluene.

6. Zusammenfassung

Im Rahmen dieser Arbeit wurden durch sichtbares Licht vermittelte Photoredoxkatalysen entwickelt und ihre Anwendungen aufgezeigt. Mittels photokatalytischer Oxidation oder Reduktion werden reaktive radikalische und elektrophile Intermediate erzeugt, die dann in unterschiedlichen organischen Transformationen umgesetzt werden. Die in dieser Arbeit entwickelten Reaktionen beinhalten die Aminoarylierung von Alkenen, die Oxygenierung von Alkinen, Alkoholoxidationen sowie die Chlorierung von Aromaten. So konnte gezeigt werden, dass Photoredoxkatalyse ein äußerst hilfreiches Werkzeug für die organische Synthese darstellt.

Im **ersten Kapitel** wird die Photo-Meerwein Additionsreaktion als effiziente Methode zur Darstellung von Amiden aus Alkenen genutzt. Diese intermolekulare Aminoarylierung verwendet Diazoniumsalze als Quelle für Arylradikale und Nitrile um in einer Ritter Reaktion ein entstehendes Carbeniumion abzufangen. Die photokatalytische Reaktion ermöglicht den Zugang zu verschiedensten Amiden unter milden Reaktionsbedingungen und toleriert zudem eine große Bandbreite an funktionellen Gruppen. Um den synthetischen Nutzen aufzuzeigen, wurde die Reaktion für die Synthese von 3-Aryl-3,4-dihydroisochinolinen eingesetzt.

Das Nitratradikal ($NO_3^\bullet$) ist ein stark oxidierendes freies Radikal mit vielseitiger chemischer Reaktivität und nachts für die meisten Oxidationsreaktionen in der Troposphäre verantwortlich. **Kapitel 2** beschreibt einen einfachen Zugang zu diesem außergewöhnlichen sauerstoffzentrierten Radikal ausgehend von gewöhnlichen Nitratsalzen. Die durch sichtbares Licht vermittelte Photokatalyse nutzt einen rein organischen Farbstoff als Katalysator und Sauerstoff als terminales Oxidationsmittel. Durch den Einsatz von spektroskopischen Methoden wurde die Wechselwirkung des angeregten Katalysators mit Nitrationen untersucht und so der Mechanismus aufgeklärt. Dabei konnte ein kurzlebiger angeregter Singulett-Zustand des Farbstoffs identifiziert werden, der für die Oxidation verantwortlich ist. Im Weiteren wurde die entwickelte Methode erfolgreich auf die $NO_3^\bullet$-vermittelte Oxygenierung von Alkinen sowie die Oxidation von Alkoholen angewendet.

Kapitel 3 beschreibt die von FAD-abhängigen Halogenasen abgeleitete oxidative Chlorierung von Arenen katalysiert durch Riboflavin. In dem photokatalytischen System wurden die Biomoleküle FAD und $NADH_2$ durch den billigen organischen Farbstoff Riboflavintetraacetat und Methoxybenzylalkohol als Reduktionsmittel ersetzt. Während die Aktivierung in einem Enzym durch eine substratspezifische Bindungstasche erfolgt und somit nur eine geringe Anzahl an

Substraten toleriert, nutzt das vorgestellte photokatalytische System eine allgemeinere Aktivierungsstrategie und erlaubt somit eine größere Substratbreite. *In situ* wird Peressigsäure erzeugt, welche dann als Mediator für die Oxidation von Chlorid fungiert. Die Reaktion wurde zur Chlorierung von aromatischen Amiden, Anisol, Anilinderivaten sowie für die α–Chlorierung von Acetophenon verwendet.

Kapitel 4 beschäftigt sich mit dem Einsatz der Photoredoxkatalyse zur Aktivierung von *N*−Chloraminen und *N*−Chlorsuccinimid (NCS). Die Photooxidation des Stickstoffes zum Radikalkation induziert eine positive Polarisierung des Chloratoms, was zu einer deutlichen Steigerung der Reaktivität in elektrophilen aromatischen Chlorierungen führt. Im Falle der *N*−Chloramine ist ein +M-Substituent am Aromaten für eine Reaktion notwendig, wohingegen das stärkere Chlorierungsreagenz NCS auch weniger elektronenreiche Substrate wie Toluol oder Xylol zulässt.

7. Abbreviations

Å	Ångström
Acr^+-Mes	9-mesityl-10-methylacridinium perchlorate
bpy	2,2'-bipyridine
CAN	ceric ammonium nitrate, $(NH_4)_2Ce(NO_3)_6$
°C	celsius
CT	charge-transfer
DCM	dichloromethane
DMSO	dimethylsulfoxide
dr	diastereomeric ratio
eq.	equivalents
ESI	electron spray ionization
ET	electron transfer
FAD	flavin adenine dinucleotide
Fc	ferrocene
Fc^+	ferrocenium
FID	flame ionization detector
GC	gas chromatography
h	hours
HAT	hydrogen atom transfer
HIV	human immunodeficiency virus
HR-MS	high resolution mass spectrometry
K	Kelvin
LE	locally excited state
LED	light emitting diode
LFP	laser flash photolysis
lm	Lumen
M	molar
mA	milli Ampere
mAU	milli absorption units
mg	milligram
MHz	Megahertz

min	minutes
mJ	milli Joule
mL	milliliter
mm	millimeter
mmol	millimole
mol%	Mole percent
Mp	melting point
MS	mass spectrometry
µm	micrometer
NAD	nicotinamide adenine dinucleotide
NCS	*N*–chlorosuccinimide
nm	nanometer
NMR	nuclear magnetic resonance
ns	nanoseconds
OD	optical density
PC	photocatalyst
*p*MBA	4-methoxybenzyl alcohol
ppm	parts per million
RFT	riboflavin tetraacetate
s	seconds
SCE	saturated calomel electrode
TBATFB	tetrabutylammonium tetrafluoroborate
TEACl	tetraethylammonium chloride
TEMPO	(2,2,6,6-Tetramethyl-piperidin-1-yl)oxyl
TFA	trifluoroacetic acid
TLC	thin layer chromatography
UV	ultra violet
V	Volt
Vis	visible light
W	Watt

8. Curriculum Vitae

PERSONAL DATA

Name:	Thea Irene Hering
Date of birth:	14.09.1987
Place of birth:	Munich
Nationality:	German

EDUCATION

12/2012 - 03/2016	**Ph.D. Thesis** at the Institute of Organic Chemistry, University of Regensburg (Supervisor: Prof. Dr. B. König) *“Activation of Ionic Species by Visible Light Photoredox Catalysis”*
10/2010 - 09/2012	**Master of Science** in Chemistry, University of Regensburg **Master Thesis:** *“Visible Light Mediated $\alpha-$Arylation of Aldehydes and Ketones”* (Supervisor: Prof. Dr. B. König)
10/2007 – 09/2010	**Bachelor of Science** in Chemistry, University of Regensburg **Bachelor Thesis:** *“Direkte Estersynthese aus Ethern durch Photokatalyse mit Riboflavintetraacetat”*(Supervisor: Prof. Dr. B. König)
09/1998 – 06/2007	**Allgemeine Hochschulreife** (A-Levels) at the Carl-Orff-Gymnasium, Unterschleißheim

AWARD, SCHOLAR- AND MEMBERSHIPS

03/2013 – 04/2015	Scholarship of the “Fonds der Deutschen Chemischen Industrie”
since 2012	Member of the DFG - Graduate Training Group GRK 1626 *“Chemical Photocatalysis”* (Graduate Speaker from 03/2014-03/2015)
since 2102	Member of the GDCh (travel grants 2014, 2015)
2012	Award of the „Dr. Alfons Paulus”-Foundation
10/2007 – 09/2012	Scholarship of the Max-Weber-Programm, Elitenetzwerk Bayern

CONFERENCES

07/2015	**7th Pacific Meeting on Radical Chemistry**, Singapore, poster presentation
04/2015	**DocDays 2015**, Graz
09/2014	**24th Lecture Conference on Photochemistry**, Köln, poster presentation
07/2014	**XXV IUPAC Symposium on Photochemistry**, Bordeaux, poster presentation
07/2014	**EUCHEM Conference on Organic Free Radicals**, Prag, poster presentation
06/2013	**63rd Lindau Nobel Laureate Meeting**, Lindau
2012 - 2016	**9th- 24th Seminar Days of the GRK 1626**, oral contributions

PUBLICATIONS

- **T. Hering**, B. Mühldorf, R. Wolf, B. König, *„Halogenase-Inspired Oxidative Chlorination Using Flavin Photocatalysis“*, *Angew. Chem., Int. Ed.* **2016**, DOI: 10.1002/anie.201600783R1.

  T. Hering, B. Mühldorf, R. Wolf, B. König, *„Halogenase-inspirierte oxidative Chlorierung mittels Flavin Photokatalyse“*, *Angew. Chem.* **2016**, DOI: 10.1002/ange.201600783R1.

- **T. Hering**, T. Slanina, A. Hancock, U. Wille and B. König, *Chem. Commun.* **2015**, *51*, 6568-6571.

- D. P. Hari, **T. Hering**, B. König, *„The Photoredox Catalyzed Meerwein Addition Reaction: Intermolecular Amino-Arylation of Alkenes“*, *Angew. Chem., Int. Ed.* **2014**, *53*, 725-728.

  D. P. Hari, **T. Hering**, B. König, *„Die Photoredoxkatalysierte Meerwein Addition: Intermolekulare Aminoarylierung von Alkenen“*, *Angew. Chem.* **2014**, *26*, 743 –74.

- D. P. Hari, **T. Hering**, B. König, *„Synthetic Applications of Aryl Diazonium Salts Enabled by Visible Light Photoredox Catalysis“, Chemistry Today* **2013**, *31*, 59-63.

- **T. Hering**, D. P. Hari, B. König, *“Visible Light Mediated α-Arylation of Enol Acetates using Aryl Diazonium Salts”, J. Org. Chem.* **2012**, *77*, 10347–10352.

- D. P. Hari, **T. Hering**, B. König, *“Visible Light Photocatalytic Synthesis of Benzothiophenes”, Org. Lett.* **2012**, *14*, 5334-5337.

9. Danksagung

Allen voran möchte ich Prof. Dr. Burkhard König herzlich danken, dass er mir die Möglichkeit gegeben hat auf einem so interessanten Thema meine Master- und Doktorarbeit zu machen. Ich bedanke mich für seine Unterstützung während der gesamten Zeit, seinen ansteckenden Enthusiasmus und die Freiheit meine eigenen Ideen zu verwirklichen.

Für die Übernahme des Zweitgutachtens, sowie die erfolgreiche Kooperation in der Flavin-Photokatalyse danke ich Prof. Dr. Robert Wolf. Ich danke Prof. Dr. Frank-Michael Matysik und Prof Dr. Olga Garcia Mancheño, dass sie sich die Zeit genommen haben in meinem Prüfungsausschuss mitzuwirken.

Dem Fonds der Deutschen Chemischen Industrie sowie dem GRK 1626 danke ich für die Finanzierung meiner Promotion. Dem GRK 1626 und dem DAAD gilt besonderer Dank für die Ermöglichung des Forschungsaufenthaltes in Melbourne.

Für die gute und erfolgreiche Zusammenarbeit auf den verschiedenen Projekten danke ich ganz herzlich Durga Prasad Hari, Tomáš Slanina, Amber Hancock, Uta Wille, Bernd Mühldorf und Robert Wolf.

Ich danke Prof. Dr. Uta Wille für die Möglichkeit einen Teil meiner Forschung an der University of Melbourne, BIO21 durchzuführen. Vielen Dank für die Einführung in die Welt der Radikale und die australische Lebensart.

Ich möchte mich auch bei Britta Badziura, Viola Rappeneger, Dr. Petra Hilgers, Simone Strauss und Ernst Lautenschlager bedanken für ihre Hilfe bei allen möglichen auftretenden Problemen, organisatorischer, bürokratischer oder technischer Natur. Besonderen Dank an Regina Hoheisel für die CV-Messungen und Dr. Rudolf Vasold für die GC-Messungen.

Ich danke den Mitgliedern der Zentralen Analytik der Universität Regensburg und der Elektronik- und Feinmechanikwerkstatt für die schnelle Bearbeitung sämtlicher Aufträge.

Meine Praktikanten Andreas Graml, Victoria Scheidler, Leonie Deichner, Marc Stierhof, Corinna Kuttenberger, Benjamin Ciszek, Daniel Weinland, Lukas Traub und Vera Hirschbeck danke ich für ihre Mitarbeit an meinen Forschungsprojekten und viel Spaß bei der Laborarbeit.

Dem GRK 1626 und allen Mitgliedern danke ich für den tiefen Einblick in die Welt der Photokatalyse, zahlreiche hilfreiche Diskussionen und nicht zuletzt die gemeinsame Zeit auf den Seminartagen.

Meinen Laborkollegen Qiu, Durga, Simone, Supratim und Daniel danke ich für die wirklich tolle Zeit im Labor, viele gute Gespräche über fachliche und weniger fachliche Themen. Danke, thank you, ధన్యవాదాలు, 谢谢!

Großer Dank für die tolle Arbeitsatmosphäre, eure Hilfsbereitschaft und natürlich die schönen Abende, International Evenings, Ski Trips oder einfach entspannende Kaffeepausen gilt allen derzeitigen und ehemaligen Mitgliedern des AK Königs, besonders: Anna, Ani, den Andis, Amrita, Benno, Durga, Caro, Leyre, Malte, Manuel, Melli, Mischko, Nadja, Natascha, Rizwan, Sanne, Simone, Swarupa. Tamal, Tonda, Troppi, Qiu, Willi. Ohne euch wäre meine Doktorarbeitszeit nur halb so schön gewesen!

Vielen lieben Dank an Carolin, Willi, Claudia, Andi, Fidi und Caro für die wöchentlichen Mensa Dates, viel Spaß und eure Freundschaft! Für ganz viel Unterstützung, schöne Momente und eure Freundschaft danke ich meinen Münchner Mädels und Jungs, Marina, Kathrin und Dirk!

Von ganzem Herzen danke ich meinen Eltern für ihre Unterstützung auf jeder Ebene, fürs Zuhören, Aufbauen und für den Rückhalt. Ohne euch wäre diese Arbeit sicher nicht möglich gewesen. Vielen Dank meinem Bruder Florian, dass du mir vorgemacht hast wie man das mit dem Doktor hinbekommt und die guten Ratschläge.

Christian, ich danke dir, dass du mit mir gemeinsam durchs Leben gehst und mit dir einfach alles ein bisschen leichter und schöner ist.

Danke!